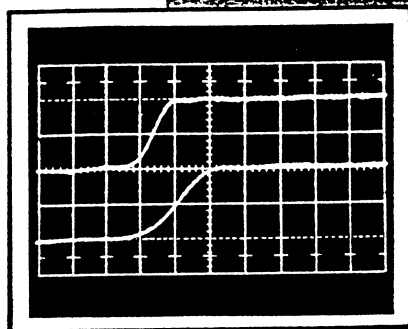
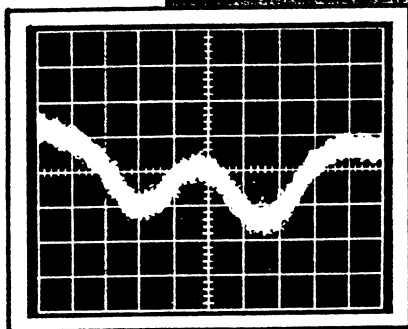
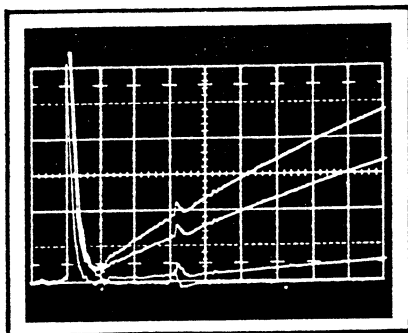


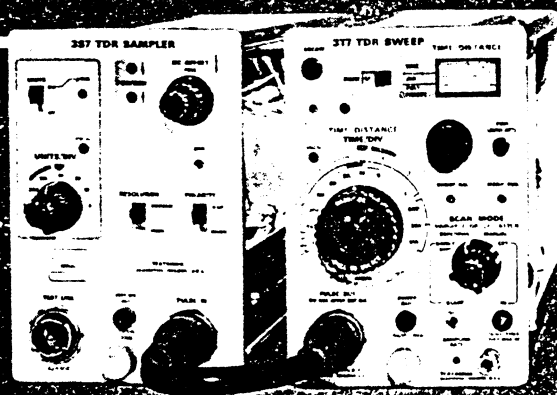


# Time-Domain Reflectometry Measurements



$$\rho = \frac{R_L - Z_0}{R_L + Z_0}$$

$$R_L = Z_0 \left( \frac{1 + \rho}{1 - \rho} \right)$$



Measurement Concept Series



# TIME-DOMAIN REFLECTOMETRY MEASUREMENTS

BY

JAMES A. STRICKLAND

Significant Contributions

by

H. ALLEN ZIMMERMAN

GORDON LONG

GEORGE FRYE



MEASUREMENT CONCEPTS



# CONTENTS

	INTRODUCTION	1
1	TRANSMISSION-LINE BASICS	3
	REALIZABLE COAXIAL TRANSMISSION LINES	5
	DIMENSION LIMITS	7
	OBTAINING ENERGY FROM A TRANSMISSION LINE	8
2	PULSE RESPONSE VERSUS FREQUENCY RESPONSE OF COAXIAL CABLES	11
	PULSES VERSUS SINEWAVES	11
	PULSE RESPONSE CHARACTERISTICS OF COAXIAL CABLES	14
	LONG CABLES	18
	SHORT CABLES	19
	MODE OF PROPAGATION IN COAXIAL CABLES	19
3	BASICS OF TDR	21
	DC ANALOGY	21
	ADDING THE TIME DIMENSION	22
	REFLECTION-SIGNAL AMPLITUDES	22
	VOLTAGE REFLECTION COEFFICIENT	23
	REFLECTIONS FROM RESISTIVE DISCONTINUITIES	26
	DISTRIBUTED RESISTANCE EXAMPLES	26
	$\rho$ CORRECTION FOR MISMATCHED-IMPEDANCE TDR	30
	$\rho$ CORRECTION FOR A SECOND DISCONTINUITY IN A MATCHED-IMPEDANCE TDR SYSTEM	31
4	TIME AND AMPLITUDE RESOLUTION RELATED TO THE FORM OF TDR SYSTEM HOOKUP	39
	AMPLITUDE RESOLUTION	39
	TIME RESOLUTION	39
	FACTORS THAT LIMIT RESOLUTION	40
	FOUR SYSTEMS	40
	CALIBRATING THE DISPLAY IN RHO/DIVISION	44

5	TDR APPLICATIONS	53
	REFLECTIONS FROM DISCRETE REACTIVE COMPONENTS	54
	IMPULSE TDR	68
	HIGH-IMPEDANCE LONG-LINE TDR USING A STEP SIGNAL	75
	CHECKING BALANCED LINES USING THE TYPE 1S2	79
	TESTING FOR FAULTS IN COAXIAL CABLES CONTAINING 60-Hz INTERFERENCE	79
	TDR USES IN THE CATV INDUSTRY	80
	TDR USED TO TUNE VHF POWER AMPLIFIER	81
	SIGNAL-GENERATOR OUTPUT IMPEDANCE	81
	BROADBAND-AMPLIFIER INPUT IMPEDANCE	81
	CIRCUIT-BOARD LEAD IMPEDANCE	82
	FREQUENCY COMPENSATION OF LOSSY CABLES	82
	EVALUATION OF FERRITE BEADS AND CORES	83
	ARTIFICIAL DELAY-LINE BALUN USE IN TDR	84
6	A COMPARISON OF SINEWAVE TESTING AND VOLTAGE STEP-FUNCTION TESTING OF COAXIAL TRANSMISSION LINES	89
	TDR VERSUS FDR MEASUREMENTS	91
	APPENDIX A	95
	APPENDIX B	97
	INDEX	103
	LIST OF ILLUSTRATIONS	105
	LIST OF TABLES	107

## INTRODUCTION

Maintaining the fidelity of electronic signals that are transmitted from point to point is of primary concern to those who design, build and maintain electronic equipment. The simple, inexpensive coaxial transmission line is perhaps the most commonly used device to accomplish this task. The techniques for determining transmission-line performance vary from simple visual inspection to elaborate instrumentation setups that require a great deal of skill and time. The availability of instruments, such as the Tektronix Type 1S2 Sampling Unit and Time Domain Reflectometer and the 3S7 TDR Sampler and 3T7 TDR Sweep units, has simplified the testing of transmission-line performance.

Time Domain Reflectometry (TDR) is the "radar" pulse testing of transmission lines. Effective use requires knowledge of both transmission lines and the TDR equipment used. Information on both subjects is included in this book – transmission lines first, then special transmission-line tests using TDR.

This book contains detailed descriptions of pulse-signal reflections from ordinary components placed into a transmission-line environment. Included are reflections from resistors (both pure  $R$  and  $Z$ ), inductors (both pure  $L$  and  $L + R$ ) and capacitors (both pure  $C$  and  $C + R$ ). Understanding such *component* pulse-signal reflections is considered important to the full analysis of transmission-line TDR plots. Thus, their descriptions fill several pages of this book.

Readers with knowledge of transmission lines may choose to be selective in using this book rather than studying the subject in the sequence offered. For quick reference, use the Index to locate selected information.





1

TRANSMISSION-LINE BASICS

A transmission line, either open-wire or coaxial-cable, gets its name from the fact that it is a transmission medium through which electrical energy is transported from one place to another. The electrical energy transported includes both a voltage between the two terminals of the line and current in both sides of the line. Once the energy has entered into a lossless line and before it reaches the output end, the voltage and current magnitudes remain constant, providing the electrical dimensions of the line remain constant.

Since a transmission line is made up of two conductors in close proximity, there is capacitance between them and inductance in series with them. (Any wire of any length has series inductance, and two adjacent wires have capacitance between them.) Fig. 1-1 is a classical diagram of a lossless transmission line and illustrates the inductance-capacitance relationship as if the line were made of discrete components. A balanced line (two parallel wire lines) is shown in Fig. 1-1A and an unbalanced (coaxial) line is shown in Fig. 1-1B. It is the combination of capacitance and inductance per unit of length that determines the major electrical characteristics of any transmission line. If a transmission line is lossless (never really true), the characteristic impedance is found by taking the square root of the ratio of the inductance per unit length,  $L$ , to the capacitance per unit length,  $C$ :

determining major electrical characteristics

$$Z_0 = \sqrt{\frac{L}{C}} \tag{1}$$

where  $L$  is in henrys,  $C$  is in farads and  $Z_0$  is in ohms.

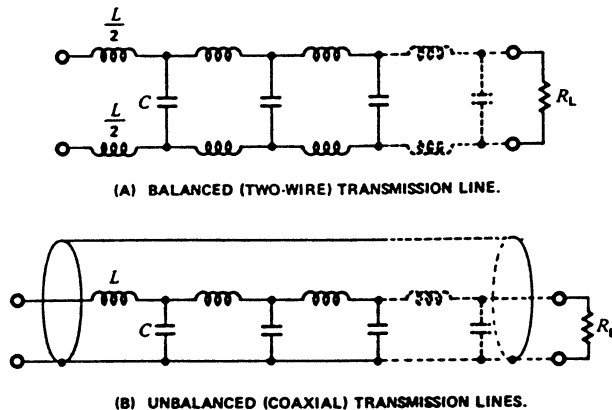


Fig. 1-1. "Lumped-constant" transmission lines.

causes  
of  $Z_0$   
changes

All matched transmission lines present a nonreactive load to their signal source. That nonreactive load appears as a lossless impedance to energy traveling in a line. The impedance does not change, providing that the physical dimensions do not change and also that the unit-length reactive components do not contain pure resistance. Any change in wire size alters the unit-length inductance and any change in wire spacing alters the unit-length capacitance. Altering either or both reactive elements can change the characteristic-impedance value of a line, causing a change in the voltage-current values of energy being transported by the line.

Using a basic definition of an inductance (it resists any change in current through it), it is possible to conceive what happens to a step signal as it reaches a discrete inductance in series with a transmission line. Before the inductance can accept the signal current, it reflects some of the energy back toward the signal source.

In a similar manner, using a basic definition of a capacitor (it resists a change in voltage across it), it is possible to conceive what happens to a step signal as it reaches a discrete capacitor shunted across a transmission line. Before the capacitor voltage can be changed to equal the signal voltage, it reflects some of the energy back toward the source.

changes  
cause  
reflections

Anytime the dimensions of a transmission line are altered over a finite length, the change can cause the line to have a new characteristic impedance. Such changes are not considered reactive, but resistive. Both reactive and nonreactive (resistive) changes within a transmission line cause some portion of a signal to be reflected back toward the source, subtracting from the energy transmitted toward the output or load end. Thus, in order to transport a maximum amount of energy through a transmission line, care must be taken to keep its characteristic impedance constant throughout its length.

It is possible to change the dimensions of a transmission line without giving it a reactive nature or changing its characteristic impedance. If, for instance, larger wire is used, even though the unit-length inductance is reduced, increasing the spacing proportionately will also reduce the unit-length capacitance and the  $Z_0$  of formula (1) remains unchanged. Changes in physical dimensions of either balanced or unbalanced lines must be made gradually over a short distance (short compared to the signal frequency wavelength) in order to avoid a sudden change in  $Z_0$ . Sometimes you will find coaxial lines with what appears as an abrupt size change. This always produces a capacitance mismatch at the point of change. Gradual size change reduces the mismatch capacitive change, thereby producing smaller signal reflections than a step change in dimension produces.

The remainder of the discussion on transmission lines deals only with coaxial lines, although either form of line may be tested with proper TDR equipment.

## REALIZABLE COAXIAL TRANSMISSION LINES

other  
losses

Other factors that must be considered in the everyday use of coaxial cables, in addition to inductance and capacitance per unit length, are:

- 1) low-frequency or DC series resistance losses,
- 2) high-frequency (HF, VHF and UHF) "skin-effect" series resistance losses,
- 3) ultrahigh-frequency (UHF) dielectric polar losses,
- 4) UHF leakage losses through the "holes" of cables that use braid as the outer conductor,
- 5) some of the energy of a UHF signal or of a very fast rise pulse changes its mode of propagation from TEM to  $TE_{11}$  if the signal frequency has a quarter wavelength shorter than the inner diameter of the outer conductor (in the circular waveguide mode,  $TE_{11}$ , energy cannot be retrieved at the cable output end<sup>1</sup>),
- 6) the rarely found shunt conductance losses and
- 7) inductance of individual braid wires that do not make good contact with neighboring wires.

Maximum power and voltage ratings will not be discussed.

series DC  
resistance

skin effect

Signal velocity of propagation is affected by the material used as the dielectric between conductors. Note that all but the DC-resistance-loss mechanisms change as a function of frequency. It is generally accepted that "skin-effect" losses predominate up to about 1000 MHz for short-length solid-polyethylene-filled braided coaxial cables.<sup>2</sup> The series DC resistance becomes apparent with long lines. (Step-signal TDR easily discloses the DC resistance in RG213/U cable of about 200 feet or longer.) Most of the losses mentioned can be minimized by using large-diameter lines with air or dry nitrogen dielectric and solid outer conductor.

<sup>1</sup>Lewis and Wells, *Millimicrosecond Techniques*, 2nd edition (Pergamon Press), pp. 27-28.

<sup>2</sup>*Ibid.*, p. 45.

minimizing  
skin-effect  
losses

Skin-effect losses are minimized best by using conductors that are clean and have very smooth surfaces. Oxidation of copper increases skin-effect losses due to both conductor surface resistance and some surface roughening. Silver plating copper conductors provides only a very small reduction in skin-effect resistance, providing that the silver is thick enough and is burnished smooth. Plating is usually porous and, if not burnished, can increase the surface length and resistance of a copper conductor. Therefore, it is common practice to silver plate (and polish) conductors used at frequencies above about 500 MHz. (Moreno<sup>3</sup> plots the RF current conduction depth for various materials versus frequency. Copper and silver being very similar, the skin depth is approximately  $6.5 \times 10^{-4}$  cm at 100 MHz; approximately  $2.1 \times 10^{-4}$  cm at 1 GHz. At those frequencies, any silver plating with less thickness actually increases the skin-effect resistance and is usually avoided.)

The characteristic impedance of short-length coaxial cables can be determined by using only formula (1). The complete formula includes series resistance (DC and skin-effect) and shunt conductance, and is:

$$Z_0 = \sqrt{\frac{R + j\omega L}{G + j\omega C}} \quad (2)$$

where  $R$  is in ohms,  $L$  is in henrys,  $G$  is in mhos (modern term for  $1/R$  is siemens) and  $C$  is in farads. " $\omega$ " relates to the signal frequency. Since most coaxial cables have insignificant shunt conductance,  $G$  can usually be left out of formula (2).

NOTE: Numerous articles and texts cover the derivation of formulas for the mathematical study of transmission lines. No derivations are offered here.<sup>4</sup>

<sup>3</sup>Theodore Moreno, *Microwave Transmission Design Data*, (New York: Dover, 1958), p. 13.

<sup>4</sup>Richard E. Matick, *Transmission Lines for Digital and Communication Networks*, (New York: McGraw-Hill, 1969).

short-length  
cable as a  
capacitor

All of the elements that make up a transmission line (resistance, reactance, conductance) are evenly distributed over its entire length. Even so, it is common to talk about a short length of line as being nothing more than a capacitor at low frequencies. Common 50-Ω flexible coaxial cables have between 28.5- and 30-pF capacitance per foot and 75-Ω cables have between 20- and 21.5-pF capacitance per foot. It is important to remember that the concept of a cable being a capacitor applies only when the line is unterminated and its electrical length is significantly shorter than the signal electrical wavelength.

### DIMENSION LIMITS

determining  
 $Z_0$

Noting the limited range of capacitance per unit length of a fixed characteristic impedance coaxial cable permits us to discuss the limits of dimension for obtaining a particular characteristic impedance. To determine the characteristic impedance of a coaxial line requires knowledge of the dielectric material and the conductor dimensions; it is determined by the formula:

$$Z_0 = \frac{138}{k} \log_{10} \frac{D}{d} \quad (3)$$

where  $k$  is the dielectric constant of the material between the conductors,  $D$  is the outer-conductor inner diameter and  $d$  is the inner-conductor outer diameter. The units of  $D$  and  $d$  must be the same.

dielectric  
material  
significance

Formula (3) includes the dielectric constant of the dielectric material placed between the two conductors. The dielectric constant is included because it affects the value of capacitance per unit of length that is part of both formula (1) and (2). Thus, it is not just the dimensions that affect the characteristic impedance of a coaxial transmission line.

A second characteristic of the dielectric material is that it affects the signal velocity of propagation through the cable. Since the signal is a form of electromagnetic energy, it travels at the velocity of light if it is propagating in a medium through which light can travel. An air dielectric line has a signal velocity of propagation,  $c$ , equal to the speed of light. Light travels at the speed of 300,000 meters per second, or 30 cm per nanosecond (ns), which is 11-13/16 inches/ns. Signals propagate through solid polyethylene dielectric coaxial cables at approximately 0.659 times that through air or about 19.77 cm/ns (which is 7-3/4 inches/ns).

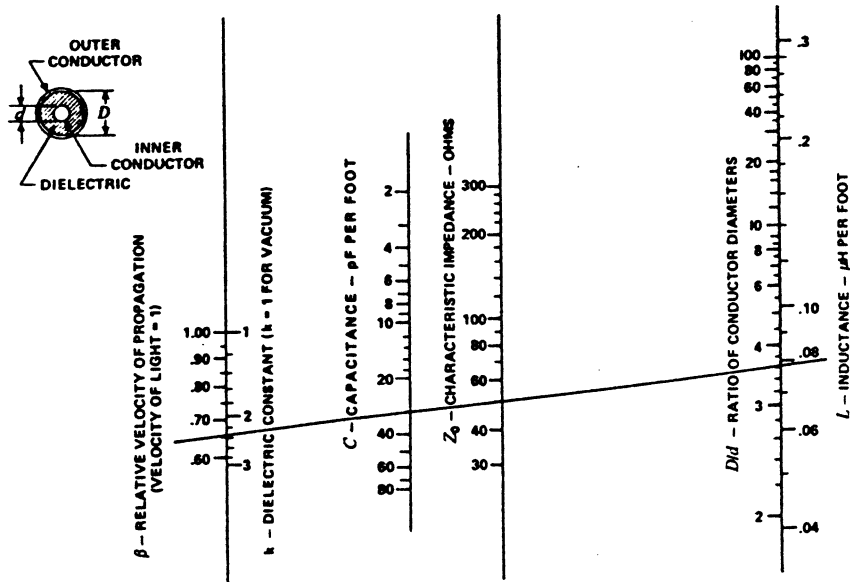


Fig. 1-2. Coaxial-transmission-line impedance nomograph.

use of  
nomograph

Six elements of a coaxial cable already discussed have been combined into a four-scale nomograph produced by Lawrence Radiation Laboratories and shown in Fig. 1-2. To use the nomograph, a single straight line that intersects the four scales represents a possible transmission line. Known points on any two scales define the location of the line. Fig. 1-2 shows a line drawn through all points that relate to a solid polyethylene coaxial cable of  $50\text{-}\Omega$  characteristic impedance. From this chart it is easy to see that changing only the dimensions of a cable changes three of the four variables, leaving the velocity of propagation unchanged. *Note that the signal velocity of propagation is related directly to the dielectric constant of the dielectric material and the inductance per foot is related directly to the ratio of the two conductor diameters.*

## OBTAINING ENERGY FROM A TRANSMISSION LINE

coaxial cable  
as a load

Energy coupled between two points by a transmission line travels through a medium said to have a characteristic impedance. The impedance is measurable at either end of the line and the  $E-I$  relationships of energy in the line respond to simple Ohm's law. There is, however, some signal loss while the signal is within the line. Therefore, it is more correct to think of a coaxial cable as *receiving* and *delivering* energy following Ohm's law rules, but with losses inside the line that may not relate to Ohm's law.

To a signal source, the coaxial cable acts as a load with a resistance value equal to  $Z_0$ . A matched source driving a matched loaded line is said to "not know" how long the transmission line is.

coaxial cable  
as a source

To a signal load, the coaxial cable acts as a signal generator with a source resistance of  $Z_0$ . The load, properly matched, is said to "not know" how long the transmission line is nor what the true generator output resistance or power level actually is.

an incorrect  
load becomes  
a "source"

If a load does not have a resistive value equal to the transmission line  $Z_0$ , there will be some energy reflected back into the line. The reflected energy travels within the line toward the source and ends up being delivered to the signal source. Under such a condition, the source is said to "find out" that the transmission line couldn't get rid of all its energy and that it was not infinitely long. A transmission line, terminated by a load with a resistive value equal to  $Z_0$ , then acts as an infinitely long line.

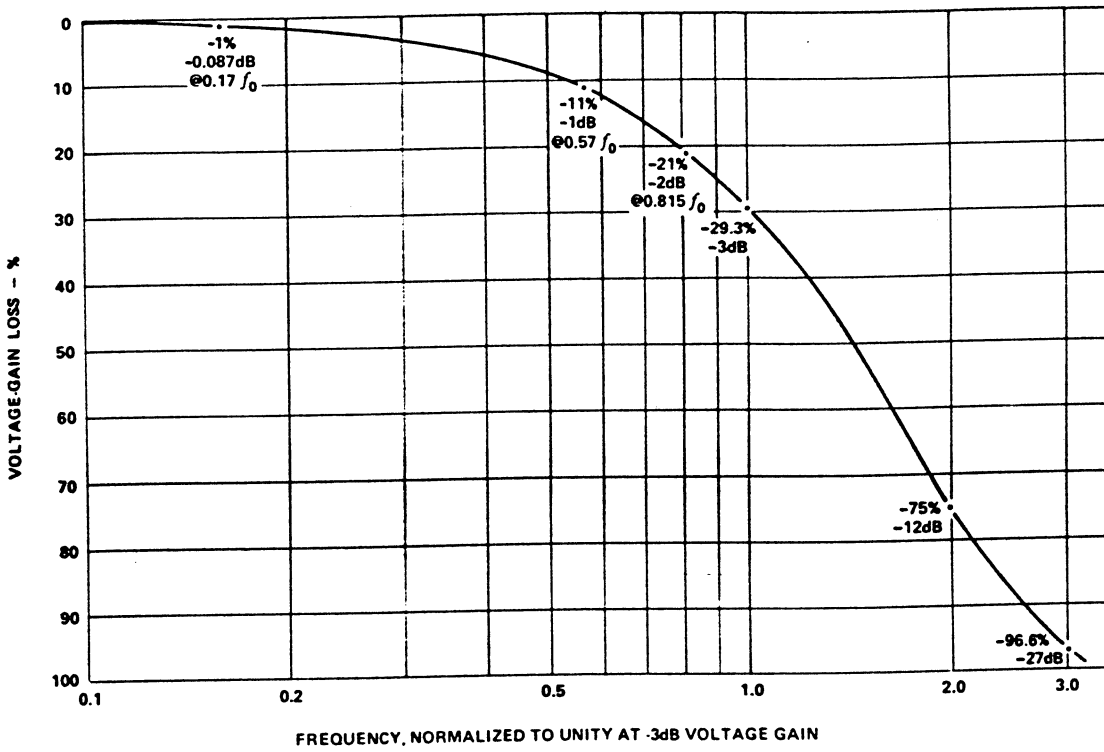


Fig. 2-1. An ideal (Gaussian) amplifier amplitude-versus-frequency response curve.



## 2

## PULSE RESPONSE VERSUS FREQUENCY RESPONSE OF COAXIAL CABLES

The following chapter introduces sinewave-oriented engineers to pulse techniques (and terminology) involving both coaxial cables and sampling oscilloscopes. In addition, the pulse response versus frequency response of real-time-oscilloscope vertical amplifiers is compared with the pulse response versus frequency response of sampling-oscilloscope vertical amplifiers. Many oscilloscope users (that are Tektronix oriented) think of amplifier frequency response only in terms of having a Gaussian response. That subject is reviewed and compared to the non-Gaussian amplitude-frequency-phase response of sampling oscilloscopes.

### PULSES VERSUS SINEWAVES

Pulse technology, used when testing real-time-oscilloscope vertical amplifiers, is often used when pulse testing the systems that use transmission lines and sampling oscilloscopes. The major signal transmission difference between an oscilloscope vertical amplifier and a coaxial cable is that the amplifier has an amplitude-frequency-phase response that is often considered Gaussian (although it actually may not be so) while a coaxial cable definitely does not. When a system contains long lengths of coaxial cable, pulse technology differs from that used with amplifiers. Systems that contain short lengths of coaxial cable have pulse responses not limited by the cable.

It is the intent of this material to point out the differences in technology used and to show that it can be misleading to state that to pulse test a transmission line also tests that line over a certain frequency range.

In amplifier testing, engineers make the mathematical translation from pulse response characteristics to amplitude-frequency response characteristics by dividing the constant of 0.35 by the time it takes the amplifier output voltage to change from 10% to 90% ( $t_r$ ) of a fast pulse. If the amplifier has a response approximately Gaussian, then its sinewave signal gain changes from its DC gain (with increasing frequency) as the square of the frequency. For example, an amplifier with a pulse risetime of 3.5 ns will have a sinewave voltage gain that is down 3 dB from the DC gain at 100 MHz ( $0.35/0.35 \times 10^{-9}$  second =  $1 \times 10^8$  cycles per second, or 100 MHz). The ideal Gaussian response curve of that amplifier is shown in Fig. 2-1.

We continue to use the above pulse-to-sinewave translation technique when testing very fast sampling oscilloscopes, even though the answers are only approximations. Fig. 2-2 shows two curves of risetime tests. Curve *A* is a real-time-oscilloscope pulse response to a 75-ps  $t_r$  signal displayed at 50 ns/div; curve *B* is a 350-ps  $t_r$  sampling-oscilloscope pulse response to the same 75-ps  $t_r$  signal displayed at 200 ps/div. Note that curve *A* shows some rounding during the rise that is normal to a Gaussian-type response but that curve *B* is more like a ramp with sharper corners at both beginning and end. The sinewave amplitude-frequency response of the real-time-oscilloscope amplifier continues to fall after the -3 dB point, but the amplitude-frequency response of the sampling oscilloscope contains several rises and falls after the -3 dB down point and may be still usable at 3 times the -3 dB frequency. Both systems have a -3 dB amplitude-frequency response near the value obtained by dividing 0.35 by the pulse display 10%-to-90% risetime. (Each sampling oscilloscope must be evaluated, especially above the -3 dB amplitude point, if it is to be used for sinewave measurements, because the amplitude-frequency response of various types of samplers differ significantly. The faster the  $t_r$  of a type of sampler, the more its amplitude-frequency response approximates a Gaussian curve.)

use of  
fast pulse  
in TDR

It is a common misconception that a fast pulse can be used in TDR to test a transmission line over the same band of frequencies that can be calculated from the pulse 10%-to-90% risetime. Page 42-5 in the 5th edition (1012 in the 4th edition) of *ITT Reference Data for Radio Engineers* shows a Fourier waveform analysis of a rectangular pulse. That concept is displayed in Fig. 2-3 by the amplitude-frequency spectrum of a 1.5- $\mu$ s-duration 250-ps-risetime pulse (using a Tektronix Type 1L20 spectrum analyzer). DC is represented at the right and each major horizontal division to the left is 5 MHz from DC. The total display then represents the voltage content of the pulse from DC through 50 MHz. Each vertical division represents 16.6% of the total pulse amplitude. Note that the pulse contains energy at 10 MHz equivalent to a sinewave with a peak voltage amplitude of only about 18% of the DC value. Note also that the amplitude is less than 6.6% for any one sinewave frequency above about 30 MHz. This then says that pulses that are used for the TDR testing of transmission lines do not contain much energy for any one sinewave frequency throughout the normal amplitude-frequency range (this can be calculated by finding the pulse response 10%-to-90% risetime).

There are several other forms of test equipment (other than TDR) that properly test transmission lines on a sinewave basis. Some of these systems are compared to TDR in Chapter 6 of this book. It is important to know that there is no TDR system that can test a transmission line on the same

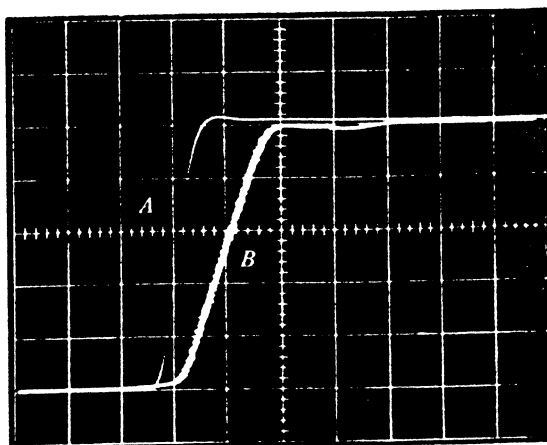


Fig. 2-2. Double exposure. Pulse tests: (A) real-time oscilloscope, 50 ns/div; (B) sampling oscilloscope, 200 ps/div.

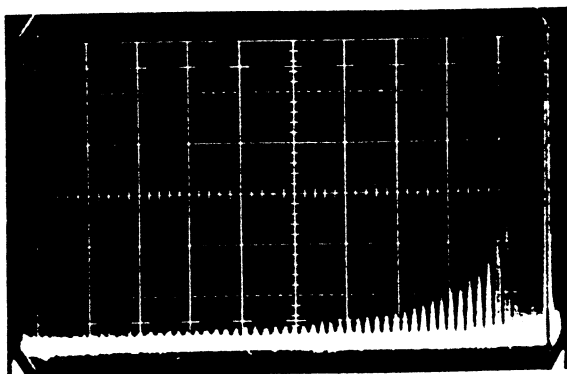


Fig. 2-3. 50-MHz dispersion display of 1.5- $\mu$ s-duration 250-ps 10%-to-90% risetime pulse.

quantitative basis as a system that uses sinewaves. It is also important to state that TDR is at times more useful than sinewave testing and the two systems are very often complementary. It can be misleading to tell an engineer who is experienced in sinewave testing (and not experienced in TDR testing) that TDR tests lines fully on a frequency basis.

A very fast transition pulse contains energy at very high frequencies. A pulse whose 10%-to-90% risetime is 90 ps commonly contains energy beyond 3800 MHz. However, the 3800-MHz equivalent sinewave does not have an amplitude similar to the pulse amplitude displayed by a TDR system.

## PULSE RESPONSE CHARACTERISTICS OF COAXIAL CABLES

step-signal  
distortion

Coaxial cables have a step-function response that distorts the original signal. The distortion is caused by several types of cable losses which are frequency dependent. The longer the cable length, the greater the distortion. Response to a step signal can be evaluated by placing the cable in a TDR system, or by placing it between a fast rise pulser and a fast risetime sampler. (When a cable is tested by a TDR device, the signal traverses the line twice; when a cable is placed between a pulser and a sampler, the signal traverses the line once.)

Engineers and mathematicians have researched the signal handling capabilities of transmission lines for many years. Their efforts have leap-frogged the advancement of testing equipment, similar to the way pulse generators and oscilloscopes have leap-frogged each other. The advent of very fast pulse generators and sampling oscilloscopes permits the confirmation of fast-pulse responses that have been predicted in technical articles during the last 10 years. This is not to imply that using fast equipment to determine the pulse response of a cable explains the loss mechanisms within the cable.

translating  
losses to  
transient  
response

Physical processes of loss are well defined by Nahman<sup>1</sup> as skin effect, dielectric effect, reflection and radiation. In the same article, Nahman presents a graphical technique for determining transient response in a cable with known losses. He uses a Laplace transformation complex variable to help explain why cables have high-frequency attenuation curves that depart from the characteristic slope of 1/2. (Nahman's method of translating attenuation data to transient response is simpler than either Bode's<sup>2</sup> integral technique or Rosenbrock's<sup>3</sup> graphical technique, even though he uses some of the work by both men.)

Another discussion of pulses in transmission lines is presented in Chapter 5 of a book by Richard E. Matick.<sup>4</sup> Matick discusses two major sources of

<sup>1</sup>N. S. Nahman, "A Discussion on the Transient Analysis of Coaxial Cables Considering High-Frequency Losses," in *IRE Transactions on Circuit Theory*, vol. CT-9, no. 2 (June, 1962), pp. 144-152.

<sup>2</sup>H. W. Bode, *Network Analysis and Feedback Amplifier Design*, (New York: D. Van Nostrand Company, Inc., 1945).

<sup>3</sup>H. H. Rosenbrock, "An Approximate Method for Obtaining Transient Response from Frequency Response," *Proceedings of the IRE* (November, 1955) vol. 102, pp. 744-752; and "Interconverting Frequency and Transient Response," *Control Engineering* (July, 1959), vol. 10.

<sup>4</sup>Richard E. Matick, *Transmission Lines for Digital and Communications Networks*, (New York: McGraw-Hill, 1969), p. 192.

pulse distortion in coaxial cables: attenuation and dispersion (“...dispersion simply indicates the dependence of phase velocity on the applied frequency, regardless of what mechanisms are responsible for this dependence.”).

long-coaxial-cable  
step response

“dribble-up”

High-frequency losses in long coaxial cables sometimes make it quite difficult to obtain an accurate 10%-to-90% risetime measurement of fast pulses. However, an interesting characteristic of coaxial cables is that they do pass some high frequencies with less attenuation than given some lower frequencies. When pulse testing a coaxial cable, this characteristic shows up as a rapid pulse transition for the first half or more of the step and thereafter the rate of step rise is slowed significantly. Therefore, the step response of long coaxial cables is often measured from the step 0% point to the step 50% amplitude point, instead of the typical 10%-to-90% risetime amplitude points. (10%-to-90% risetime is labeled  $t_r$  and 0%-to-50% risetime is labeled  $t_0$ .) The resultant display of a pulse passed through a long cable is said to “dribble-up” to the 100% point. Limits of dribble-up, calculated for skin-effect losses only, are described in a Lawrence Radiation Laboratory in-house report<sup>5</sup> which states that the 10%-to-90% risetime ( $t_r$ ) through a cable usually takes 28 times longer than the 0%-to-50% risetime ( $t_0$ ). Modern testing equipment permits more accurate data than calculations allow. RG213/U cable has a  $t_r$ -to- $t_0$  changing ratio of  $\leq 16:1$ , depending upon the general length of cable used. The ratio is maximum for 250-foot long cables.

Two types of modern JAN (Joint Army Navy) coaxial cable were pulse tested using both TDR and one-way-signal tests to record differences in both  $t_r$  and  $t_0$  for different cable lengths. Purpose of the testing was to verify the LRL article and another article on the same subject by R. L. Wigington and N. S. Nahman.<sup>6</sup> Pulse testing included three different pulse sources. Two of them in the Tektronix Type 1S2 Sampling Unit and Time Domain Reflectometer; the third was the Tektronix Type S-50 Pulse Generator Head. (The three systems have 10%-to-90% risetimes of 1 ns, 150 ps and 45 ps.) The two cables tested have JAN designations of RG63B/U (125- $\Omega$   $Z_0$ ) and RG213/U (50- $\Omega$   $Z_0$ ), both single-braid shielded and with a braid inner diameter slightly greater than 1/4 inch.

<sup>5</sup>Q. Kerns, F. Kirsten, and C. N. Winningstad, “Pulse Response of Coaxial Cables,” *Counting Notes*, Rad. Lab., File No. CC2-1 (Berkeley, California: University of California, March, 1956).  
Revised by F. Kirsten (January 15, 1959).

<sup>6</sup>R. L. Wigington and N. S. Nahman, “Transient Analysis of Coaxial Cables Considering Skin Effect,” *Proceedings of the IRE* (February, 1957), vol. 45, pp. 166-174.

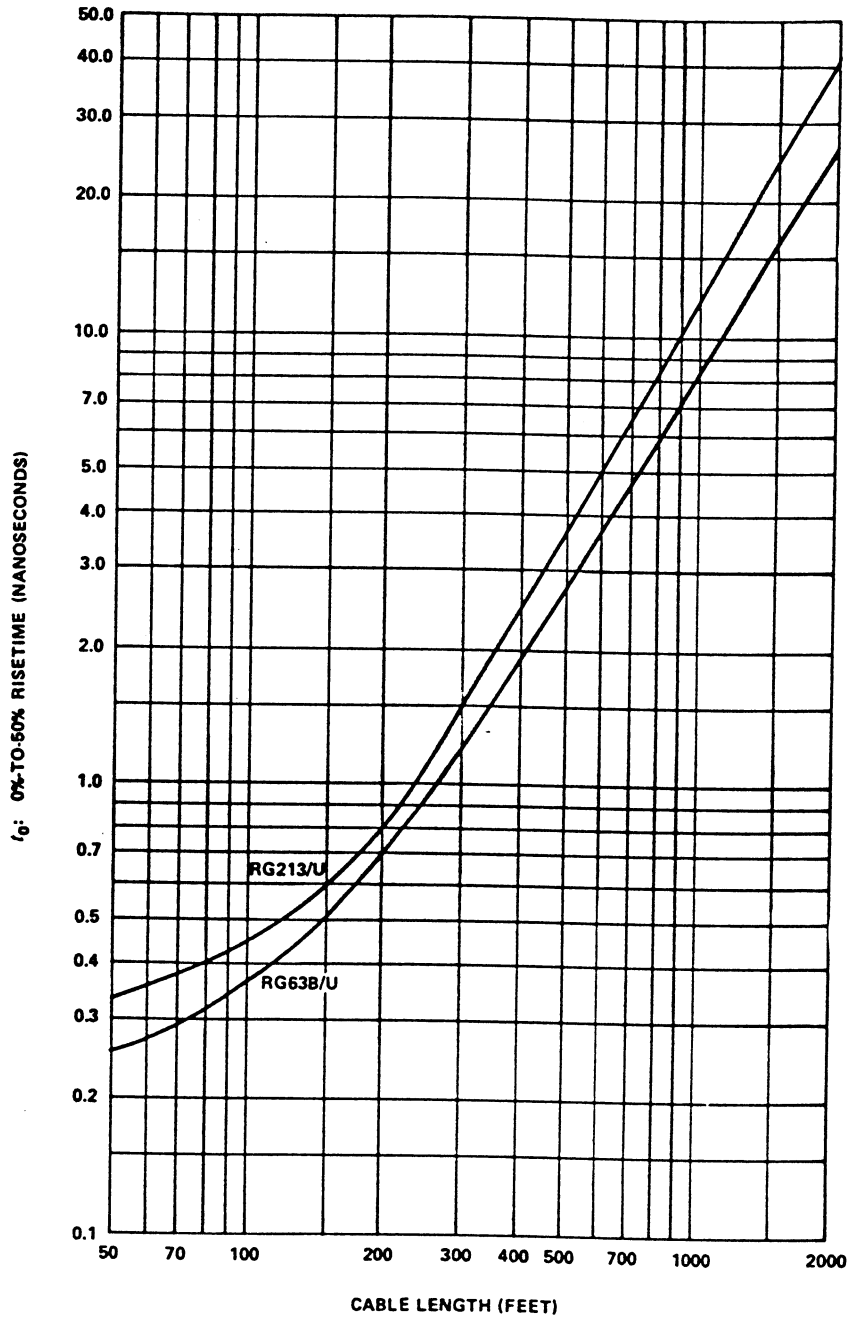
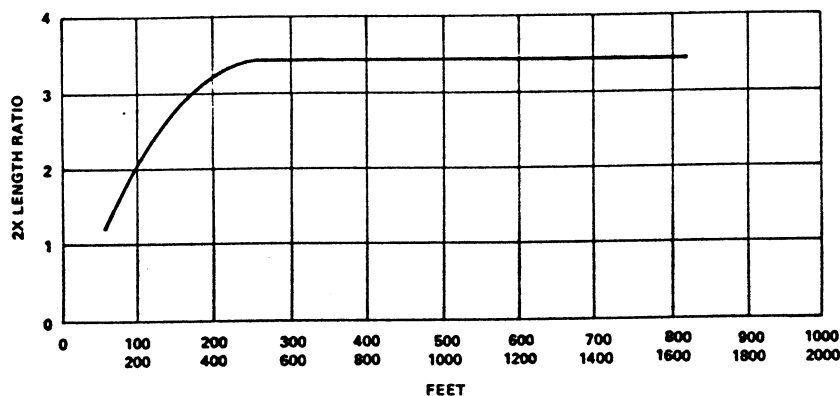


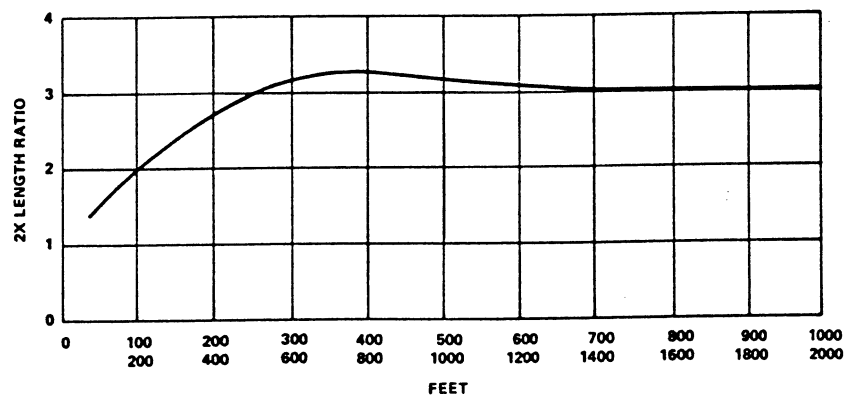
Fig. 2-4. Coaxial-cable 0%-to-50% pulse risetime versus length.

Tested cables had lengths ranging from 50 feet to 2000 feet. Data was converted to the graphs of Fig. 2-4 and Fig. 2-5. Fig. 2-4 shows changes in  $t_0$  risetime (limited by the coaxial cable only) over the range of lengths tested. Fig. 2-5 shows the changing ratios of  $t_0$  when doubling a cable length. (For years engineers have said that to double a coaxial cable's length slows the  $t_r$  or  $t_0$  by a factor of 4. Note that the cables tested never reached the 2X length ratio of 4:1, but the ratio varies for short cable lengths and is fairly stable at about 3.3:1 for cable lengths greater than about 300 feet.)

Comparison of  $t_r$  to  $t_0$  for each length shows a changing ratio for different cable lengths. It is this ratio ( $t_r$  to  $t_0$ ) that is difficult to measure accurately because lengths greater than about 250 feet showed a lot of "dribble-up." The longer the cable, the greater inaccuracy of the  $t_r$  measurement. Even though the  $t_r$  measurements contained an accuracy error, it is still significant to note that the ratio of  $t_r$  to  $t_0$  never exceeded 16:1 for a 250-foot length and was less than that for all other lengths.



(A) CHANGING RATIO OF 0%-TO-50% RISETIME ( $t_0$ ) FOR 2X CABLE LENGTHS OF RG213/U COAX.



(B) CHANGING RATIO OF 0%-TO-50% RISETIME ( $t_0$ ) FOR 2X CABLE LENGTHS OF RG638/U COAX.

Fig. 2-5. RG213/U and RG638/U ratios of  $t_0$  for 2X change in cable length.

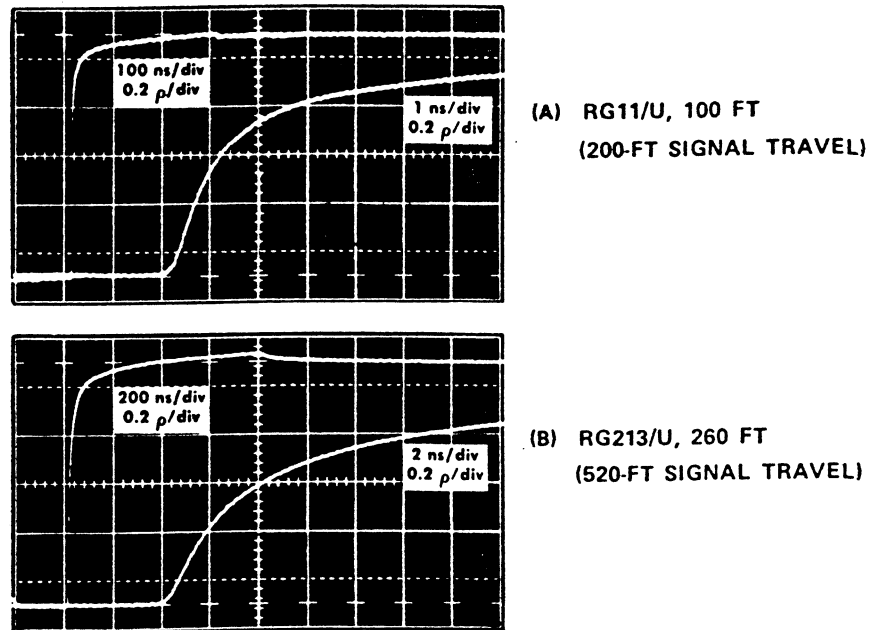


Fig. 2-6. RG11/U and RG213/U distortion to a step signal. Waveforms are reflections from cable open end.

## LONG CABLES

dribble-up  
examples

“Dribble-up” distortion to pulse signals in coaxial cables is most easily displayed on a CRT when the cable is long. A long cable is here defined as one that exhibits significant losses in the system in which it is used. The tests shown in Fig. 2-6 were made on a 100-foot section of RG11/U and a 260-foot section of RG213/U. In each case the signal traversed the line twice in a normal TDR manner. The far end of the cable was left an open circuit so that a return signal with a  $\rho$  of +1 could be observed. (See pages 23 and 24 for a definition of  $\rho$ .) This gives the same effect as having sent the pulse signal through a line twice as long.

Fig. 2-7A is a double exposure using the 260-foot length of RG213/U connected between the Tektronix Type 1S2 1-ns  $t_r$  pulser and the terminated Thru Signal Channel. Both traces were made at 1000 ns/div, the upper trace at 0.2  $\rho$ /div and the lower trace at 0.05  $\rho$ /div. The lower trace leads us to believe that the output pulse reaches 100% amplitude sometime between 4000 and 5000 ns after the initial step rise. More exact measurements can be made by comparing the cable output with the Type 1S2 no-cable response as shown in Fig. 2-7B. Here both traces were made at 1000 ns/div and 0.02  $\rho$ /div with an intentional small vertical repositioning. When the two traces become a constant distance apart, you can be relatively certain the cable output signal has reached 100% amplitude. Fig. 2-7B indicates a possibility that the output signal had not completely reached 100% amplitude even after 8000 ns (8  $\mu$ s).



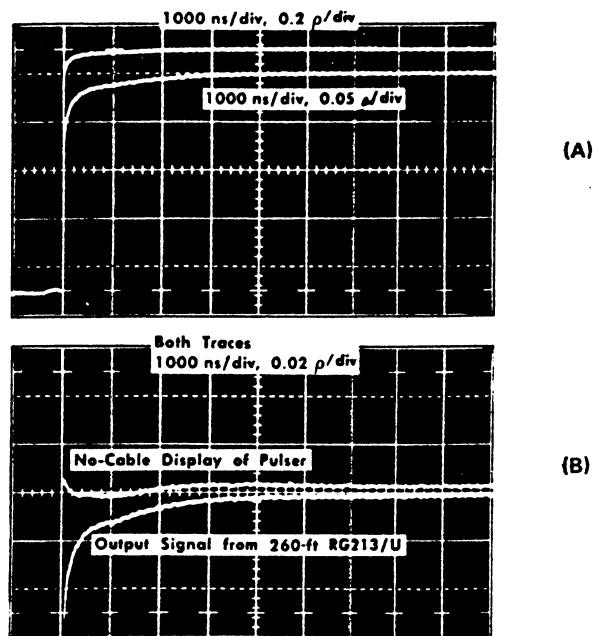


Fig. 2-7. "Dribble-up" output signals from 260-ft RG213/U.

## SHORT CABLES

Even though information just given on long cables is true for any length cable, a physically short cable can be treated as if it has no dribble-up or losses. A short cable will have a  $t_0$  sufficiently faster than the Type 1S2 50-ps pulser's 10%-to-90%  $t_r$  and the long slow rise ("dribble-up") of Fig. 2-7 will not be evident. Under these short-cable conditions, it is reasonable to assume that the bandpass upper limit of a cable and its system can be approximated from the 10%-to-90% risetime display.

## MODE OF PROPAGATION IN COAXIAL CABLES

cause of  
mode change

Energy traveling within a coaxial cable travels in what is termed the Transverse ElectroMagnetic (TEM) mode. It must remain in the TEM mode from cable input to output so that the load receives the energy at the cable output in a form similar to what it was when it entered the cable. There can be a change in the mode of propagation, should the energy contain frequencies whose electrical quarter wavelength is approximately equal to the cable outer-conductor inner diameter. If that condition exists, then any discontinuity within the cable will likely cause some of the energy to change from TEM propagation to  $TE_{11}$  (Transverse Electric, circular waveguide mode) propagation at the instant it reaches the discontinuity. For this reason, users of TDR test equipment do not normally drive a transmission line with a step pulse that has a  $t_r$  that is "too fast." For example, users of the Tektronix Type 1S2 should usually avoid using fast 0.25-volt pulser ( $t_r \leq 50$  ps) to test cables whose outer-conductor inner diameter is equal to or larger than one-quarter wavelength at 3500 MHz.

Fig. 2-8 shows two tests of an air dielectric line whose outer-conductor inner diameter is 3-1/8 inches. Fig. 2-8A used the Type 1S2 1-ns  $t_r$  pulser. Fig. 2-8B used the Type 1S2 50-ps  $t_r$  pulser. The line elements were the same in each case: 1) a short section of RG213/U cable between the Type 1S2 and a tapered line section, 2) the tapered line section and 3) the section of 3-1/8-inch-diameter rigid air line with a 90° elbow in the display time window. The numerous aberrations of Fig. 2-8B are due to a change in propagation mode when the signal arrived at the 90° elbow. The resulting multiple reflections are of very little value to the operator testing the line.

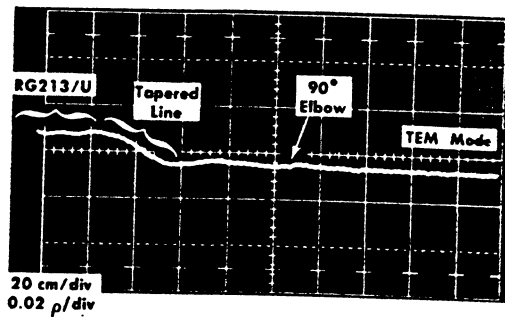
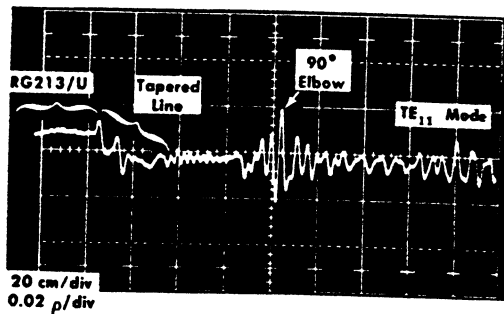
(A) 1-ns  $t_r$  PULSER(B) 50-ps  $t_r$  PULSER

Fig. 2-8. Propagation-mode change in large-diameter transmission line when driven by the Type 1S2 fast pulser.

## 3

## BASICS OF TDR

This chapter discusses the basic principles of TDR reflection-signal amplitude, voltage reflection coefficient, reflections from discrete resistive discontinuities, distributed resistance reflections and differences between small lossy cables and normal power-handling quality cables. The whole discussion relates to a TDR system which uses a matched-pulse signal source and a "fly-by" through-signal sampling oscilloscope (Tektronix Type 1S2 or 3S7/3T7 units).

## DC ANALOGY

Signal reflection amplitudes from nonuniform transmission-line loads are easily related to a simple DC circuit.

Fig. 3-1 illustrates three simple circuits that relate to transmission lines and TDR. Fig. 3-1A is the diagram of an ordinary resistance voltage divider, where the voltage across  $R_2$  is

$$E_{R2} = \frac{R_2}{R_1 + R_2} \times E \text{ of the battery.} \quad (1)$$

Fig. 3-1B substitutes  $R_{line}$  (or  $Z_0$ ) for  $R_2$ , and substitutes  $R_g$  (generator resistance) for  $R_1$ . It is assumed the battery has zero internal resistance and that  $R_g$  is an inserted series generator resistance. If the battery is 1 volt and if  $R_g = R_{line}$ , then a voltmeter across  $R_{line}$  will indicate 0.5 volt when the switch is closed.

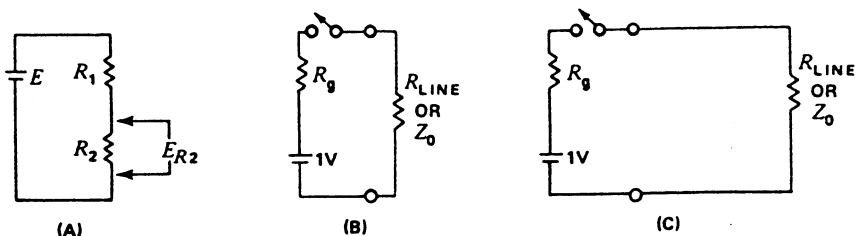


Fig. 3-1. Circuits showing DC analogy of TDR.

In Fig. 3-1C, a pair of zero resistance wires of the same physical length connect  $R_{line}$  to the battery and switch. A voltmeter across  $R_{line}$  will still indicate 0.5 volt when the switch is closed.

### ADDING THE TIME DIMENSION

Fig. 3-2 substitutes a step signal generator for the battery and switch of Fig. 3-1. The generator has zero source resistance, so  $R_g$  is again added in series with the generator. The generator and  $R_g$  drive a finite-length transmission line that has a characteristic impedance of  $Z_0$ . The transmission line has output terminals that permit connecting a load,  $R_L$ . An oscilloscope voltmeter measures the voltage signal(s) at the input end of the transmission line.

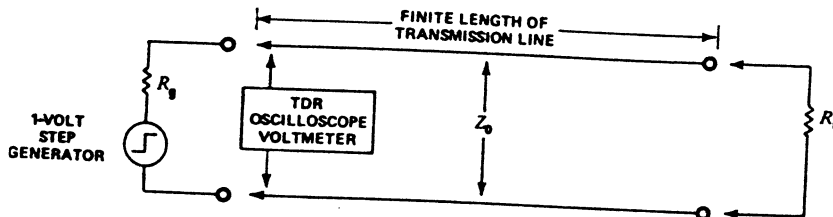


Fig. 3-2. Adding the time dimension to the circuit of Fig. 3-1.

Assume that no load resistance is connected to the transmission-line output terminals ( $R_L = \infty$ ) and that  $R_g = Z_0$  ( $Z_0$  acts exactly as the DC resistor  $R_{line}$  of Fig. 3-1). As the zero-impedance step generator applies its 1-volt step signal to  $R_g$ , the oscilloscope voltmeter indicates 0.5 volt. The oscilloscope voltmeter will continue to indicate a 0.5-volt signal until the wave travels down the line to the open end, doubles in amplitude due to no current into  $R_L = \infty$  and is reflected back to the generator end of the line. A 1-volt signal is finally indicated on the oscilloscope after the measurable time required for the step signal to travel down and back in the finite length of open-ended transmission line.

### REFLECTION-SIGNAL AMPLITUDES

Fig. 3-3 illustrates TDR oscilloscope (voltmeter) displays related to the value of  $R_L$  versus the value of the transmission-line  $Z_0$ . Apply resistance values of  $50 \Omega$  to  $R_g$  and  $Z_0$ , and  $75 \Omega$  to  $R_L$  of Fig. 3-2. By formula (1), the oscilloscope display of the reflected signal amplitude will be 0.6 volt. The actual reflection, however, is only +0.1 volt added to the 0.5-volt incident step.

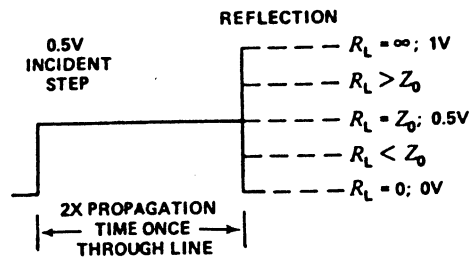


Fig. 3-3. Oscilloscope voltmeter displays for circuit of Fig. 3-2, dependent upon value of  $R_L$  versus  $Z_0$ .

### VOLTAGE REFLECTION COEFFICIENT

rho ( $\rho$ )

A somewhat more convenient method of handling signal reflections than has just been suggested is to consider the voltage reflection as having been added to or subtracted from the incident pulse. Thus, the reflected signal amplitude is not measured from zero volts, but is referenced to the incident signal amplitude. This permits establishing a ratio between the incident and reflected voltage signals which is called the voltage reflection coefficient, rho ( $\rho$ ). The value of  $\rho$  is simply the reflected pulse amplitude (the total display amplitude minus the incident pulse amplitude) divided by the incident pulse amplitude,

$$\rho = \frac{E_{\text{reflected}}}{E_{\text{incident}}} \quad (2)$$

Fig. 3-4 shows the two parts of a TDR display appropriately labeled to identify the incident and reflected voltage signals.

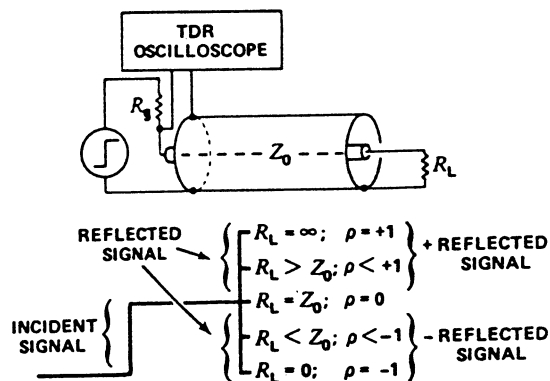


Fig. 3-4. TDR oscilloscope displays for various values of  $R_L$  versus  $Z_0$ .

When  $\rho = 0$ , the transmission line is terminated in a resistance equal to its characteristic impedance,  $Z_0$ . When  $\rho$  equals +1, the transmission-line load is an open circuit. When  $\rho$  is -1, the transmission line load is a short. If the line is terminated in  $R_L > Z_0$ ,  $\rho$  is positive. If the line is terminated in  $R_L < Z_0$ ,  $\rho$  is negative. The dependence of  $\rho$  on the transmission-line load is

$$\rho = \frac{R_L - Z_0}{R_L + Z_0} \quad (3)$$

If  $\rho$  is known,  $R_L$  can be found by rearranging formula (3);

$$R_L = Z_0 \frac{1 + \rho}{1 - \rho} \quad (4)$$

Formula (4) applies to any reflected voltage display that results from a purely resistive load. The load shown in Fig. 3-4 is assumed to be at the end of a lossless coaxial transmission line. (Reflected current signals are not considered in TDR.<sup>1</sup>)

determining  
resistive-  
load value

Substituting 50  $\Omega$  for  $Z_0$  in formula (4), calculations for small values of  $\rho$  show that each division of reflected signal is approximately equal to a certain number of ohms. Table 3-1 lists the ohms per division for vertical deflection factors of 0.005  $\rho$ , 0.01  $\rho$  and 0.02  $\rho$ . Or, for  $R_L$  values near 50  $\Omega$ , you may use the approximation formula

$$R_L \approx 50 + 100\rho.$$

This formula has a  $\leq 2.2\%$  error for absolute values of  $\rho \leq 0.1$  and a  $\leq 8\%$  error for absolute values of  $\rho \leq 0.2$ .

$R_L$  for reflections with  $\rho$  up to essentially +1 or -1 can be quickly determined using the graph of Fig. 3-5. Fig. 3-5 is based upon a 50- $\Omega$  transmission-line impedance just prior to the discontinuity that causes the reflection signal.

$\rho/\text{DIV}$	$\Omega/\text{DIV}$	ERROR/DIV
0.005	1/2	$\sim 0.016\Omega$
0.01	1	$\sim 0.066\Omega$
0.02	2	$\sim 0.2\Omega$

Table 3-1.  $R_L$  approximations for reflection coefficients of 0.005, 0.01 and 0.02 related to a 50- $\Omega$  transmission line.

<sup>1</sup>Richard E. Matick, *Transmission Lines for Digital and Communication Networks* (New York: McGraw-Hill, 1969) pp. 44-45.

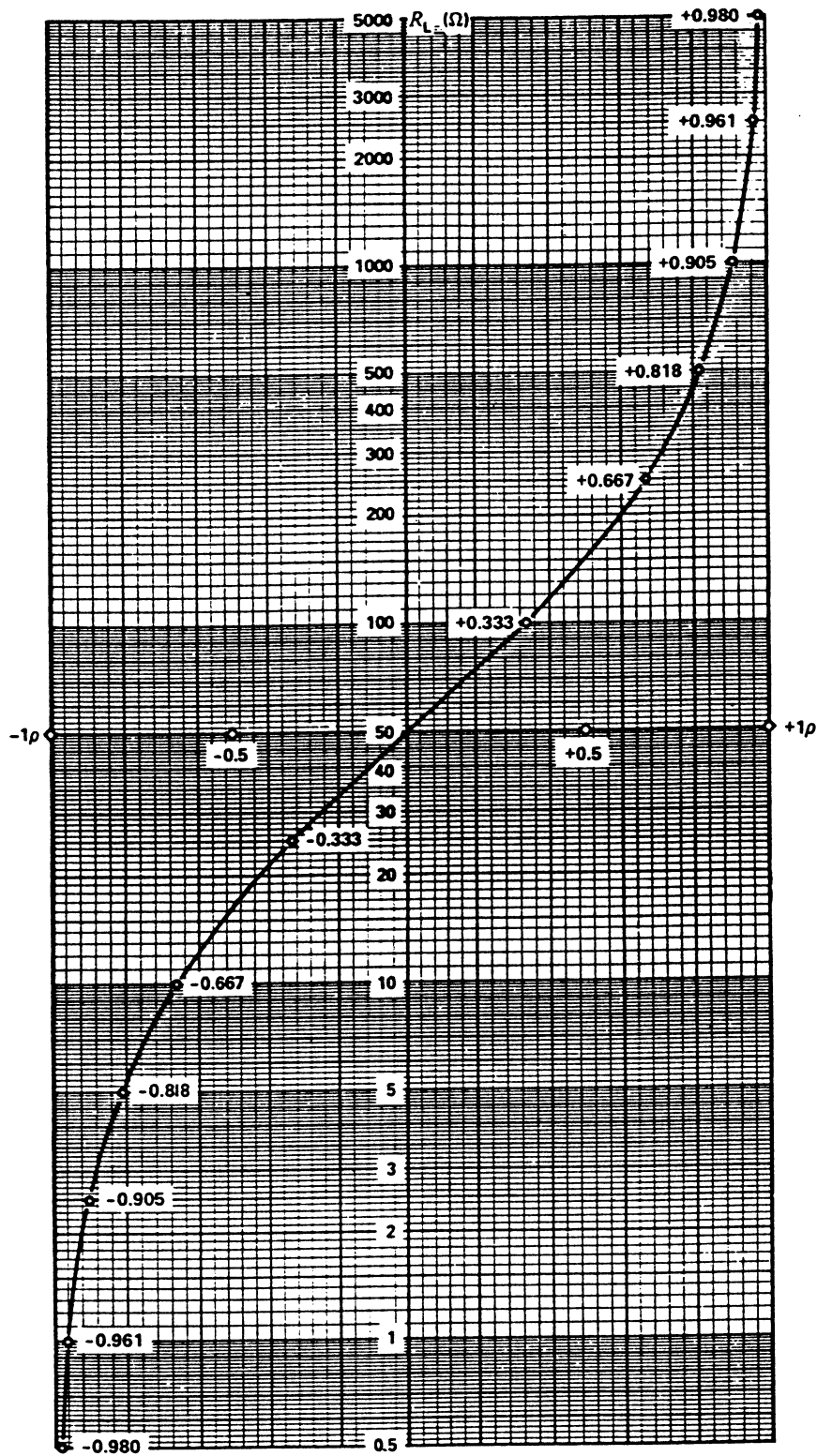


Fig. 3-5. Values of  $R_L$  versus reflection coefficient when reflection is compared to 50- $\Omega$  transmission line.

## REFLECTIONS FROM RESISTIVE DISCONTINUITIES

Two types of reflections occur from two types of resistive discontinuities. They are a step reflection and a continuously changing reflection. A resistance in series with a transmission line causes a positive reflection. A resistance in parallel with a transmission line causes a negative reflection. Discrete single resistors cause a step reflection, while distributed resistance causes a continuously changing reflection. The discrete resistor reflections are shown in ideal form in Fig. 3-6, and the distributed resistance reflections are shown in ideal form in Fig. 3-7.

Fig. 3-7 has been exaggerated by showing the distributed resistance beginning at a particular point in the line. Normally, such series or shunt distributed resistance will be found in the total length of any coaxial line tested.

discrete  
distributed

All four forms of resistance are an indication of signal losses between the input and output ends of the transmission line. The single-resistor discontinuities can occur from discrete components or may indicate a loose connector with added series resistance. Such discontinuities can be physically located by TDR. Distributed losses are usually part of the particular line being tested and the TDR display can be of value for quantitative analysis of resistance per unit of line length.

No reflection should occur from a properly fabricated matched attenuator. Therefore, a TDR unit will not indicate losses when matched attenuators are used.

## DISTRIBUTED RESISTANCE EXAMPLES

The examples of distributed-resistance reflections that follow deal with the normal characteristics of transmission lines. Both small-diameter lossy cables and moderate-diameter quality cables are discussed.

small,  
lossy  
cables

returned  
signal  
attenuation

A small-diameter 50- $\Omega$  transmission line (such as 1/8-inch-diameter cable) will have sufficient DC resistance to mask "skin-effect" losses. The DC resistance in its center conductor will cause a nearly exponential changing reflection. See Fig. 3-8A. As the incident signal propagates down the line away from the TDR unit, the small series resistance causes small reflections to return to the TDR unit. If you mentally divide the line into small increments of series resistance, each increment causing a small signal reflection, you can then understand the continuous return of energy to the input end of the line. Each reflected energy increment is additionally attenuated on its way back to the TDR unit. This return attenuation is the factor that prevents the display from being a linear ramp and converts it into a nearly exponential reflection. (Note the curve of the reflection between the incident signal plus step and the termination of Fig. 3-8A.)



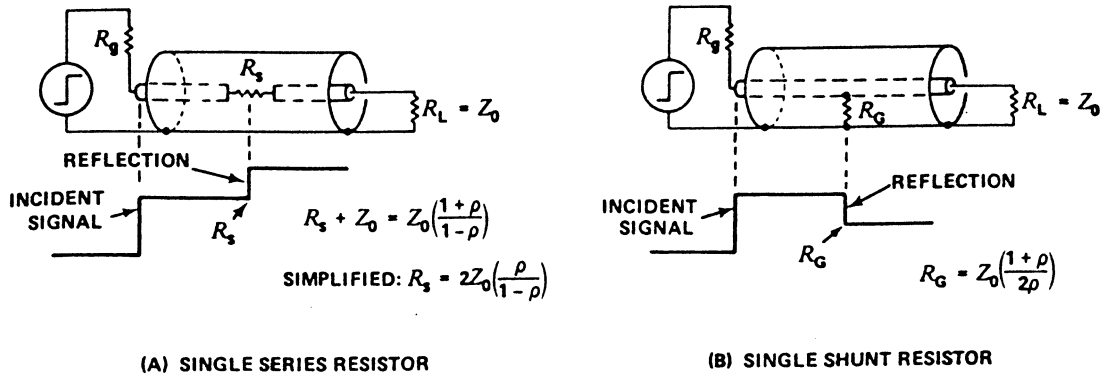


Fig. 3-6. Single-resistor discontinuities and their reflections.

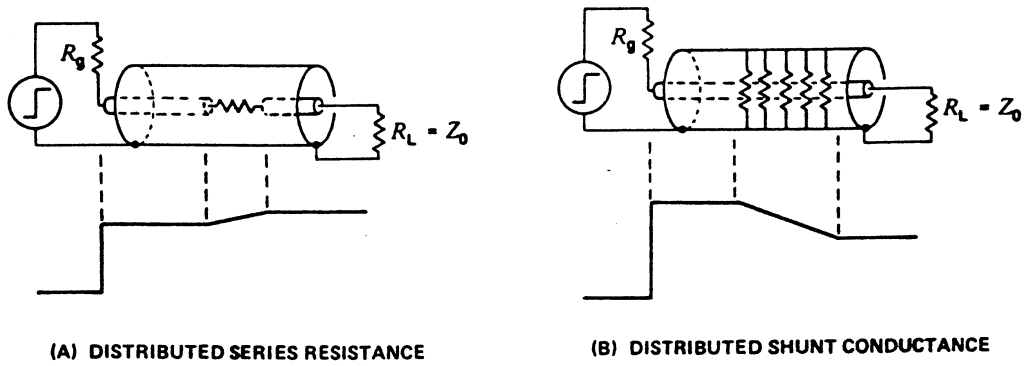


Fig. 3-7. Distributed-resistance discontinuities and their reflections.

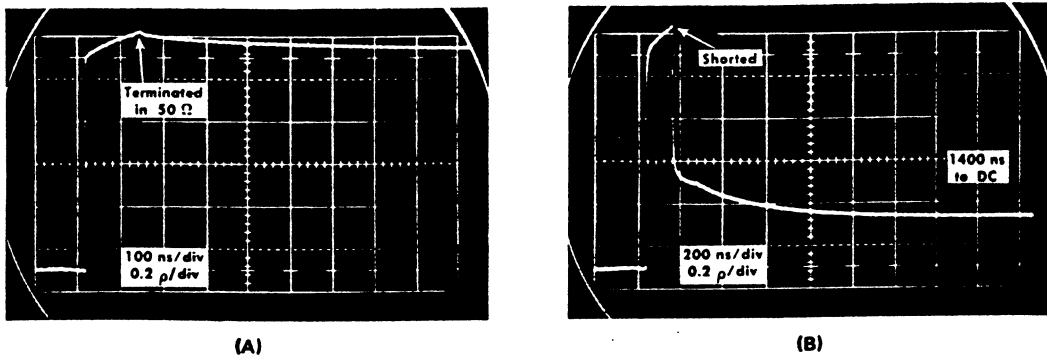


Fig. 3-8. Waveforms of 1/8-inch-diameter lossy 50-Ω cable.

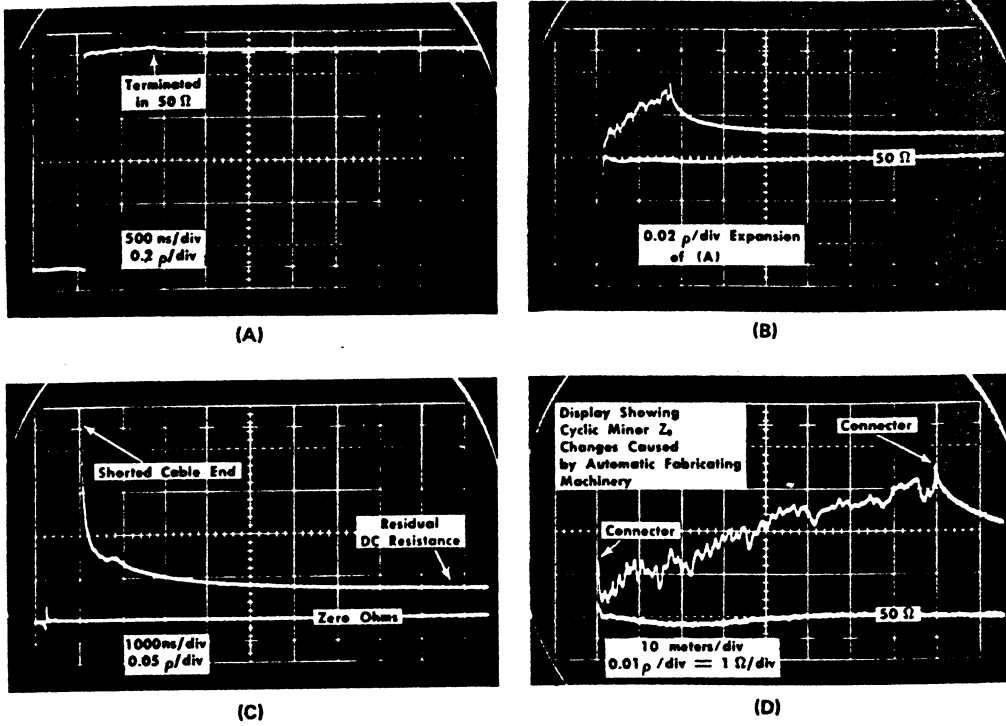


Fig. 3-9. Quality RG213/U-cable resistance and  $\Delta Z_0$  characteristics. (Cable tested was 260 feet long.)

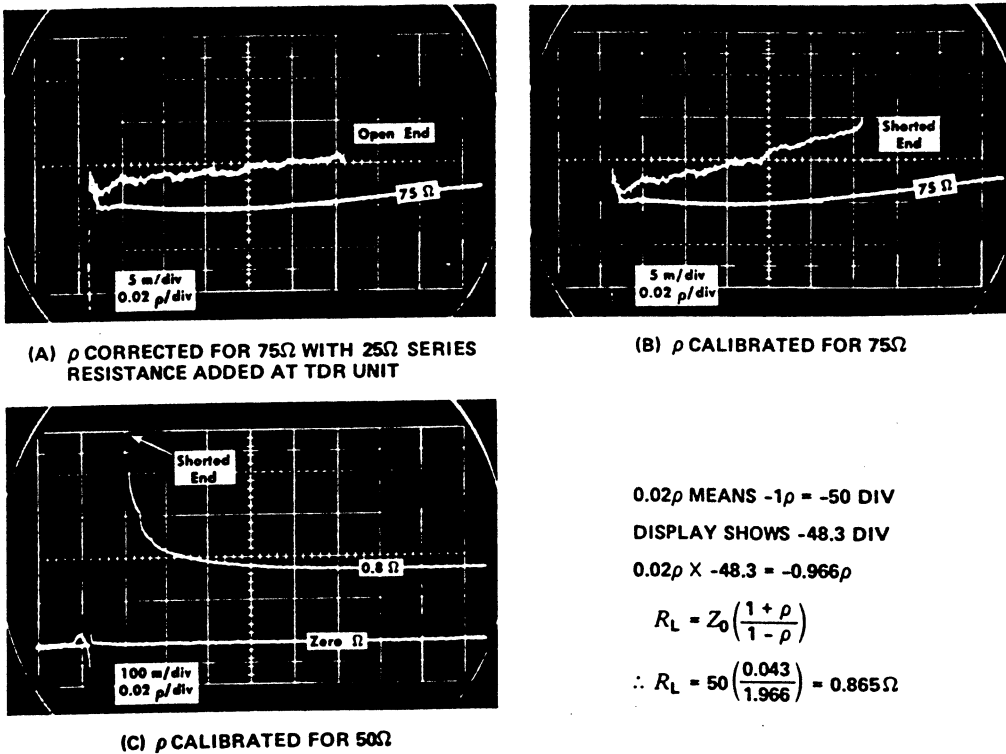


Fig. 3-10. Quality RG11/U-cable resistance and  $\Delta Z_0$  characteristics. (Cable tested was 100 feet long.)

input  
impedance  
changes  
with time

Another way of expressing the effect of the nearly exponential reflection is to say that the transmission-line input impedance changes with time. Fig. 3-8A shows the line characteristic impedance to be essentially  $50\ \Omega$  at the beginning of the exponential reflection and to be approximately  $64\ \Omega$  after  $130\ \text{ns}$  ( $+0.12\ \rho = 64\ \Omega$ ).

The long, nearly exponential, decay after the termination of Fig. 3-8A is related to high-frequency losses. The negative reflection occurs at the termination because the  $50\text{-}\Omega$  termination was driven by approximately  $64\ \Omega$ .

If the small-diameter cable is shorted at its output end instead of terminated, the TDR display will appear similar to Fig. 3-8B. A lossless line would have a full  $-1\ \rho$  after the short, but the small lossy cable not only has attenuation of the signal to the short but attenuation of the reflected signal back to the TDR unit. Again, the long, nearly exponential, curve after the short is caused by the cable distorting the reflected step signal.

measuring  
cable DC  
resistance

Fig. 3-8B also allows measurement of the total cable DC resistance between the TDR unit and a short circuit. The vertical distance between the incident-pulse peak level and the flat right-end portion of the reflected signal is due strictly to the cable DC resistance. In this case  $-3.8$  divisions =  $-0.76\ \rho$ , which is equal to  $6.5\ \Omega$  (from curve of Fig. 3-5). (A bench multimeter-type ohmmeter indicated  $6.8$  ohms for the same cable.)

quality  
cables

A quality cable, such as RG8A/U ( $52\ \Omega$ ), RG213/U ( $50\ \Omega$ ) or RG11/U ( $75\ \Omega$ ), will exhibit similar characteristics to the small lossy cable just described, but the cable must be much longer to obtain a similar display of series resistance. Fig. 3-9A and B show the same rising type of waveform caused by center-conductor series resistance in RG213/U. Fig. 3-9C shows the residual DC resistance of the line when shorted. Fig. 3-9D is a time and voltage expansion of the (A) and (B) waveforms showing a possible use for TDR in troubleshooting cable-fabricating equipment.

measuring  
series  
resistance

Fig. 3-10 shows the same series-resistance characteristics for RG11/U cable. However, instead of terminating the cable end, the series resistance was measured first with the end open and then with the end shorted. Note the difference in waveform slope (apparent change in resistance) after the signal has traveled halfway through the line. The change in slope is due to distortion of the originally flat incident pulse by traveling through the cable once. As the nonflat signal reaches the cable end, its reflection back through the cable is altered a second time. The net result is an obvious distortion to the true resistive slope of the reflected "bits" of the distributed series resistance during the second half of the reflection. This example is given to show the desirability of properly terminating any line section in which you wish to measure total distributed series resistance. (Conditions leading to this changing slope phenomenon are described by H. H. Skilling on page 397 of his text *Electronic Transmission Lines*, McGraw-Hill, 1951.) Each of the three waveform pictures of Fig. 3-10 is a double exposure with the lower waveform showing the TDR-system no-cable response to a termination resistance in (A) and (B) and a short circuit in (C).

## $\rho$ CORRECTION FOR MISMATCHED-IMPEDANCE TDR

Mismatched-impedance TDR is defined as driving (and observing reflections from) a coaxial cable with a  $Z_0$  different from the TDR-unit source impedance.

direct  
connection

inserting  
matching  
resistors

Fig. 3-10 shows a display from a 75- $\Omega$  cable attached directly to a 50- $\Omega$  TDR unit with corrected voltage reflection coefficient. Two connection methods are available when the cable being tested has a characteristic impedance that does not match the TDR-unit output impedance. One is to connect the cable directly to the TDR unit, the other is to insert minimum-loss matching resistors at the mismatched connection. In the case shown in Fig. 3-10, a 25- $\Omega$  resistor was inserted in series with the 75- $\Omega$  cable so that signals reflected from the 75- $\Omega$  line were not re-reflected back into the line by a 75- $\Omega$  to 50- $\Omega$  mismatch at the pulse generator. The load driven by the TDR unit then was  $75 + 25 = 100 \Omega$ , creating a significant driving mismatch for the TDR unit. The Tektronix Type 1S2 used has the sampling-oscilloscope input located very close to the junction between the 50- $\Omega$  source and the 100- $\Omega$  load. This connection causes a small reflection at the instant the signal enters the 75- $\Omega$  line, but permits reflected signals to be displayed without connector distortion.

adjusting  
vertical-  
deflection  
factor

$\rho$  correction is most easily accomplished by changing the sampling-oscilloscope vertical-deflection factor. In Fig. 3-10, the VARIABLE units/div control was adjusted (clockwise) until a +1  $\rho$  reflection from a 3-foot length of open-end 75- $\Omega$  cable spanned 5 vertical divisions when the VERTICAL UNITS/DIV switch was at 0.2  $\rho$ /div. This caused the incident pulse to be considerably greater than seen with a matched system, but the incident pulse is never evaluated; only reflected signals have meaning.

Leaving the VARIABLE control at its new position then places the numbers around the VERTICAL UNITS/DIV switch back into calibration for all positions of the switch.

testing  
length

Usually, if a mismatched line is to be tested for length only, it is not necessary to make resistive or deflection-factor corrections.  $\rho$  calibration is not important; only the propagation velocity or DISTANCE calibration is important.

#### $\rho$ CORRECTION FOR A SECOND DISCONTINUITY IN A MATCHED-IMPEDANCE TDR SYSTEM

A matched-impedance TDR system is one in which both the generator and the load match the transmission-line  $Z_0$  at their connection points.

Multiple discontinuities in a transmission line always cause energy due to reflection to travel in both directions.

second  
discontinuity

The goal of this discussion is to point out that a matched-impedance TDR system gives a second-discontinuity reflection coefficient that deviates from the reflection value that will result from a single discontinuity of the same magnitude  $Z_0$  change. The examples chosen to support this are illustrated in Fig. 3-11, Fig. 3-12 and Fig. 3-13. Calculations are included for two different approaches. The first approach describes conditions where three impedances are known (Fig. 3-12A). The second approach is with only the generator impedance known and a method is given for calculating the resistive value of the second discontinuity (Fig. 3-12B).

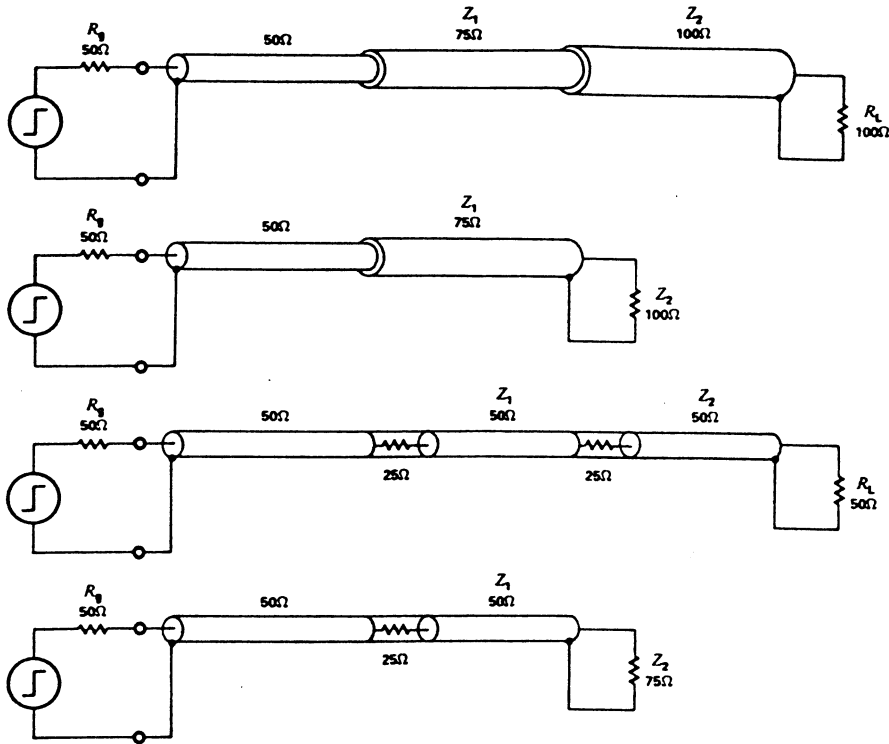


Fig. 3-11. Four mismatch conditions that lead to identical reflection coefficients similar to Fig. 3-12A.

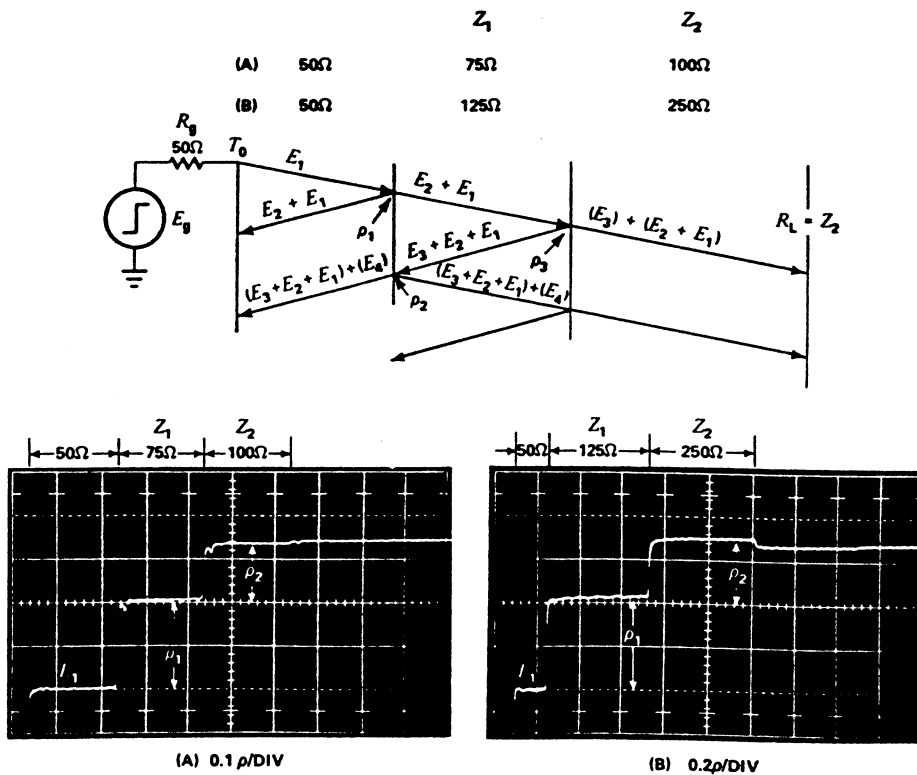


Fig. 3-12. Two examples of second-discontinuity reflections. Error of second reflection caused by first discontinuity.

## FIRST EXAMPLE — 50-Ω TO 75-Ω TO 100-Ω

Fig. 3-12 includes a signal flow chart<sup>2</sup> that helps keep track of the energy as it moves through the transmission line. It is important to remember that once energy is within a coaxial line it travels with the voltage and current magnitudes calculable by Ohm's law. The CRT display in Fig. 3-12A shows an amplitude at the 100-Ω level that is 1.12% greater than if there was no intermediate 75-Ω discontinuity. If two successive resistive discontinuities are of the type shown in Fig. 3-11, the second discontinuity will always produce a reflection amplitude that is greater than that produced by a single discontinuity of the same value.

Calculations here apply to Fig. 3-12A, the 50-Ω to 75-Ω to 100-Ω example.

Since the 50-Ω line  $Z_0$  equals  $R_g$ , then the incident signal  $E_1$  sent into 50 Ω is:

$$E_1 = \left( \frac{50}{50 + 50} \right) E_g = \frac{50}{100} E_g = 0.5E_g.$$

The reflection coefficient  $\rho_1$  at the 50-Ω to 75-Ω discontinuity is:

$$\rho_1 = \frac{Z_1 - 50}{Z_1 + 50} = \frac{75 - 50}{75 + 50} = \frac{25}{125} = 0.20.$$

The voltage  $E_2$  is defined as the reflected voltage only, not including the incident voltage, but the TDR-unit CRT display shows  $E_2$  added to  $E_1$ . Therefore, the total amplitude of the TDR-unit CRT display is  $E_2 + E_1$ :

$$E_2 = (\rho_1)(E_1).$$

$$(\rho_1)(E_1) + E_1 = (0.2)(0.5E_g) + 0.5E_g = 0.6E_g.$$

<sup>2</sup>Millman and Taub, *Pulse, Digital and Switching Waveforms* (McGraw-Hill, 1965), p. 98.

It is important to note that  $0.6 E_g$  is the total voltage propagating away from the  $50\text{-}\Omega$  to  $75\text{-}\Omega$  junction in both directions. The signal heading toward the  $100\text{-}\Omega$  discontinuity is now an incident signal (with  $0.6E_g$  amplitude) within a  $75\text{-}\Omega$  transmission line. The reflected signal is an incident signal (with  $0.1E_g$  amplitude) within a  $50\text{-}\Omega$  transmission line.

The reflection coefficient  $\rho_3$  at the  $75\text{-}\Omega$  to  $100\text{-}\Omega$  discontinuity is:

$$\rho_3 = \frac{Z_2 - Z_1}{Z_2 + Z_1} = \frac{100 - 75}{100 + 75} = \frac{25}{175} = 0.1429.$$

The voltage  $E_3$  is defined as the reflected voltage only, not including the  $0.6E_g$  incident voltage, but the signal propagated toward the  $100\text{-}\Omega$  load has an amplitude of  $0.6E_g + E_3$ . Since  $E_3$  is:

$$E_3 = (\rho_3)(E_2 + E_1) = (0.1429)(0.6E_g) = 0.08574E_g \cong 0.086E_g,$$

then the signal heading toward the  $100\text{-}\Omega$  termination is:

$$0.6E_g + 0.086E_g = 0.686E_g.$$

$E_3$  heading toward the  $75\text{-}\Omega$  to  $50\text{-}\Omega$  discontinuity is an incident signal within a  $75\text{-}\Omega$  transmission line.  $E_3$  amplitude will be reduced at the time it encounters the  $50\text{-}\Omega$  line impedance. The new signal traveling toward the generator within the  $50\text{-}\Omega$  line is known as  $E_4$  and is found by multiplying  $\rho_2$  and  $E_3$ . The CRT display voltage is found by adding that product to the sum of  $E_2 + E_1$ .

$$\rho_2 = \frac{50 - Z_1}{50 + Z_1} = \frac{50 - 75}{50 + 75} = \frac{-25}{125} = -0.20,$$

$$E_4 = (\rho_2)(E_3) = (-0.20)(0.086E_g) = -0.0172E_g.$$

Therefore, the CRT display, due to the  $100\text{-}\Omega$  transmission line, is:

$$(E_3 + E_2 + E_1) + (E_4) = 0.686E_g - 0.017E_g = 0.669E_g = +0.335\rho$$



That amplitude can be compared to the amplitude that would occur from a single 50- $\Omega$  to 100- $\Omega$  discontinuity. Under these conditions, the actual reflection coefficient is:

$$\rho = \frac{Z_2 - 50}{Z_2 + 50} = \frac{100 - 50}{100 + 50} = \frac{50}{150} = 0.333.$$

The amplitude of the 50- $\Omega$  to 100- $\Omega$  TDR-unit CRT display will then be:

$$(\rho)(0.5E_g) + 0.5E_g = (0.333)(0.5E_g) + 0.5E_g = 0.666E_g.$$

% error

Since the sum of  $\rho_1$  and  $\rho_2$  (in Fig. 3-12A) is +0.335 and  $\rho$  of the 50- $\Omega$  to 100- $\Omega$  discontinuity is +0.333, the two resistive discontinuities in series create a total display error for the 100- $\Omega$   $Z_2$  of +0.6%. Larger mismatches from 50- $\Omega$  to  $Z_1$  and from  $Z_1$  to  $Z_2$  will produce a greater + $\rho$  error for the reflection coefficient display of  $Z_1 + Z_2$ . Fig. 3-12B shows an example of a + $\rho$  error of 5.02% for  $Z_2$ .

All the above calculations assume a lossless transmission line. Normal series DC resistance is removed from the  $\rho$  reading by extending the reference 50- $\Omega$  or  $Z_1$  slope to a point directly under the reflection point of measurement. This technique is used in obtaining  $\rho$  from Fig. 3-13 and is described below.

#### SECOND EXAMPLE — A FORMULA FOR CALCULATING $Z_0$ OF A SECOND (RESISTIVE) REFLECTION IN A 50- $\Omega$ MATCHED TDR SYSTEM

The laborious procedure just used to determine the percent error produced by reading a second reflection  $\rho$  between 50  $\Omega$  and  $Z_2$  of a *known* system is of no value when measuring  $Z_2$  of an *unknown* system. It is easy to calculate the resistive value that causes the first mismatch reflection of a double reflection display. However, a special formula is needed to calculate the resistive value that causes the second mismatch reflection. The following formula makes use of the first reflection resistive value, as calculated from a TDR-unit display, in calculating the resistive value of  $Z_2$ .

Fig. 3-12B is used here with the reflection between  $50 \Omega$  and  $Z_1$  shown in Fig. 3-13A and the reflection between  $Z_1$  and  $Z_2$  shown in Fig. 3-13B.  $\rho_1$  and  $\rho_2$  of Fig. 3-12B are the same in Fig. 3-13 except the vertical deflection factor is changed in both Fig. 3-13 displays.

$\rho_1$  allows  $Z_1$  resistance value to be calculated relative to  $50 \Omega$ . However,  $\rho_2$  is the "observed" reflection from  $Z_2$  relative to  $Z_1$  and contains an error because of energy reflections not displayed. When the incident step into the first section of known  $50\text{-}\Omega$  line is normalized to unity,  $Z_2$  can be calculated using the following formula:

$$Z_2 = (Z_1) \frac{200Z_1 + \rho_2(Z_1 + 50)^2}{200Z_1 - \rho_2(Z_1 + 50)^2} \quad (5)$$

(Formula derivation given in Appendix A.)

Before measuring the reflection coefficient of  $Z_1$ , the display must be treated to ignore both dribble-up and DC resistance. This is accomplished by extending the DC slope of the  $50\text{-}\Omega$  reference line to be directly under a point in the  $Z_1$  display after the completion of dribble-up. See the scribed line in Fig. 3-13A between the end of the  $50\text{-}\Omega$  display and the graticule centerline. The same technique is used between  $Z_1$  and  $Z_2$  when measuring  $\rho_2$  (Fig. 3-13B).

From Fig. 3-13A,  $\rho_1$  reads +0.435. Calculating for  $Z_1$ :

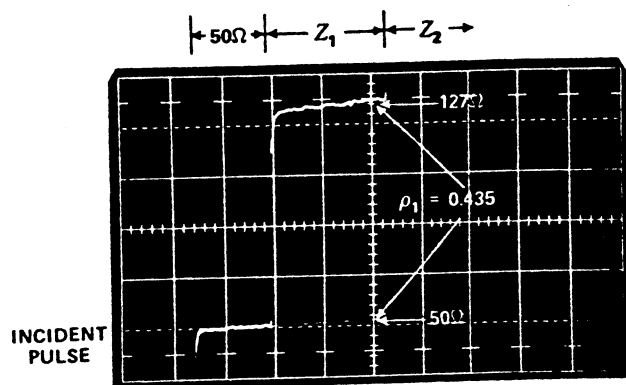
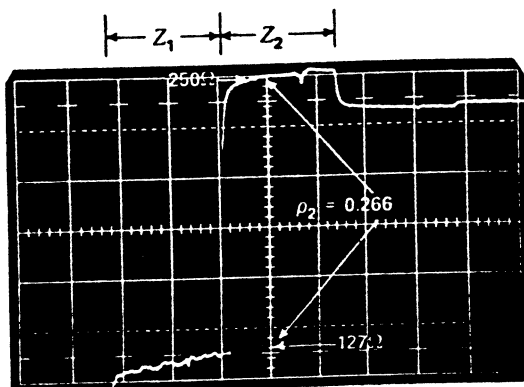
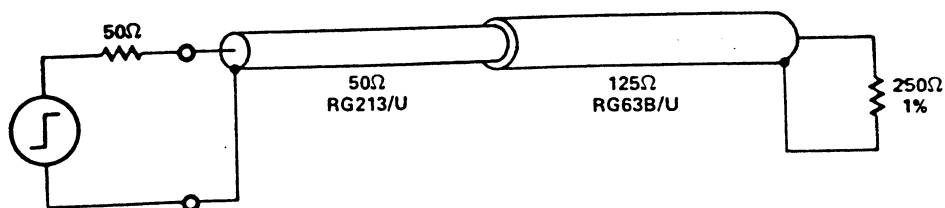
$$Z_1 = 50 \left( \frac{1 + \rho_1}{1 - \rho_1} \right) = 50 \frac{1.435}{0.565} = 127 \Omega.$$

The CRT display is altered in position and deflection factor so  $Z_1$ -to- $Z_2$  reflection can be measured with the greatest accuracy.

From Fig. 3-13B,  $\rho_2$  reads +0.266. Using formula (5) to calculate the  $Z_0$  value of  $Z_2$ :

$$\begin{aligned} Z_2 &= 127 \frac{(200)(127) + (0.266)(127 + 50)^2}{(200)(127) - (0.266)(127 + 50)^2} \\ &= 127 \frac{25,400 + (0.266)(31,350)}{25,400 - (0.266)(31,350)} = 127 \frac{33,740}{17,060} = 251 \Omega. \end{aligned}$$

$251 \Omega$  checks very well with the 1%  $250\text{-}\Omega$  resistor used as the  $Z_2$  termination when taking the photographs of Fig. 3-13.

(A)  $50\Omega - 125\Omega$  EXPANDED DISPLAY,  $0.1 \rho/\text{DIV}$ (B)  $125\Omega - 250\Omega$  EXPANDED DISPLAY,  $0.05 \rho/\text{DIV}$ 

(C) CIRCUIT THAT PRODUCED DISPLAYS (A) AND (B)

Fig. 3-13. Second-reflection measurement using expanded displays of system shown in Fig. 3-12B.



## 4

## TIME AND AMPLITUDE RESOLUTION RELATED TO THE FORM OF TDR SYSTEM HOOKUP

Resolution in TDR is basically the ability of a system to identify very small discontinuities (reflection visible in the CRT displayed noise) or identify two closely spaced discontinuities as having separate reflections (two "bumps" instead of one). We thus define both amplitude resolution and time resolution in this chapter. It is desirable that a TDR system have both good amplitude and good time resolution.

### AMPLITUDE RESOLUTION

Amplitude resolution refers to the ability of a TDR system to display a reflection signal from a discontinuity that produces a very small reflection coefficient. Very small impedance discontinuities along the length of a transmission line can be displayed by a system having good amplitude resolution. A discontinuity causing a reflection signal that is smaller than the system displayed noise is difficult to observe. Displayed noise is therefore a good reference to use in comparing the amplitude resolution of various TDR systems.

*The amplitude resolution of a TDR system may be defined as: That reflection coefficient which is equivalent to the displayed noise amplitude.*

### TIME RESOLUTION

Time resolution, on the other hand, refers to the ability of a TDR system to distinguish between two point discontinuities that are located very close together.

*The time resolution of a TDR system may be defined as: The minimum time spacing of two equal point discontinuities which give rise to a 50% valley between the two displayed reflections. The pulse signal risetime and high-frequency losses of a TDR system affect its time resolution.*

## FACTORS THAT LIMIT RESOLUTION

system  
noise  
and  
risetime

For a distributed discontinuity — like a section of 49- $\Omega$  transmission line in a 50- $\Omega$  TDR system — the *amplitude resolution* is usually limited by system noise. For a point discontinuity — or one which is distributed over a short distance relative to the equivalent length of the system risetime — the amplitude resolution is usually limited by both system noise and risetime. Unwanted reflections or signal aberrations which happen to fall on top of the desired reflection can also limit amplitude resolution. It is usually possible to shift these disturbances out of the time region of interest by adding a judiciously chosen length of delay cable in the right place.

*Time resolution* is primarily limited by system risetime. It must be emphasized that the transmission system or device under test should be considered as part of the overall TDR system and as such may introduce a significant limitation on time resolution. Thus, it may be possible to resolve two closely spaced discontinuities 10 feet down a coaxial line while the same two discontinuities may appear smeared together at 50 feet.

From the foregoing discussion it would appear that one should select the TDR system having the fastest risetime and the least noise. Unfortunately, it is not that easy — partly because these are, to some extent, mutually exclusive characteristics and partly because the configuration of the TDR system plays a major role in determining the actual noise and risetime.

## FOUR SYSTEMS

Four major TDR system configurations are shown in block diagram form in Fig. 4-1. Because of practical instrument considerations, the systems vary widely in their advantages and limitations. It should also be said that the configuration which gives the best amplitude resolution will probably not give the best time resolution. Fig. 4-2 compares resolution and configuration for five instrument combinations of Tektronix instruments.

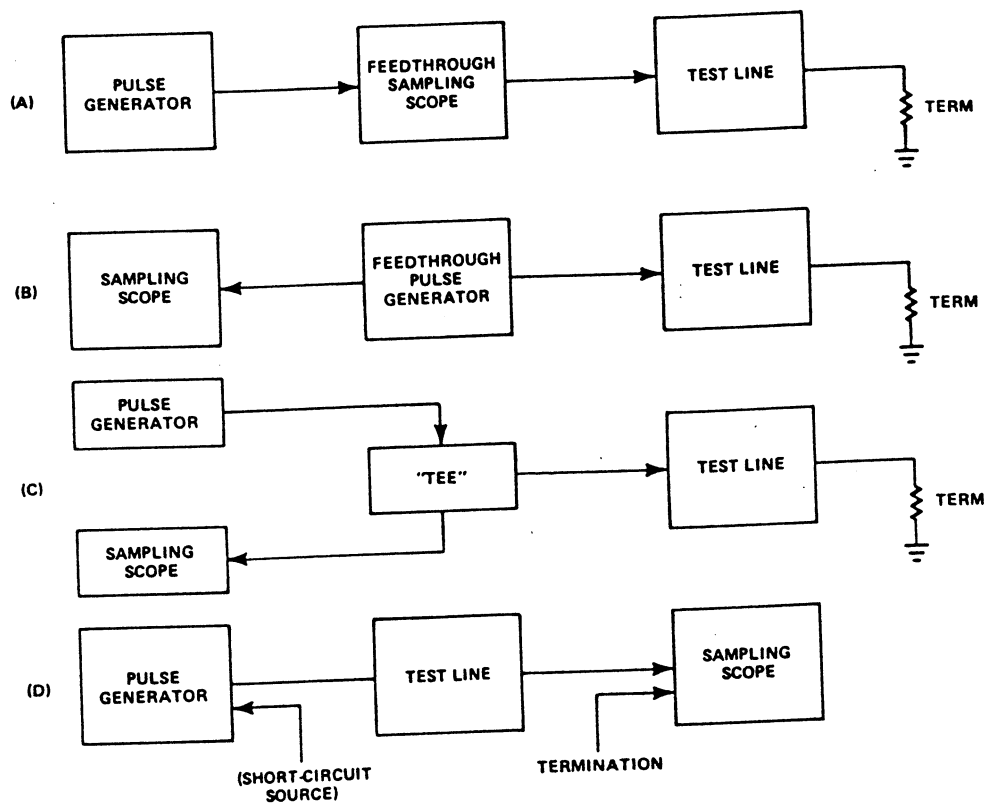


Fig. 4-1. TDR-system configurations.

EXAMPLE	TYPE OF CONFIGURATION	INSTRUMENT TYPES (TEKTRONIX)	PULSE AMPLITUDE	SYSTEM RISETIME <sup>1</sup>	MAX AMPLITUDE RESOLUTION <sup>2</sup>	MAX TIME RESOLUTION
1	A (FEEDTHROUGH SAMPLER)	TYPE 1S2 REFLECTOMETER	1.0V	1.1ns	$\rho = 0.0004$	670ps
			250mV	150ps	$\rho = 0.001$	85ps
2	B (FEEDTHROUGH PULSER)	TYPE 281 TDR PULSER TYPE 3S1 SAMPLING UNIT	460mV	1.0ns	$\rho = 0.001$	600ps
3	C ("TEE")	TYPE S-50 PULSER TYPE S-4 SAMPLING HEAD	400mV	40ps	$\rho = 0.01$	35ps
4	C ("TEE")	TYPE 111 PULSE GENERATOR TYPE S-1 SAMPLING HEAD	5V (ATTENUATED TO 1.0V)	610ps	$\rho = 0.001$	400ps
5 <sup>3</sup>	D (IN-LINE)	TYPE S-50 PULSER TYPE S-4 SAMPLING HEAD	400mV	40ps	$\rho = 0.004$	35ps

<sup>1</sup>INCLUDES EFFECTS OF PULSE-SOURCE, SAMPLER AND CONFIGURATION  
<sup>2</sup>TYPICAL PERFORMANCE FIGURES  
<sup>3</sup>EXAMPLE DEMONSTRATED

Fig. 4-2. Typical TDR resolution.

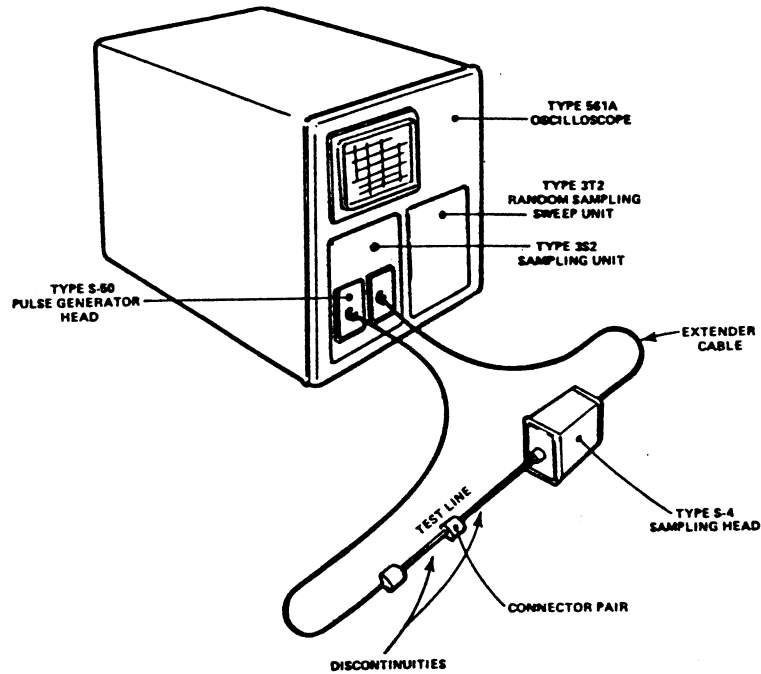


Fig. 4-3. Application example 5 – demonstration setup.

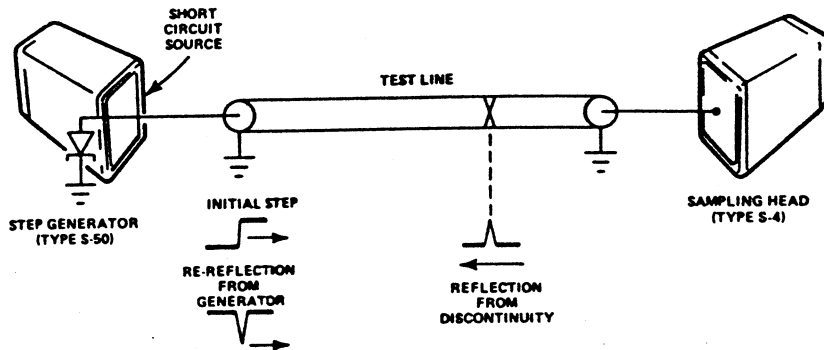


Fig. 4-4. In-line TDR configuration.

Example 5 from Fig. 4-2 is illustrated in Figs. 4-3 and 4-4. The in-line configuration is particularly well suited for studying discontinuities in relatively short, high-quality transmission systems.

A tunnel diode supplies the exciting pulse directly into the test line. The pulse propagates down the test line until it encounters a discontinuity, whereupon energy is reflected back toward the generator. The short-circuit ( $3\text{-}\Omega$ ) source impedance of the generator then re-reflects this energy back through the test line and into the sampler for observation. Since reverse termination in the pulse generator is not required — indeed, not allowed — the full amplitude of the tunnel-diode step signal is available to drive the test line for the best signal-to-noise advantage. The example uses a short, high-quality test line so risetime losses are held to a minimum.



Fig. 4-5 shows the amplitude resolution of the system. The observed reflection coefficient of 0.004 corresponds to a shunt capacitance of 0.008 picofarad. A similar reflection coefficient of the opposite polarity would indicate a series inductance of 20 picohenries.

state-of-the-art  
time  
resolution

Fig. 4-6 shows the time resolution of the system. The two discontinuities indicated are separated by 7.4 millimeters of solid TFE transmission line. This corresponds to a time separation of 35 picoseconds in the test line which, due to the required round-trip propagation, becomes a 70-picosecond indication in the TDR display.

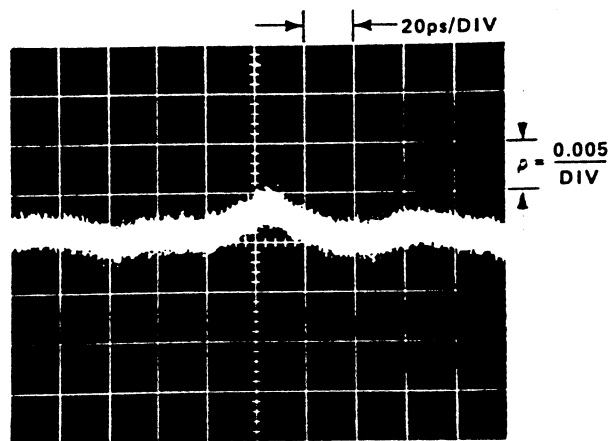


Fig. 4-5. Maximum amplitude resolution.

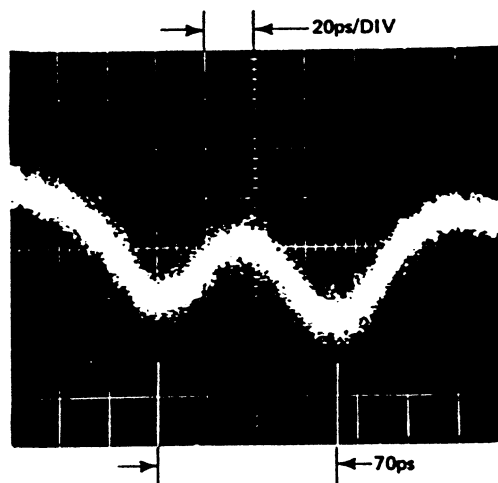


Fig. 4-6. Maximum time resolution.

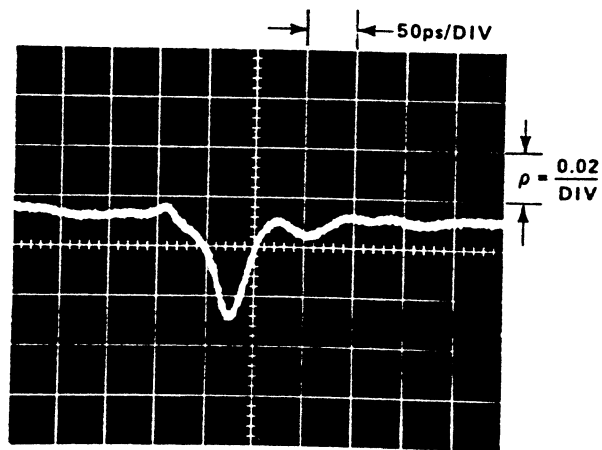


Fig. 4-7. Reflection from connector pair.

Fig. 4-7 shows a typical reflection from a mated pair of 3-mm connectors from one manufacturer. Obviously, quite a bit of improvement to the connectors is possible before the TDR resolution limits are reached!

#### CALIBRATING THE DISPLAY IN RHO/DIVISION

Fig. 4-8 shows the Tektronix Type S-4 Sampling Head and the Type S-50 Pulse Generator Head in three high-resolution TDR interconnections. Each system requires special adjustment for calibrating the CRT display so reflection coefficients can be read directly.

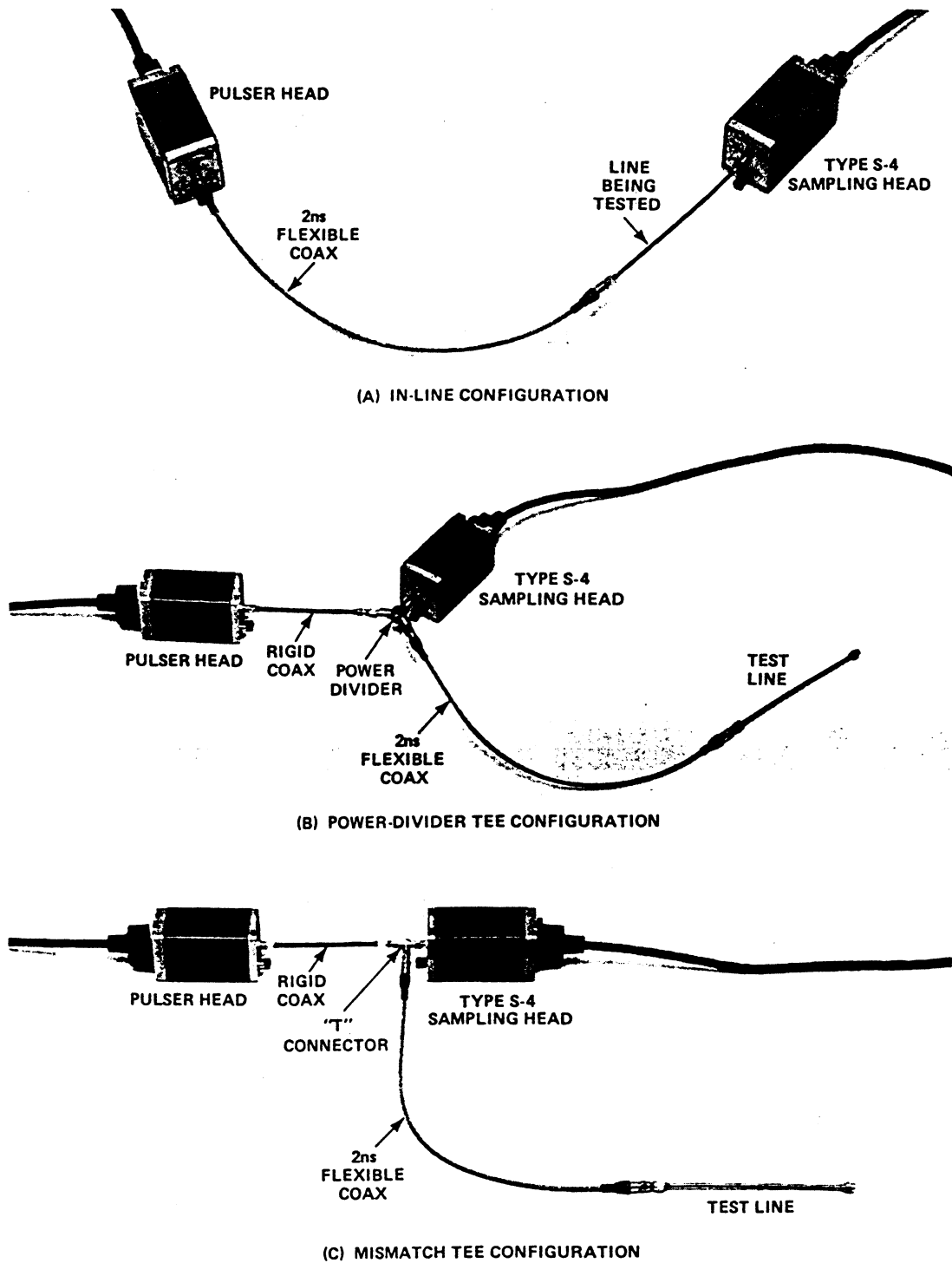


Fig. 4-8. Three examples of high-resolution TDR connections. Both heads are operating on extender cables, outside the parent sampling unit (vertical-channel plug-in unit).

### “IN-LINE” CONFIGURATION

reference  
signal

The “in-line” configuration shown in Fig. 4-8A is described first. A typical display using this setup is shown in both simple and expanded forms in Fig. 4-9. *When using the “in-line” connections, the fast-rise portion of the pulse-generator output signal is used as the reference for calibrating the display deflection factor in  $\rho/\text{div}$ .* (The calibration does not apply for any portion of the display that is horizontally flat when high-resolution — less than  $\pm 1 \rho$  reflection coefficient — TDR is the objective.)

The fast-rise step displayed in Fig. 4-9A is about three major divisions from the left graticule edge. The fast transition is defined as having a signal amplitude of  $\pm 1 \rho$ , covering about 2.5 major vertical divisions in this case. Therefore, Fig. 4-9A has a high-resolution TDR deflection factor of approximately  $0.4 \rho/\text{div}$  ( $\rho/2.5 \text{ div} = 0.4 \rho/\text{div}$ ).

Since a deflection factor of  $0.4 \rho/\text{div}$  is difficult to work with, the display amplitude can be adjusted to a more convenient value by using the sampling-unit VARIABLE control. Make the adjustment so the incident transition spans 1, 2 or 5 major divisions. In Fig. 4-9B, the sampling-unit VARIABLE control was adjusted for a reference signal amplitude of 2 divisions. That display has a calibrated high-resolution deflection factor of  $0.5 \rho/\text{div}$ .

The portion of Fig. 4-9B outlined by the second bracket is time-expanded twice in Fig. 4-9C and D. Fig. 4-9B includes the entire length of the test line as well as the sampling-head input. The final display (Fig. 4-9D) includes an increase in vertical gain and shows less than the whole test line in the time window. The vertical gain change was made by changing the sampling-unit VERTICAL UNITS/DIV switch from 200 mV/div to 5 mV/div, for a deflection factor of  $0.0125 \rho/\text{div}$ . The VARIABLE control was left as set for Fig. 4-9B to not disturb the deflection-factor accuracy. The final display sweep rate was 100 ps/div. The noise level (Fig. 4-9D) has an amplitude of about one-fifth division (one minor division). At  $0.0125 \rho/\text{div}$ , the system amplitude resolution in this case is then approximately  $0.0025 \rho/\text{div}$  ( $0.2 \text{ div} \times 0.0125 \rho/\text{div}$ ).

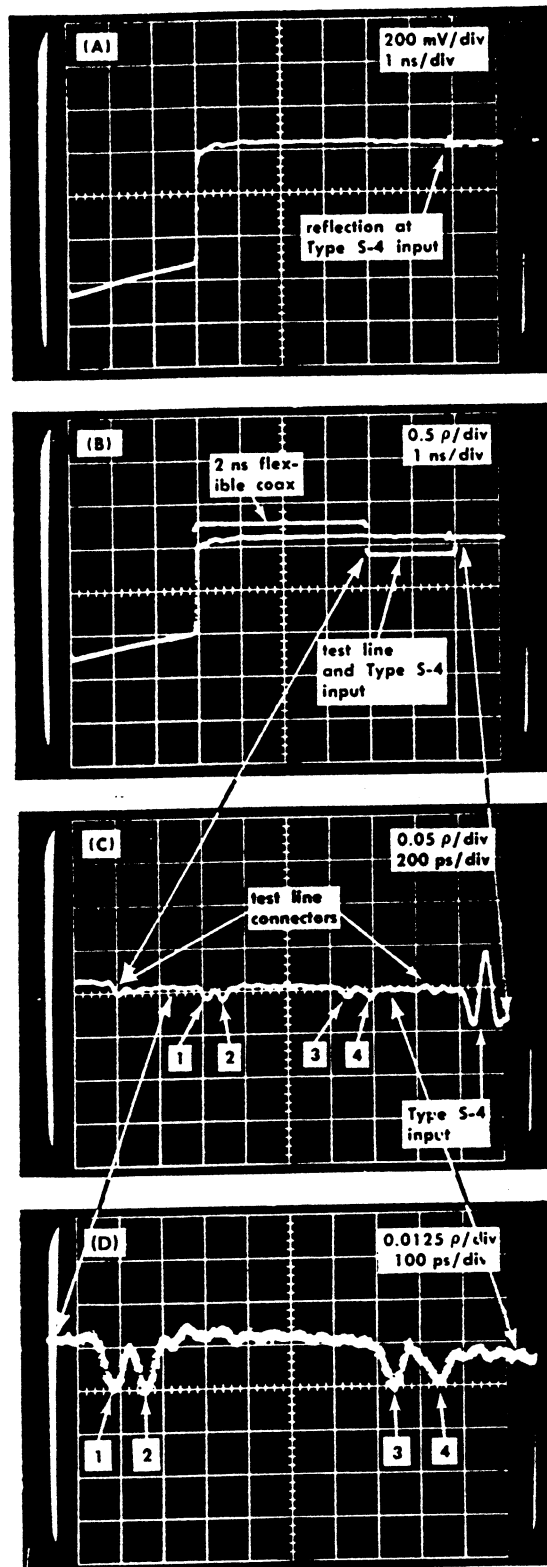


Fig. 4-9. Displays while calibrating the deflection factor in  $\rho/\text{div}$  using the "in-line" hookup.

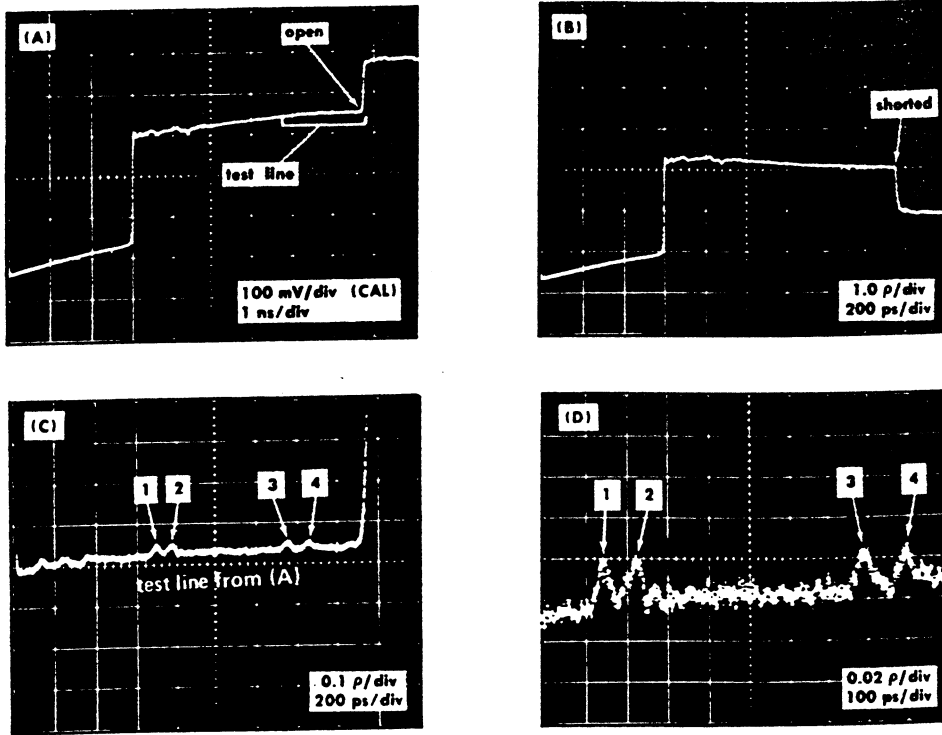


Fig. 4-10. Displays while calibrating the displays in  $\rho/\text{div}$  using either "Tee"-hookup TDR system.

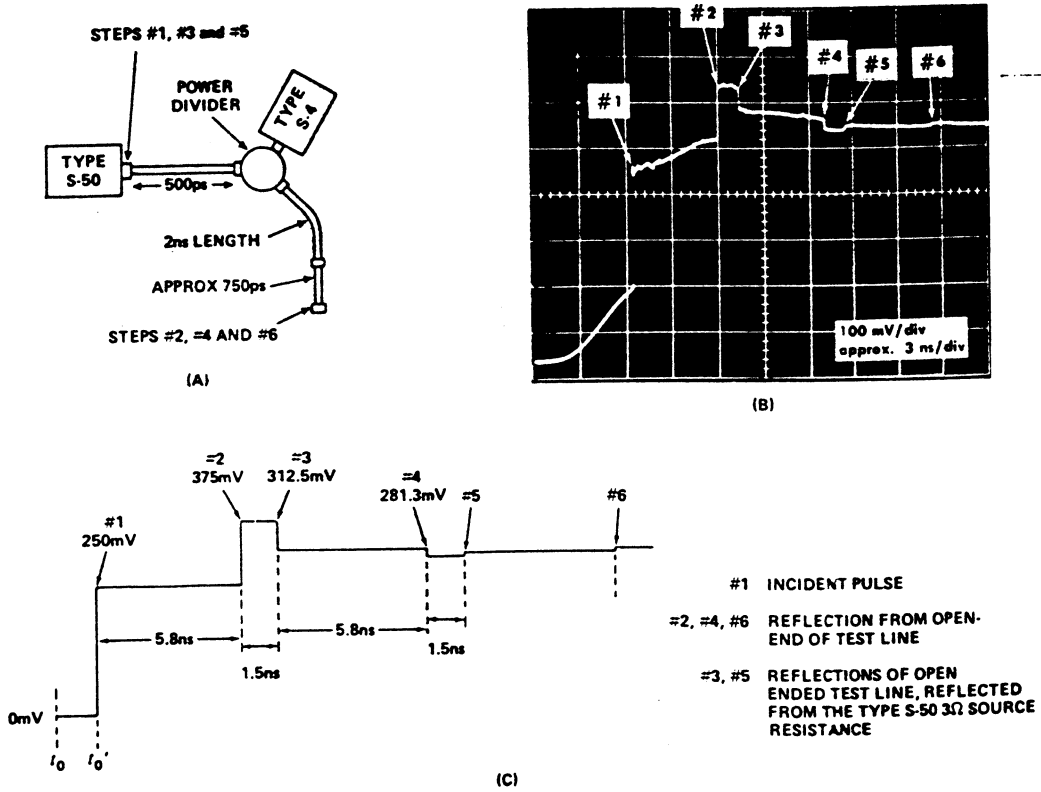


Fig. 4-11. Analysis of display when using a "Power-divider Tee."

**“MISMATCHED TEE” AND/OR  
“POWER-DIVIDER TEE” CONFIGURATION**

“Power-divider Tee” hookup of Fig. 4-8B is described here. Fig. 4-10 is a typical display of an open-ended test line when using a Power-divider-Tee TDR system and the Tektronix Type S-4 and Type S-50 heads; sweep rate is 1 ns/div and the vertical deflection factor is 100 mV/div. The incident-pulse fast-rise transition is located three major divisions from the left graticule edge. The lower-amplitude (about 1.2 major divisions) transition near the graticule right is from the test-line open end.

reference  
signal

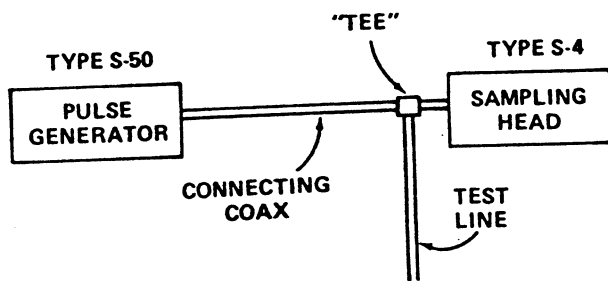
*When using a “Tee” configuration, the displayed reflection from an open or shorted test-line end is the reference signal of  $\pm 1 \rho$ . A Power-divider-Tee-system  $\pm 1 \rho$  reference signal has only one-quarter the amplitude of the previously described “in-line” configuration. This is caused by a 2X attenuation of the signal each time it passes through the matching Power Divider.*

Fig. 4-10B shows the test-line shorted-end reflection spanning one major vertical division — adjusted by the sampling-unit VARIABLE control. The TDR display is now calibrated at 1  $\rho$ /div.

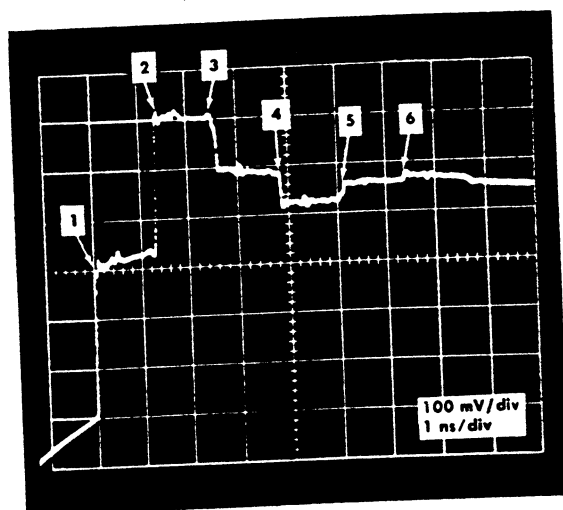
Both Fig. 4-10A and B show a slow ramp between the incident pulse and the  $\pm 1 \rho$  reflection. That slope is a natural reflection of the pulse-generator arming ramp and is not due to either test-line series resistance or losses.

Fig. 4-10C and D show two time and vertical expansions of the test-line time window. Fig. 4-10D time window displays less than the total test line and includes two dual reflections. Note that the display noise is greater than for the in-line system.

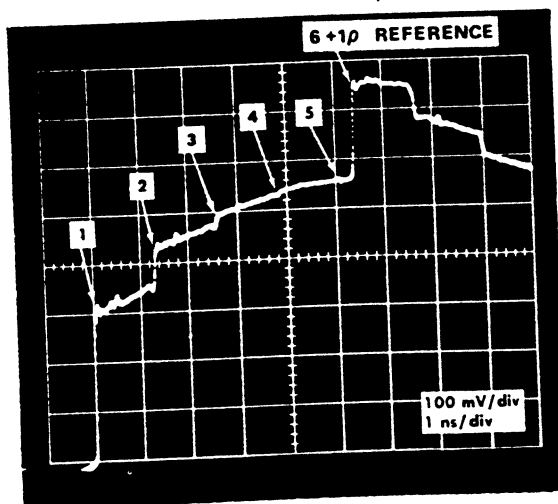
The system of Fig. 4-8B produced the displays in Fig. 4-10. The same system produces a confusing display of multireflections if the sweep rate is made to be slow. Such a multireflection (longer time window) display is shown in Fig. 4-11 with each step numbered to aid in identifying its source.



(A) TEST SETUP



(B) 500ps TEST LINE; UNUSABLE SYSTEM



(C) 2500ps TEST LINE; USABLE SYSTEM

Fig. 4-12. Regular "Tee" connected to Type S-50 Pulse Generator through a 500-ps section of rigid coaxial line.



### “MISMATCHED TEE” CONFIGURATION

reference  
signal

Fig. 4-12 shows a mismatched-tee hookup and reflections. Step 2 of Fig. 4-12C is the calibrating  $+1 \rho$  reference step — in this case from an open-end test line. Note that in Fig. 4-12B step 2 does not represent a  $+1 \rho$  reflection because the open-end reflection has been exalted on the incident-signal re-reflection from the tee to the S-50 and back. This condition occurs whenever the connecting-cable and test-cable signal delays are equal, and is to be avoided. Fig. 4-12C is a display from a usable system with step 6 the reference  $+1 \rho$  signal. Reflections 2, 3, 4 and 5 are not from the open end, but are multiple reflections caused by the tee and the pulse-generator  $3\text{-}\Omega$  source resistance.

A mismatched-tee-configuration  $\pm 1 \rho$  reflection has less loss in its signal path and is therefore about two times the matched power-divider-tee-configuration  $\pm 1 \rho$  amplitude.

The displays shown in Fig. 4-9 through Fig. 4-12 are discussed in greater detail in the Tektronix Type S-4 and Type S-50 instruction manuals. Fig. 4-2 of this chapter lists the different typical resolution characteristics of the TDR systems available from Tektronix as of January 1970.

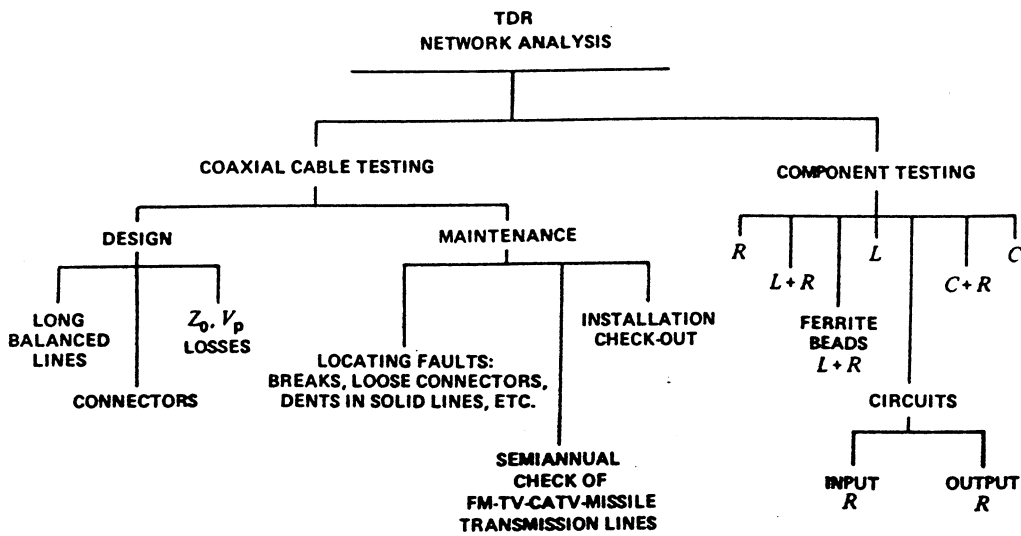


Table 5-1.

## 5

## TDR APPLICATIONS

Time-Domain-Reflectometry equipment is a measuring tool that permits analysis of many items related to transmission lines. The number of applications included here is not an exhaustive study, but does include many practical uses of a TDR system. Those items related to transmission lines that cannot be tested by TDR are discussed in Chapter 6.

A general view of application categories is presented in Table 5-1. We do not recommend TDR as a normal method of testing components, but for academic reasons extensive descriptions of reflections from components placed in coaxial environments are included. The TDR operator that thoroughly understands component TDR reactions is then more fully qualified to analyze TDR plots of transmission lines. An experienced operator's analysis of a TDR plot reveals a component's electrical parts measured in a series equivalent circuit.

Chapter 2 includes TDR testing of coaxial cables to determine their pulse response characteristics. Chapter 3 discusses spatially locating discontinuities, measuring:  $Z_0$ ,  $R_L$ , series DC resistance, shunt conductance,  $Z_0$  of a second resistive discontinuity, coaxial-cable fabricating-equipment mechanical problems and  $\rho$  correction in mismatched-impedance TDR systems. Chapter 4 shows one example of evaluating two mating coaxial connectors with a high-resolution TDR system. Chapter 6 compares frequency-domain reflectometry with TDR and tells how TDR can quickly (and roughly) check the frequencies at which an antenna radiates energy.

**CAUTION:** It is normal that most TDR equipment uses a sampling oscilloscope to read the reflections. Most sampling oscilloscopes do not contain over-voltage protection. Some coaxial cables stored on large reels contain a high-voltage (capacitive) charge, left there from some test before being shipped by the manufacturer. Other transmission lines may be charged with either DC or AC as a result of some fault. It is therefore important that all TDR equipment operators take precautions to ensure that a line to be tested is not *hot*, thus protecting the TDR-unit sampling oscilloscope from damage.

## REFLECTIONS FROM DISCRETE REACTIVE COMPONENTS

Inasmuch as the rest of this book deals with resistive-mismatch TDR displays, this chapter begins with a discussion of reactive-mismatch displays.

Contrary to frequency-domain measurements, TDR response to a reactance is only momentary. Thus an inductor or a capacitor located in a transmission line will give only a short-duration response to the TDR incident pulse. Analysis of large reactances is relatively simple and makes use of time-constant (T) information contained in the reflection display. Small reactances are not so simple to evaluate quantitatively, so will be treated separately.

### LARGE REACTANCES

The difference between a "large" and a "small" reactance is not a fixed value of capacitance or inductance, but is instead related to the TDR display. If the displayed reflection includes a definite exponential curve that lasts long enough for one time constant to be determined, the reactance is considered "large."

fully charged  
capacitor

fully "charged"  
inductor

Discrete (single) capacitors connected in series or parallel with a transmission line start to charge at the instant the incident pulse arrives. Inductors start to conduct current at the arrival of the incident pulse. Both forms of reactance cause an exponentially changing reflection to be sent back to the TDR unit. When a capacitor is fully charged, the TDR unit indicates an open circuit. When an inductor is fully "charged" (current through it reaches its stable state), the TDR unit indicates a short circuit. The TDR unit will indicate an inductor's series DC resistance if its value is significant in relation to  $Z_0$ . The general form of reflection and long-term effect upon the TDR display by both inductors and capacitors is listed in Tables 5-2 and 5-3.

accurately  
measuring one  
time constant  
(T)

In practice, TDR reactance displays usually contain aberrations during the desired pure exponential reflection. Such aberrations prevent finding the normal 63% one-time-constant point of the curve accurately. (The aberrations are due to either the environment around the reactance, i.e. stray inductance in series with a capacitor, or stray capacitance in parallel with an inductor, or secondary system reflections.) However, accurate time-constant information can be obtained from less than a complete exponential curve. The principle used requires that a "clean" portion of the display must exist. The "clean" portion used must include the right-hand "end" of the displayed curve (a capacitor is then fully charged, or an inductor current has stopped changing). The "end" of the curve will appear on the display to be parallel to a horizontally scribed graticule line. Thus, aberrations that exist at the beginning of the curve can be ignored.

REACTANCE	IN SERIES WITH LINE	IN PARALLEL WITH LINE	LINE IMPEDANCE AT REACTANCE
CAPACITOR			SERIES: $2Z_0$ PARALLEL: $\frac{Z_0}{2}$
INDUCTOR			SERIES: $2Z_0$ PARALLEL: $\frac{Z_0}{2}$

Table 5-2. Single capacitor or inductor TDR displays related to terminated transmission lines.

REACTANCE	DISPLAY	LINE IMPEDANCE AT REACTANCE
CAPACITOR		$Z_0$
INDUCTOR		$Z_0$

Table 5-3. Single capacitor or inductor TDR displays when connected across end of transmission line.

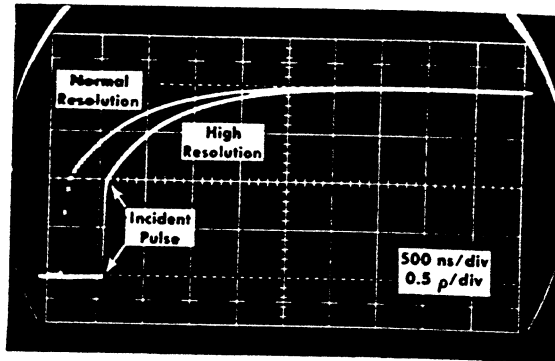
CIRCUIT	EQUIVALENT CIRCUIT	FORMULA	DISPLAY
SERIES WITH TERMINATED LINE 		$C = \frac{1T}{2Z_0}$ (1)	
PARALLEL WITH TERMINATED LINE 		$C = \frac{1T}{Z_0}$ (2)	
ACROSS LINE END 		$C = \frac{1T}{Z_0}$ (3)	

WHERE C = FARADS; T = TIME CONSTANT;  $Z_0$  = LINE CHARACTERISTIC IMPEDANCE

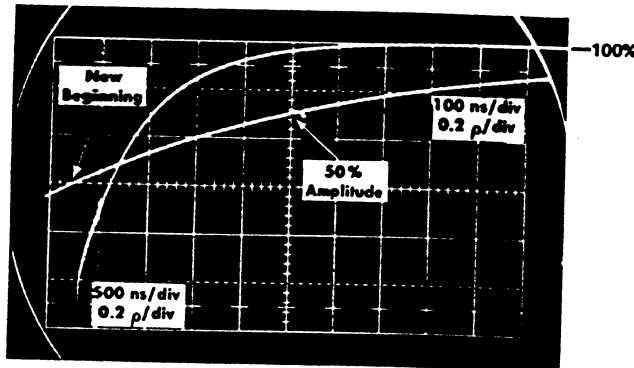
Table 5-4. "Large"-capacitor circuits and formulas.

50% =  
0.693T

Fig. 5-1 shows the first example of obtaining valid time-constant information from less than a full 100% exponential curve. The technique is to choose any "clean" portion of the display that includes the "end" of the exponential curve and find the half-amplitude point. The time duration from the beginning of any new curve section to its 50% amplitude point is always equal to 69.3% of one time constant. Thus, the time duration for a 50% change divided by 0.693 is equal to one time constant.



(A)



(B)

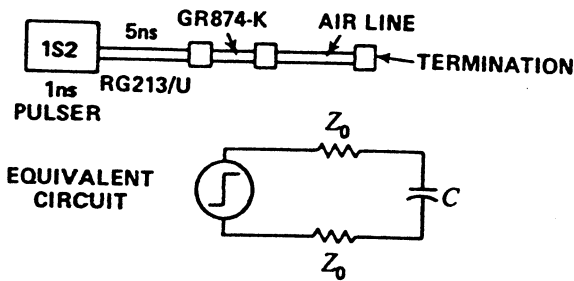


Fig. 5-1. Exponential curves and circuit of 6.5-nF capacitor in series with terminated transmission line.

Fig. 5-1 shows the TDR displays of a capacitor placed in series with a transmission-line center conductor ( $2Z_0$  environment). This and the other waveform pictures shown in this reactive-display discussion were taken with a Tektronix C-27 Camera mounted on a Tektronix Type 547 Oscilloscope with a Tektronix Type 1S2 Sampling Unit and Time Domain Reflectometer. Fig. 5-1A is comprised of a double exposure with the left curve taken while the Type 1S2 RESOLUTION switch was at NORMAL and the right curve taken when the switch was at HIGH. Both curves give sufficient information to measure one time constant. Note that the top of the incident pulse is indefinite (in the displays) due to the sweep rate and short length of cable used between the Type 1S2 and the capacitor. Such a display does not have a definite beginning of the normal 100% exponential curve. This prevents 63% of the total curve from being read directly from the display. [It is also quite possible for lead inductance to cause a capacitor to ring. When a TDR display shows capacitor ringing, the ringing can sometimes be reduced by: 1) using a slower risetime pulse and/or 2) changing the transmission-line environment to place a lower value  $Z_0$  in parallel with the capacitor.]

The double exposure of Fig. 5-1B shows a full exponential curve beginning in the vicinity of 1 division from the graticule bottom. Then the same curve has been time-expanded for easier reading. The indefinite beginning of the 500-ns/div exponential curve prevents finding one time constant by measuring the time of 63% of the total curve amplitude. The new arbitrarily chosen 100%-amplitude portion of the curve begins at the graticule center horizontal line and extends (off the right of the graticule) to the top graticule line. Three divisions were chosen for the new 100% exponential curve, with the 100% and 50% points marked. Then, dividing the time for the 50% amplitude change by 0.693 gives a total one-time-constant time value of 650 ns. Since the equivalent circuit shows two  $Z_0$  in series with the capacitor, its value is found by formula (1) (Table 5-4) to be 6.5 nanofarads.

## LARGE CAPACITORS

The difference between a "large" and a "small" capacitor is not a fixed value of capacitance, but is instead related to the TDR display. If the display includes a definite exponential curve that lasts long enough to permit one RC time constant to be determined, the capacitor value can be found by using a normal RC time-constant formula. The actual formula varies according to the equivalent circuit in which the capacitor is located. Table 5-4 lists the possible configurations and their related formulas.

The first example of "large"-capacitance measurement was given in the previous discussion on finding one time constant ( $50\% = 0.693T$ ). The large-value capacitor used is easy to measure and usually causes only one aberration to the exponential curve — the indefinite curve beginning.

moving a  
reflection  
aberration

When testing small capacitors that still produce a usable exponential curve, it may be difficult to get accurate time-constant data when there are reflections within the system. For example, a 100-pF disc ceramic capacitor was soldered into a General Radio Radiating Line section (Fig. 5-2). The Type 1S2 1-volt pulser was used; re-reflections from the pulser distort the exponential curve in Fig. 5-2A. The re-reflection is moved to the right just outside the time window by placing a 20-ns signal-delay RG213/U cable between the pulser and the sampler. The acceptable waveform is shown in Fig. 5-2B. Fig. 5-2C is a double exposure showing first how the “end” of the exponential curve is set to a graticule line. Then the display is time expanded to 500 ps/div (leaving the vertical position as adjusted) and the new arbitrary 100% exponential curve is chosen and marked. The capacitor’s value, taken from the time-expanded curve of Fig. 5-2C and using formula (2) is 104 pF ( $1.8 \times 10^{-9} \div 0.693 \div 25 = 1.04 \times 10^{-10} = 104 \text{ pF}$ ). Note that the vertical  $\rho$  factor was changed for Fig. 5-2C to make the time-constant measurement from a clean section of the curve near its end.

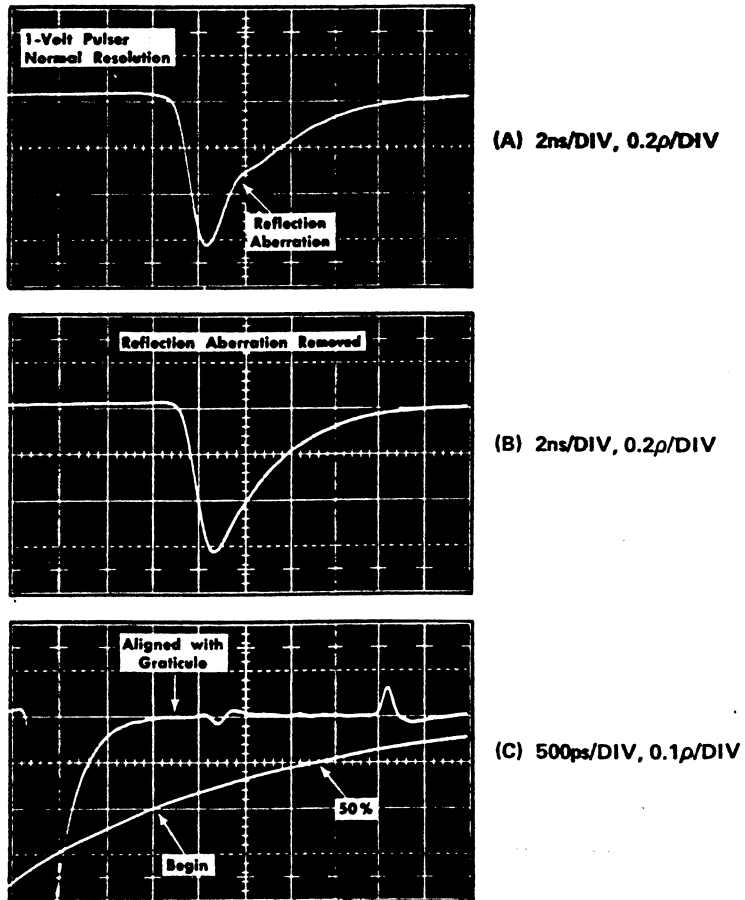
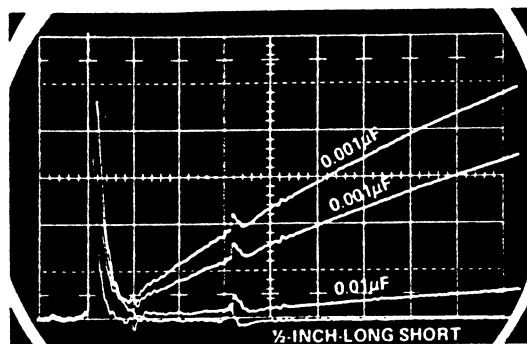
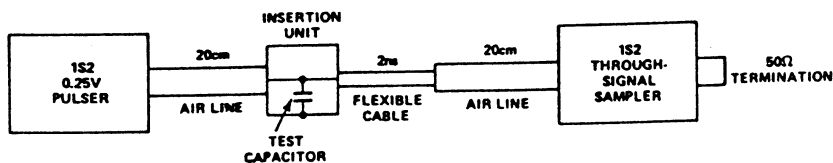
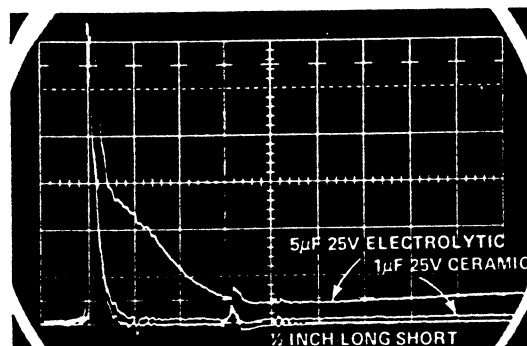


Fig. 5-2. Example of moving display reflection aberrations to obtain a “clean” exponential curve.





(A) 0.1 $\rho$ /DIV, 2ns/DIV,  
3 CERAMIC CAPACITORS



(B) 0.1 $\rho$ /DIV, 2ns/DIV

**Fig. 5-3. Special non-TDR high-speed pulse tests of by-pass capacitors.**

special  
capacitor  
testing

Non-Reflection Time-Domain testing using the Type 1S2 is another method of testing capacitors described here. The particular value of this method is that the display allows a direct comparison of the abilities of various capacitors to function in a high-speed pulse circuit. The method discloses a capacitor's series lead inductance, its series  $X_C$  (its lowest possible impedance) and its capacitance value all in one display. Lead inductance is compared to the "reference" inductance of a piece of wire that has the same length as the capacitor's signal path. The series  $X_C$  is measured in ohms and the capacitance is measured by normal time-constant information.

The circuit, shown in Fig. 5-3, makes use of the Type 1S2 fast (50-ps  $t_r$ ) 0.25-V pulser and the fast (90-ps  $t_r$ ) sampler. The capacitor is soldered into a component insertion unit (or GR 874-LR Radiating Line) in parallel with the transmission line, effectively shorting the pulser signal during the time the capacitor is a low impedance. (The insertion-unit part numbers are given in the discussion about Fig. 6-1 on page 91.)

Fig. 5-3A shows a multiple exposure of four traces. The bottom trace is from a reference 1/2-inch-long shorting wire of the same diameter as the capacitor leads. The other three traces are of three different ceramic (sometimes called discap) capacitors, each with total visible lead lengths of about 3/8 inch (the invisible leads are coated by the capacitor's normal protective coating). The small positive impulse at 4.2 major divisions from the graticule left edge is a re-reflection of the inductance impulse that went back toward the pulser source; it is not caused by a fault of the capacitor or the insertion unit. At 0.1  $\rho$ /div, the 0.01- $\mu$ F capacitor shows a  $X_C$  value of less than 0.2  $\Omega$  for about 4 ns after the inductive impulse; the capacitor then starts its RC charge about 3 major divisions after the pulse began to rise. The two 0.001- $\mu$ F capacitors (made by two different manufacturers) begin to charge almost instantly and are at about 1- $\Omega$  reactance 4 ns after the pulse began to rise.

Fig. 5-3B shows a multiple exposure of three traces. The bottom trace is again a reference short, 1/2-inch long. The other two traces compare a 1- $\mu$ F 25-V ceramic and a 5- $\mu$ F 25-V electrolytic capacitor. The 1- $\mu$ F trace was purposely offset vertically from the shorted-trace position to show that it identically follows the shorted trace for longer than the 18 ns that is visible after the pulse starts to rise. The 5- $\mu$ F trace is not offset and shows a significant series resistance that changes with time. It takes about 8 ns for the 5- $\mu$ F capacitor to become a true low reactance which is then equal to about a 4- $\Omega$  resistance for several ns. It is also interesting that the 5- $\mu$ F capacitor begins its RC charge before the 1- $\mu$ F capacitor does.

The two illustrations are not exhaustive, but give only the basic idea of how a fast pulse and fast sampler can evaluate the high-speed characteristics of bypass capacitors. (It was such a test that helped an engineer select a particular 1- $\mu$ F capacitor as a power-supply decoupling device in several Tektronix sampling circuits.)

## LARGE INDUCTORS

inductors  
without  $R$

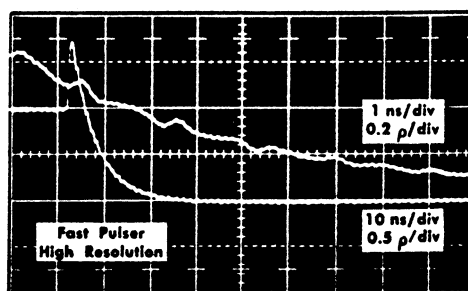
The difference between "large" and "small" inductors in TDR testing follows the same general display limits as for large or small capacitors. A "small" inductor in series with a transmission-line center conductor will give a display that does not permit normal time-constant analysis. The same inductor in parallel with a terminated transmission line may give a display that does allow normal time-constant analysis.

ringing

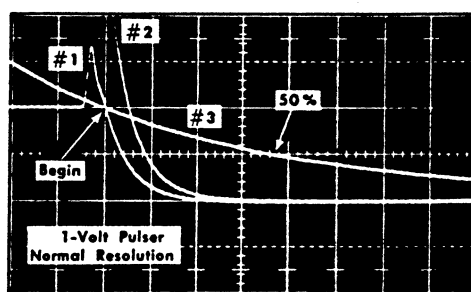
Ringling in the exponential TDR display is often observed when measuring inductors. It is usually caused by distributed capacitance across the coil that has not been adequately damped by transmission-line characteristic impedance. Since an inductor with stray capacitance will ring unless adequately damped, an inductor in parallel with a transmission line ( $Z_0/2$  environment) will be less likely to ring than the same inductor in series with a line ( $2Z_0$  environment).

changes  
to prevent  
ringing

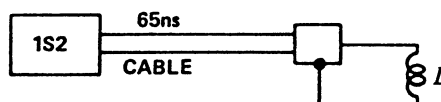
Fig. 5-4 shows waveforms of the reflections from a seven-turn 3/8-inch-diameter coil. The coil was connected across the end of a 50- $\Omega$  transmission line ( $Z_0$  environment). Fig 5-4A was made using the Type 1S2 0.25-volt fast pulser with the RESOLUTION switch at HIGH. The ringing makes it impossible to obtain an accurate time-constant measurement from the display. Fig. 5-4B was made using the Type 1S2 1-volt pulser with the RESOLUTION switch at NORMAL. Here the slower-risetime incident pulse does not excite the ringing. In addition, the time averaging of fast changes by normal-resolution operation permits a time constant to be measured. Ringing could also have been reduced by a  $Z_0/2$  environment by placing a termination across the inductor or by placing the inductor at a convenient midpoint of a long line.



(A)



(B)



(C)

Fig. 5-4. Seven-turn coil across end of 50- $\Omega$  line.

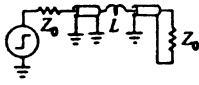
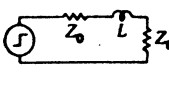

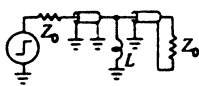
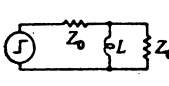

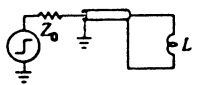
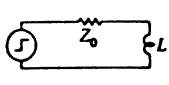

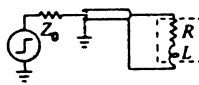
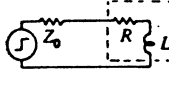

CIRCUIT	EQUIVALENT CIRCUIT	FORMULA	DISPLAY
SERIES WITH TERMINATED LINE 		$L = 2Z_0 \times 1T$ (4)	
PARALLEL WITH TERMINATED LINE 		$L = \frac{Z_0}{2} \times 1T$ (5)	
ACROSS LINE END 		$L = Z_0 \times 1T$ (6)	
INDUCTIVE RESISTOR ACROSS LINE END 		$L = (Z_0 + R) \times 1T$ (7)	

Table 5-5. "Large"-inductor circuits and formulas.

The triple exposure of Fig. 5-4B includes three curves: #1, the total reflected signal at 10 ns/div and 0.5  $\rho$ /div; #2, increased vertical deflection and the exponential-curve end positioned one division below the graticule center horizontal line; and #3, the #2 curve time-expanded to 1 ns/div for measurement of the  $L/R$  time constant. The new 100%-to-50%-amplitude time duration of curve #3 is shown as 3-3/4 ns.  $3.75/0.693 = 5.41$  ns for 1 time constant. Since the coil is at the end of a 50- $\Omega$  transmission line, the inductance is calculated to be 270.5 nH by formula (6) in Table 5-5 [ $L = 50 \times (5.41 \times 10^{-9}) = 2.705 \times 10^{-7} = 270.5$  nH].

inductor  
with  
pure R

In the event an inductor has pure resistance as part of its equivalent circuit, the TDR display will deviate from that of a pure inductor. The fourth example in Table 5-5 shows one such lossy-inductor case. Note that the inductor's pure  $R$  is included in series with the transmission-line environment driving  $Z_0$  and becomes part of the formula for determining pure  $L$ . That principle must be considered in all cases when a large inductance is displayed by a TDR system. (Read about measurement of ferrite cores near the end of this chapter for the proper method of including the core loss resistance in the formula for calculating pure  $L$ .)

### SMALL REACTANCES

"Small" reactances are here defined as series-connected inductors and shunt-connected capacitors that cause TDR reflections without apparent time-constant reaction to the incident pulse. Some small reactances are capable of reaching a "charged" state (capacitor voltage is stable; inductor current is stable) faster than the TDR-pulser incident-pulse rate-of-rise. (The Type 1S2  $\leq 50$ -ps pulser is used in the following examples.) If the TDR display has no exponential section, normal  $RC$  and  $L/R$  calculations cannot be made. All "small" reactances generate TDR reflections with less than +1  $\rho$  or -1  $\rho$ .

Small discrete capacitors with leads always include a significant amount of stray series inductance. Fig. 6-1 and the associated discussion is an example of such a capacitor with inductive leads. Small shunt capacitors without leads may be produced by either an increase in a coaxial-cable center-conductor diameter or a reduction of its outer-conductor diameter. Leadless capacitors are sometimes treated as a small reduction in  $Z_0$  rather than as a capacitor. Usually, such small discontinuities are considered capacitance when the section of reduced  $Z_0$  line is so short physically that no level portion can be seen in the TDR display.

Small series inductors rarely have sufficient parallel (stray) capacitance to be significant in the TDR display. However, the coaxial environment around such a small conductor does affect the TDR display. Small series inductors without capacitive strays are sometimes caused by changes in coaxial-cable diameter – decreased center-conductor diameter or increased outer-conductor diameter. This form of inductor is usually treated as a small increase in  $Z_0$  rather than as an inductor. Usually, such discontinuities are considered to be inductance when the section of increased  $Z_0$  line is so short physically that no level portion can be seen in the TDR display.

assumptions  
permitting  
small-reactance  
analysis

The usual TDR system does not have the required characteristics for accurately measuring small reactances. Yet small reactances can be measured, provided the following assumptions are made regarding the TDR system:

- 1) The actual TDR system may be adequately described by a model having a simple ramp as the pulse source and a lossless transmission line with an ideal sampler.
- 2) The rounded “corners” of the actual step transition may be ignored.
- 3) The transmission-line high-frequency losses, classed as “skin effect” or “dribble-up”, are not significant. (The significance of dribble-up to this type of measurement is explained later in connection with Fig. 5-8.)
- 4) The sampler is nonloading, nondistorting and of infinitesimal risetime.
- 5) The element being analyzed is either pure  $L$  or pure  $C$  and does not contain any opposite sign reactance.

The formula for small series inductance and small shunt capacitance in a transmission line contains factors for: 1) the system risetime at the spatial location of the reactance, 2) the observed reflection coefficient and 3) the transmission-line characteristic impedance.

The system risetime may be measured from the display by placing either an open circuit or a short circuit at the spatial location of the reactance.

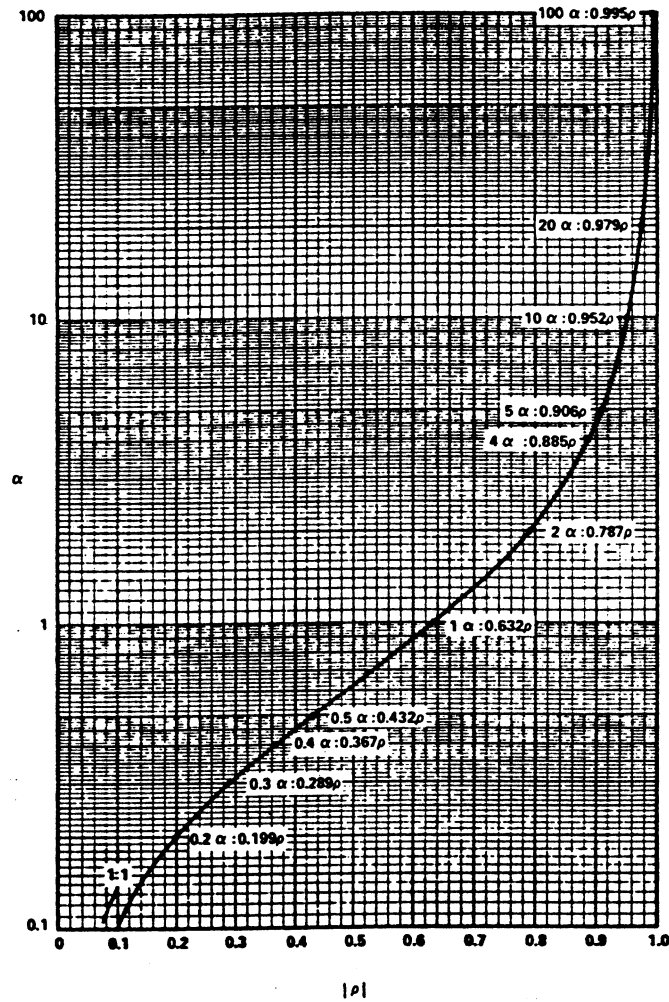


Fig. 5-5. Graph for conversion of small reactance observed  $\rho$  to  $\alpha$  for use in formulas (7) and (9).

The value for a small series inductor can be calculated using the formula

$$L = 2.5 \alpha Z_0 t_r \quad (7)$$

where  $L$  is in henries,  $Z_0$  is in ohms,  $t_r$  is the system 10%-to-90% risetime in seconds, and  $\alpha$  is a dimensionless coefficient related to the observed reflection coefficient  $\rho$  by either the graph of Fig. 5-5 or formula (8).

$$|\rho| = \alpha \left(1 - \epsilon^{-\frac{1}{\alpha}}\right) \quad (8)$$

A small shunt capacitor's value can be calculated using the formula

$$C = \frac{2.5 \alpha t_r}{Z_0} \quad (9)$$

where  $C$  is in farads and the other units are as in formula (7).

small  
series  
inductor

Fig. 5-6 is an example of TDR displays from a small (1-3/4-turn) inductor placed in parallel with a 50-Ω line (A) and in series with the 50-Ω line (B). Calculations were made first on Fig. 5-6A because the display is a clean exponential that permits  $L/R$  time-constant analysis. Fig. 5-6A shows first the full exponential decay through five CRT divisions; then the waveform was positioned vertically with the exponential end at -1 division; using the same vertical calibration, it was then time expanded to obtain the new 100%-to-50% time duration.

The time duration of the 50%-amplitude-change section of the exponential curve is 450 ps. This time divided by 0.693 produces a one-time-constant time duration of  $650 \times 10^{-12}$  seconds. Then from formula (5), the value of the inductor is 16.22 nH ( $1.622 \times 10^{-8}$  H).

The waveform of Fig. 5-6B has an observed reflection coefficient of +0.58. From the graph of Fig. 5-5, 0.58  $\rho$  is equal to 0.82  $\alpha$ . The risetime of the system was found to be 160 ps by disconnecting the insertion unit in which the inductor was located and measuring the reflection signal risetime. These figures placed into formula (8) give a value for the series inductor of 16.4 nH ( $1.64 \times 10^{-8}$  H). This correlates very well with the previous parallel measurement.

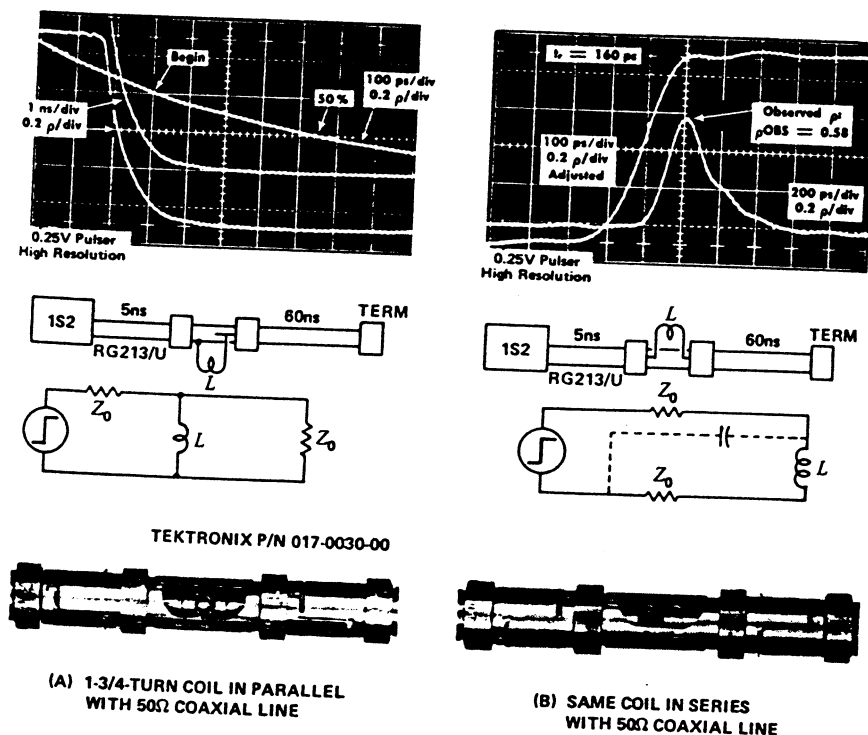


Fig. 5-6.

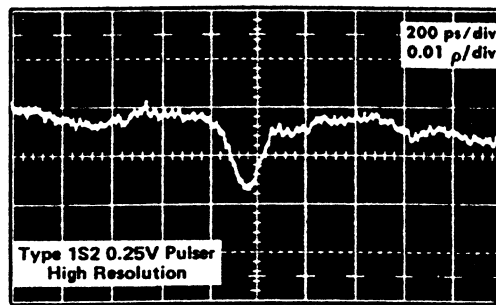


Fig. 5-7. Shunt capacitor,  $\sim 0.085$  pF, caused by compressing RG8A/U coaxial cable with pliers.

small  
shunt  
capacitor

Fig. 5-7 is an example of a small shunt capacitor placed across a  $50\text{-}\Omega$  coaxial cable by compressing the cable outer diameter. Since the cable (RG8A/U) has normal impedance variations along its length, the peak reflection from the capacitor can only be approximated. Assuming a  $\rho$  of  $-1$  division in Fig. 5-7, then by formula (9), the capacitance is approximately  $0.085$  picofarads.

measuring  
small  
reactances

The measurement of the small series inductor in Fig. 5-6B is explained here to point out necessary techniques for measuring small reactances.

In evaluating small reactances with the TDR system, we have assumed the driving pulse to be a linear ramp; therefore, the ramp risetime must be determined for each change in the test system. The word "dribble-up" refers to the coaxial-cable characteristic of transporting a step signal with distortion. The time required for the cable output signal to reach 100% of the step-signal input amplitude is many times longer than the interval needed for the output signal to change from 0% to 50%. If we consider that the small reactance receives a pure ramp signal, then the rounded corners of the output pulse must be ignored.

Fig. 5-8 shows the degradation of the Type 1S2 incident signal pulse by two different lengths of RG8A/U<sup>1</sup> coaxial cable. Fig. 5-8A is the reflection from a 96-cm-long open cable (192-cm signal path equals 75 inches or 6.25 feet) and Fig. 5-8B is the reflection from a 550-cm-long open cable (1100-cm signal path equals 432 inches or 36 feet). The upper waveform in each case was made with the Type 1S2 VERTICAL UNITS/DIV control set to  $0.5 \rho/\text{div}$ , calibrated. The lower waveform in each case was made with the Type 1S2 VERTICAL VARIABLE control advanced slightly clockwise to approximate a deflection factor of  $0.5 \rho/\text{div}$  for just the ramp portion of the waveform. In each case the signal continues to rise after the initial step but Fig. 5-8B shows the "dribble-up" characteristic very plainly. The lower waveforms of Fig. 5-8A and B do not permit an accurate measurement of the system risetime because the waveforms as shown are not large enough.

<sup>1</sup>RG8A/U cable has a nominal  $Z_0$  of  $51.7 \Omega$ , RG213/U has a nominal  $Z_0$  of  $50.0 \Omega$ . Tektronix no longer supplies RG8A/U for interconnection purposes. RG213/U is considered more appropriate for  $50\text{-}\Omega$ -TDR-equipment support.



However, the upper waveforms of Fig. 5-9A and B are large enough to permit a reasonable measurement of the 10%-to-90% risetime of the ramp that drives the small inductor. It is also obvious from Fig. 5-9A and B that the series-inductor peak reflection is truly caused by just the ramp portion of the driving signal and not by the "dribble-up" portion.

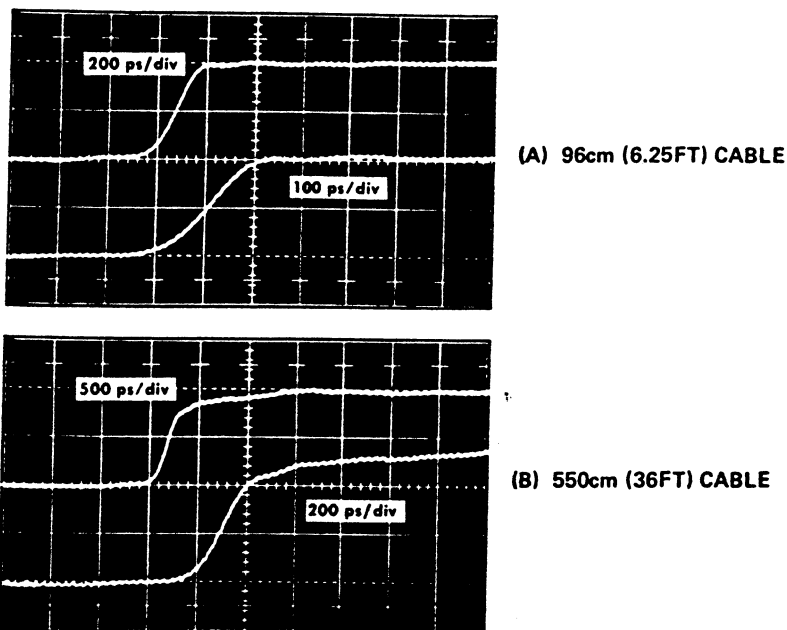


Fig. 5-8. "Dribble-up" characteristics of two lengths of RG8A/U.

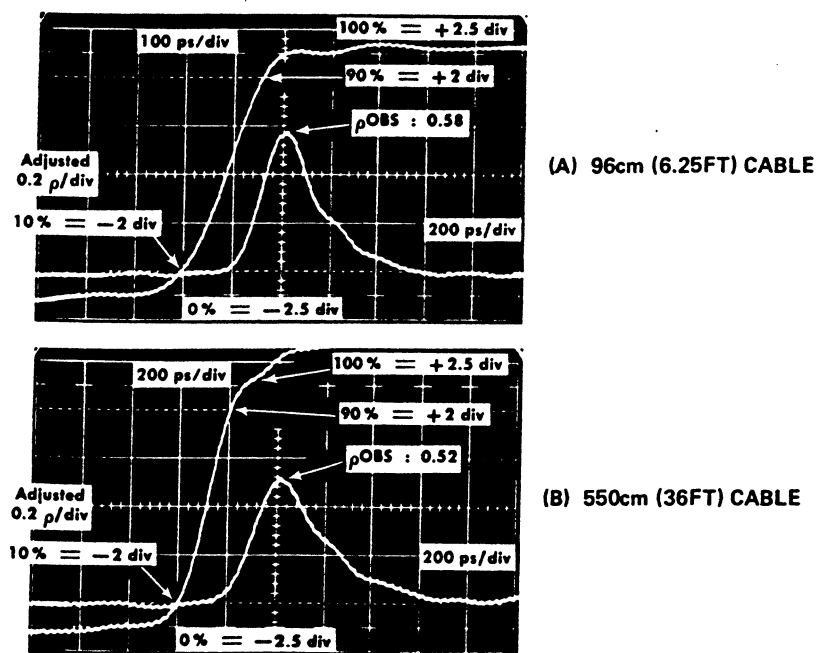


Fig. 5-9. Small series inductor measured 96 cm and 550 cm away from Type 1S2 in RG8A/U coaxial cable.

Calculations made from Fig. 5-9A and B using formula (8) and the curve of Fig. 5-5 indicate the series coil has an inductance of 16.40 nH in Fig. 5-9A and inductance of 16.51 nH in Fig. 5-9B. (Fig. 5-9A:  $L = (2.5) (0.82) (50) (1.60 \times 10^{-8}) = 1.64 \times 10^{-8}$  H. Fig. 5-9B:  $L = (2.5) (0.66) (50) (2.0 \times 10^{-8}) = 1.651 \times 10^{-8}$  H.) This indicates that an inductor in series with a coaxial transmission line can be accurately measured so long as the risetime of the ramp portion of the incident signal can be measured. Fig. 5-9B indicates that a cable of RG8A/U a bit longer than 550 cm (40 feet) might make it difficult to measure the ramp risetime from the display. If a cable has sufficient length to prevent a reasonable display for measuring the ramp 10%-to-90% risetime, the small series inductor cannot be measured.

a limitation

Calculations of cable risetime will not permit small inductor measurements because the Type 1S2 vertical  $\rho/\text{div}$  calibration must be adjusted in each case. Once the vertical gain has been increased to measure the ramp risetime, the same newly adjusted vertical  $\rho/\text{div}$  setting is used for measuring the observed  $\rho$  from the series inductor. If the cable is long enough to make it impossible to "see" the top of the ramp, the inductor cannot be measured. The same limitations apply when measuring small shunt capacitors.

locating  
small  
reactances

The discussion of small reactances has thus far assumed that the TDR operator has access to all the cable between the TDR unit and the reactance being measured. This is, of course, not always the case. When a long length of cable indicates a fault, the reflected signal has not only been reduced in amplitude, it has also been smeared in time. The discontinuity is then located in time, closely related to the approximate 1%-amplitude point on the beginning edge of the display rather than, as might be expected, at 50% of the reflection.

This completes the discussion of reactive mismatch TDR displays.

## IMPULSE TDR

A special high-voltage impulse-TDR system was assembled to permit analyzing a functional FM-radio-station transmission line that contained approximately 350 mV peak-to-peak of 100-MHz interference from other stations that were on the air at the time of testing. The high-voltage impulse-testing system was needed to obtain an adequate signal-to-noise (interference) ratio so that small discontinuities in the transmission line could be resolved.

EQUIPMENT AND HOOK-UP

+100-V  
signal

Fig. 5-10 shows both the equipment and the connections of the high-voltage impulse-TDR system. The impulse duration used was 4 ns and its amplitude into the 50-Ω 3-1/8-inch-diameter station coaxial line was 100 V. (Table 5-6 lists minimum pulse durations, required by the various sweep rates of the Type 1S2, for observing a 100% or +1 ρ reflection at full amplitude.) Pulse risetime (10%-to-90%) at the transmission-line input was approximately 300 ps. Other types of sampling equipment could be used (such as a Type 3S1 with Type 3T2), but the Type 1S2 VERTICAL UNITS/DIV switch is calibrated properly to read in ρ directly for the signal amplitude used. In addition, using the Type 1S2 as the sampling unit permitted its TDR performance to be compared directly with the impulse system.

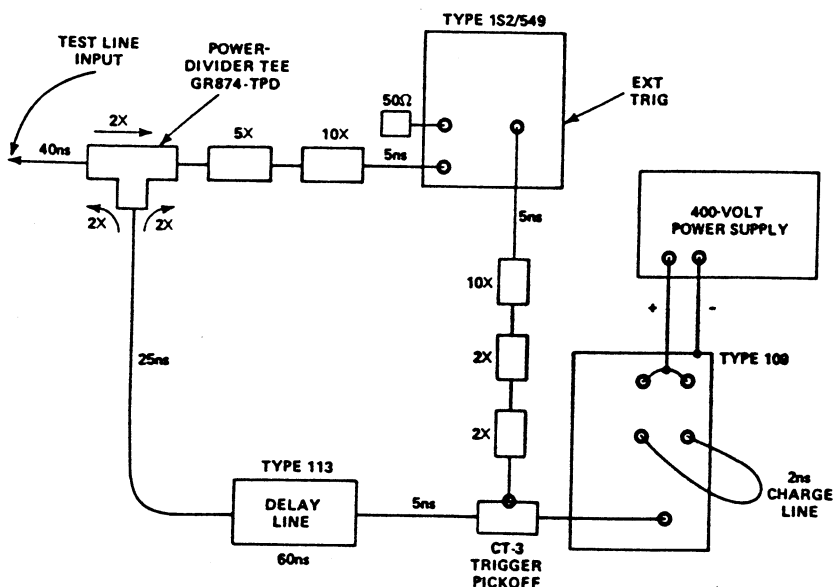
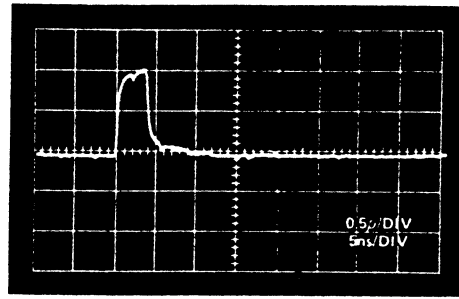


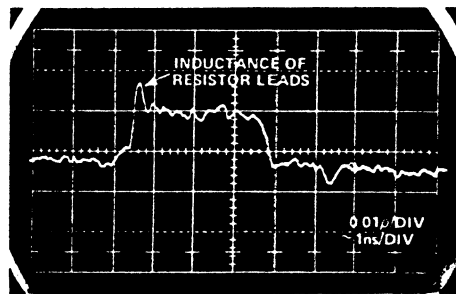
Fig. 5-10. Special high-voltage impulse-TDR system.

RANGE SWITCH SETTING	MAGNIFIER SETTING	ONE TIME WINDOW (10-DIV TOTAL)		RANGE END POSITION: 9.90		IMPULSE TDR MIN PULSE DURATION
		TIME	DISTANCE	TIME	DISTANCE	
10µs/1km	X1	10µs	1000m (3,281ft)	19.9µs	1990m (6,529.2ft)	80ns
	X2	5µs	500m (1,640.5ft)	14.9µs	1490m (4,888.7ft)	40ns
	X5	2µs	200m (656.2ft)	11.9µs	1190m (3,904.4ft)	20ns
	X10	1µs	100m (328.1ft)	10.9µs	1090m (3,578.3ft)	10ns
	X20	.5µs	50m (164.05ft)	10.4µs	1040m (3,402.25ft)	4ns
	X50	.2µs	20m (65.62ft)	10.1µs	1010m (3,313.8ft)	2ns
	X100	.1µs	10m (32.81ft)	10.0µs	1000m (3,281.0ft)	2ns
1µs/100m	X1	1000ns	100m (328.1ft)	1990ns	199m (652.9ft)	10ns
	X2	500ns	50m (164.05ft)	1490ns	149m (488.9ft)	4ns
	X5	200ns	20m (65.62ft)	1190ns	119m (390.4ft)	2ns
	X10	100ns	10m (32.81ft)	1090ns	109m (357.6ft)	1ns
	X20	50ns	5m (16.4ft)	1040ns	104m (341.2ft)	0.4ns
	X50	20ns	2m (6.56ft)	1010ns	101m (331.4ft)	0.2ns
	X100	10ns	1m (3.28ft)	1000ns	100m (328.1ft)	0.2ns

Table 5-6. Type 1S2 suggested impulse duration related to range and magnifier controls. (The RESOLUTION switch must be at its HIGH position.)

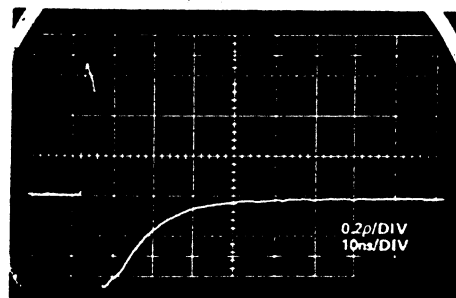


(A) +1p REFLECTION FROM OPEN CIRCUIT

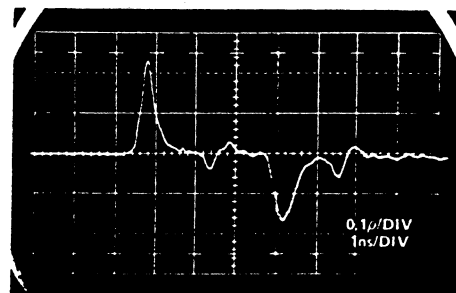


(B) 52.6Ω TERMINATION ON 50Ω LINE

Fig. 5-11. Impulse-TDR resistive-reflection displays.



(A) 0.5μH COIL ACROSS END OF 50Ω LINE



(B) 18.2nH COIL IN SERIES WITH 50Ω LINE

Fig. 5-12. Impulse-TDR inductive-reflection displays.

The Type 109 Pulse Generator is capable of delivering pulse amplitudes up to 300 V. The variable-voltage (regulated) power-supply output was set to a value of approximately +400 V (producing a +200-V pulse); its final value was set to produce a +1  $\rho$  reflection from an open circuit at the junction between the TDR-system-output line and the station transmission line. The sequence of pulse-amplitude changes from the Type 109 to the Type 1S2 is: Type 109 output, +200 V; pulse into station transmission line, +100 V; +1  $\rho$  reflection received at the Type 1S2 input, +1 V (attenuation of 100X by the GR874-TPD and two 50- $\Omega$  GR attenuators as diagrammed in Fig. 5-10).

mismatch  
examples

Several known mismatch items were placed at the end of the TDR-system 40-ns-output line so that reflections could be recognized from the 4-ns-duration impulse. Those mismatch items are identified and their reflections shown in Figs. 5-11, 5-12 and 5-13. The sweep rate of Fig. 5-12A is the same as the sweep rate used when checking the FM-station transmission line (Fig. 5-16).

The Type 109 Pulse Generator is a 50- $\Omega$  source only during the time the pulse is being delivered to its output terminal. At all other times the output resistance is about 25 k $\Omega$ . Signals reflected from mismatches may therefore be seen a second time approximately 170 ns later at one-quarter amplitude. (No significant Type 109 re-reflections appeared in the station-transmission-line plot, so no special attempt was made to make the Type 109 output look like 50  $\Omega$  at all times.)

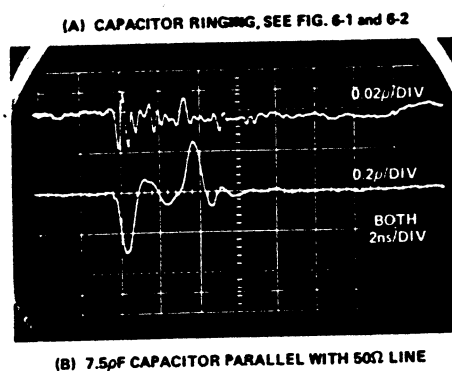
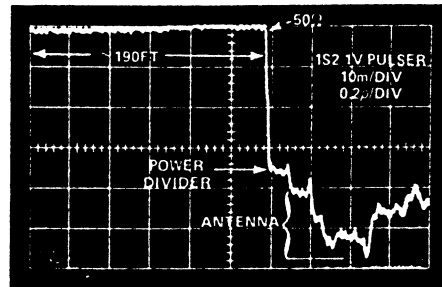
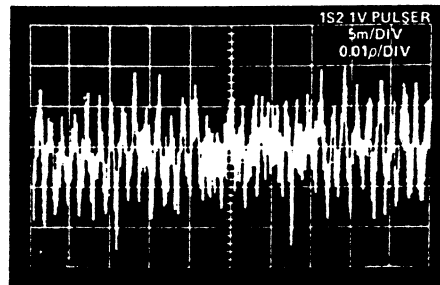


Fig. 5-13. Impulse-TDR capacitive-reflection displays.



(A) FM STATION ANTENNA



(B) 164FT OF 50Ω LINE WITH 100MHz INTERFERENCE

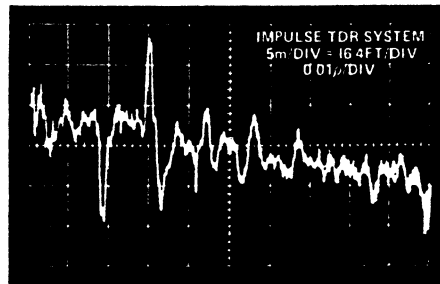
(C) SAME AS B, WITH INTERFERENCE ATTENUATED  
100X BY IMPULSE TDR SYSTEM

Fig. 5-14. Comparison of Type 1S2 and special impulse-TDR system.

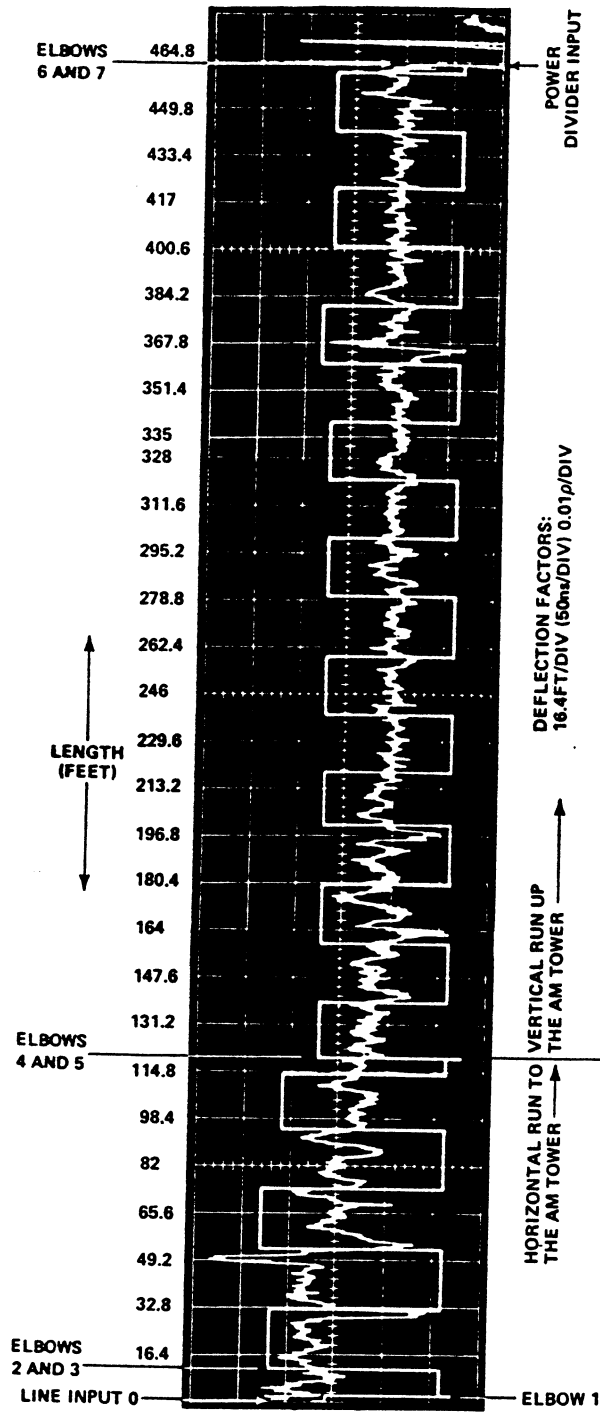


Fig. 5-16. Three-time-window impulse-TDR plot of FM station 466-foot-long transmission line.

transmission-  
line impulse-  
TDR plot

The whole transmission line, from the transmitter room to the antenna, is shown in Fig. 5-16 and consists of three photographs placed end-to-end. The first 120 feet of the line runs horizontally from the transmitter room to the base of an AM tower and is indicated in Fig. 5-16. Each 20-foot line section and three shorter sections are identified by what appears as a squarewave laced over the impulse-TDR plot. Also, each elbow location is identified. Note that the transmission-line junctions do not always produce a significant reflection.

In Fig. 5-16, the vertical-deflection factor of 0.01  $\rho$ /div means that the display shows only very small impedance deviations from the nominal 50- $\Omega$   $Z_0$ . To the untrained eye, the plot looks like the line is in terrible shape — in reality, it is in good shape, because the VSWR at the station frequency near 100 MHz is approximately 1.022:1. For example, the first significant negative pip (30 feet into the line) represents a resistive deviation from 50  $\Omega$  (reference taken about 25 feet into the line) by just -2.45  $\Omega$ , or it represents a momentary  $Z_0$  of 47.55  $\Omega$ . The TDR display shows 47.55  $\Omega$  for a period of time twice as long as the actual discontinuity, therefore 47.55- $\Omega$   $Z_0$  covers an actual time span of only about 5 ns. The transmitter frequency has a one-cycle time of about 10 ns, it therefore stands that the short-duration  $Z_0$  discontinuity does not cause a significant VSWR at the frequency of operation. However, the second major discontinuity, about 50 feet into the line, is inductive and will contribute to the overall system VSWR.

The major value of such a TDR plot is that it can be repeated periodically and helps foretell failures by comparing one plot against the next.

### HIGH-IMPEDANCE LONG-LINE TDR USING A STEP SIGNAL

Modern very high-voltage (AC or DC) power-distribution transmission lines can be evaluated for constancy of impedance very easily. Large distribution systems require that the high-tension open-wire lines have a fairly uniform characteristic impedance for the purpose of minimizing multiple high-voltage transient reflections at the occurrence of corona impulses or lightning discharges. There follows a short description of a special TDR system used by the College of Engineering Research Division, Washington State University, when testing a Bonneville Power Administration EHV DC test transmission line. The work was performed in 1967 and is described here with permission of both WSU and BPA.



A comparison of system displays is shown in Fig. 5-14. Fig. 5-14A shows a Type 1S2 1-volt-pulsar (normal use of the Type 1S2) display of a portion of the station transmission line which includes the antenna at the tower top. (The antenna is eight bays, fed at a common point by a 50-to-6.25- $\Omega$  power divider identified in Fig. 5-14A.) Fig. 5-14B shows the first third of the transmission line, also using the Type 1S2 1-volt pulsar but at a vertical-deflection factor of 0.01  $\rho$ /div. Fig. 5-13C shows the same portion of the transmission line at the same horizontal- and vertical-deflection factors but using the impulse-TDR system. Note that only the impulse-TDR display allows any analysis of the transmission line (the 100-MHz interference that makes up the major part of Fig. 5-14B prevents analysis of the line).

Both Fig. 5-14C and Fig. 5-15 show a falling slope (exponential in Fig. 5-15) which is due to improper adjustment of Type 1S2 sampling-gate "blowby" compensation and not to anything in the transmission line being tested.

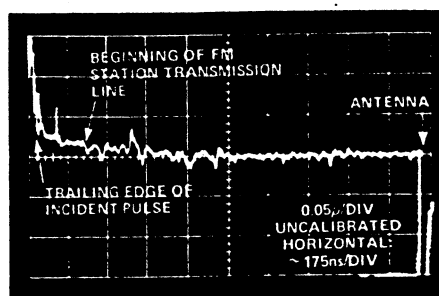


Fig. 5-15. Complete FM station line using impulse-TDR system.

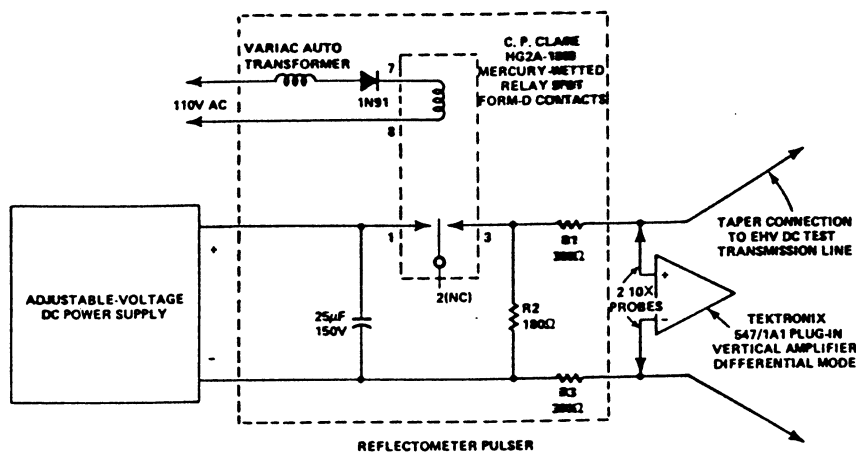


Fig. 5-17. WSU-BPA special Hg pulser and matching network used for testing an EHV DC test transmission line.

equipment

Fig. 5-17 shows the equipment used. The mercury-wetted relay was a make-before-break type that connected a fixed DC voltage to a matching network at the test-transmission-line input end. The incident step and reflection signals were monitored by a Tektronix Type 547 Oscilloscope with a Type 1A1 Plug-In. (A Type 109 Pulse Generator and a 500-series oscilloscope with a Type 1A5 can also be used. Suggested Type 109 connections are shown in Fig. 5-19.) Because the Type 1A1 was not designed for high common-mode signal rejection, it was necessary to vary the 60-Hz amplitude to the mercury relay. The change in 60-Hz amplitude provided a limited phasing adjustment between the pulse time and the common-mode 60 Hz of the test transmission line. (The Type 1A5 has a CMRR of 10,000:1 from DC through 1 MHz, well above the pulse repetition rate of a Tektronix Type 109 Pulse Generator – allowing the Type 109 ~750-Hz repetition rate to be useful without special regard for the 60-Hz common-mode interference. A 60-Hz pulser should be used if the oscilloscope CMRR is too low.)

$Z_0$   
determined

Special tests were run on the transmission line to determine its characteristic impedance. The value was determined by TDR-pulsing the line and changing a far-end termination resistor until the line-end  $Z_0$  signal amplitude and the termination-resistor  $R_L$  signal amplitude were equal. After the impedance value (of 780  $\Omega$ ) was determined, then the driving and matching network was assembled to allow the incident pulse and reflection signals to be measured without significant re-reflections originating at the sending end. Those connections are shown in Fig. 5-17.

calibrating

A TDR plot and the EHV DC test-line profile are shown in Fig. 5-18. The vertical reflection coefficient was calibrated by first using an unterminated far-end and setting the oscilloscope controls and the DC power-supply voltage for a +1  $\rho$  amplitude between CRT graticule lines. Then the gain was increased to obtain the 0.066- $\rho$ /div display for the terminated line. The oscilloscope DELAY-TIME MULTIPLIER was used to move the “display window” along the line, allowing six successive photographs to be pieced together for the continuous TDR plot.

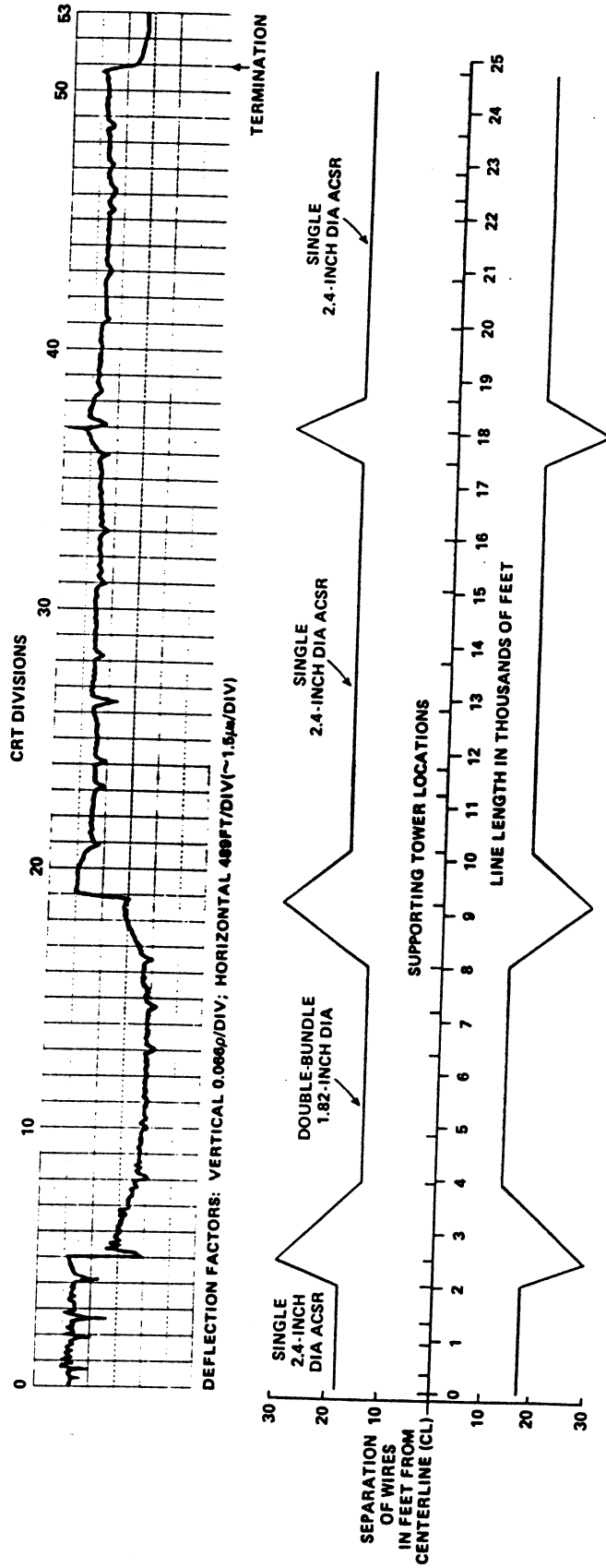


Fig. 5-18. TDR trace and line profile for BPA EHV-DC test line.  
By permission of WSU and BPA.

The line tested is a two-wire line with a single overhead ground conductor. Fig. 5-18 shows plainly the effects of towers and changing characteristic impedance along the line. Note that the line has considerable high-frequency attenuation and that ringing caused by the fast incident pulse, five divisions (2540 feet) into the line, is not repeated at other discontinuities farther down the line. Even though there was considerable high-frequency loss, the five-mile-line TDR plot provided much useful information to the EHV DC transmission-line design engineers.

We are grateful to Mr. James Logan of WSU for his cooperation in helping us include this report in this book on TDR measurements.

The Tektronix Type 109 will provide an approximate 750-Hz-pulse repetition-rate step signal for a similar high-impedance TDR test. Use the principles suggested by WSU and BPA and the diagram shown in Fig. 5-19. The 180- $\Omega$  resistor assures both a fixed load for the pulser and a current path for discharge of the long line between successive pulses. That resistor is not part of the source resistance during the time the step pulse is "up". The other two resistors, both 390  $\Omega$  in Figs. 5-17 and 5-19, provide a proper drive to the line and a balanced reflection measurement circuit to allow differential cancellation of any common-mode 60-Hz (or other) interfering frequency. All three resistors discharge the line between pulses. The pulse duration will be slightly longer than 0.5 ms, allowing TDR of lines about 0.25-ms long (air dielectric: 0.25 ms  $\cong$  16,000 feet).

NOTE: All remaining applications apply to unbalanced TDR test equipment such as the Tektronix Type 1S2 Reflectometer.

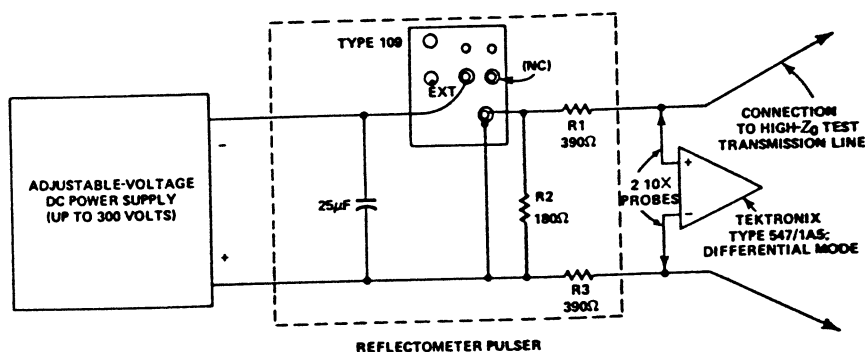


Fig. 5-19. Type 109 Pulse Generator special application for driving high- $Z_0$  transmission-line TDR system.

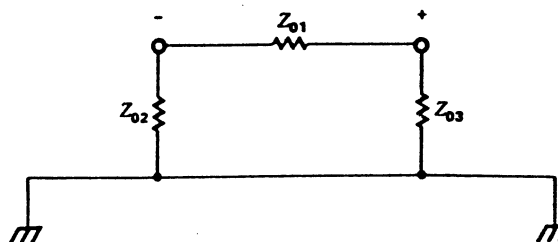


Fig. 5-20. Parallel transmission-line impedance relationships between conductors, and between individual conductors and a ground plane.

### CHECKING BALANCED LINES USING THE TYPE 1S2

The unbalanced (coaxial) output of the Type 1S2 can be used to check balanced (parallel or twisted pair) lines by using special connections. Such TDR testing is described briefly as checking each side individually against ground while the other side is grounded. Fig. 5-20 shows a normal two-wire line near a ground plane. Note that there are three resistors drawn, each resistor representing a  $Z_0$  value. Thus, with the Type 1S2 frame always grounded through the power cord, the unit cannot properly drive such a balanced-line system by directly connecting the two halves of the line to the output connector.

Assume the negative (-) lead of Fig. 5-20 is connected to both the ground plane and the Type 1S2 output-connector outer conductor. The positive (+) lead is driven by the Type 1S2 output-connector center conductor. Even if the line is useful (without a failure) and it is properly terminated by  $Z_{01}$ , a TDR display will indicate that the line is incorrectly terminated. This is because  $Z_{02}$  is in parallel with  $Z_{01}$ . Thus, testing of this type requires checking both sides of the line and then observing the two displays for dissimilarities. Such testing can determine which side contains a fault and locate where an open line is open.

### TESTING FOR FAULTS IN COAXIAL CABLES CONTAINING 60-Hz INTERFERENCE

An excellent example of 60-Hz interference was encountered in a CATV (Community Antenna Television) 3/4-inch-diameter 75- $\Omega$  distribution system. (The coaxial cable has a solid-aluminum outer conductor.) State electrical safety codes often require that such a cable, strung between power poles, be connected to the individual-power-pole ground return lead. Those ground return leads often carry enough 60-Hz current of different magnitudes to introduce a significant 60-Hz current in the coaxial-cable outer conductor. The case checked showed about 1-V (into 1 M $\Omega$ ) 60 Hz between cable conductors when the line was terminated in 75  $\Omega$  about 2200 feet away; the line also showed about 0.5-V (into 1 M $\Omega$ ) 60 Hz when the far end was *not* terminated.

A low-inductance 500-pF capacitor was placed in series with a 50- $\Omega$  insertion-unit center conductor (insertion-unit part number is located on page 91) and the unit was placed at the Type 1S2 output. 500pF has an  $X_C$  of about 5  $M\Omega$  at 60 Hz, thereby isolating the line 60 Hz from the Type 1S2 50- $\Omega$  input. The TDR display is now a normal fast step with a 50-ns time-constant charge of the 500-pF capacitor. 50-ns time constant gives about a 350-ns exponential curve. The curve lasts for an air-dielectric line length of about 100 feet. Therefore, after 100 feet of the line being tested have been displayed, the trace is back at zero volts. Thereafter, any discontinuity will cause a return-pulse echo which allows a fault location to be determined.

Once the 60 Hz was eliminated, the quality of the whole 2200 feet of line was effectively evaluated. A customer signal-takeoff tee showed ringing, and the far-end open or short circuit (test condition) returned an impulse that was about 75% the amplitude of the 1-V incident pulse.

## TDR USES IN THE CATV INDUSTRY

TDR test equipment can prove very valuable in the CATV industry for use as a system maintenance aid. It does not, however, have great value for testing cables before installation. Other types of test equipment do a significantly superior analysis of a coaxial cable's attenuation over the band of frequencies used in CATV. TDR equipment does permit the quick location of a cable break or the location of a defective customer takeoff tee that is just bad enough to bother the other customers on the same feeder line.

The relationship between a step pulse and its sinewave-frequency content is discussed at the beginning of Chapter 2. That information describes why it can be misleading to claim that TDR test equipment (step-pulse or impulse) can test a coaxial cable over a band of frequencies equal to the Fourier frequency content of the incident signal.

Any person wishing to further understand how the CATV industry checks out a coaxial cable before installation should read Chapter 10, "Sweep Frequency Testing of Coaxial Cables", *Technical Handbook for CATV Systems*, (Philadelphia, Pennsylvania: 1968) Jerrold Electronics Corporation. That chapter, plus other information in the handbook, supplies a wealth of information for the serious CATV system engineer.

Proper use of the Tektronix Type 1S2 requires that the 1-ns  $t_r$  pulse be used, not the 50-ps  $t_r$  pulse. The 1-ns risetime pulse contains frequencies up through about 350 MHz and will not cause propagation mode changes at discontinuities. The faster pulse will sometimes give trace information that is not significant to the CATV user and, therefore, should not be used. In all uses, *check that there is no AC or DC voltage on the coaxial cable before connecting it to the TDR unit.*

## TDR USED TO TUNE VHF POWER AMPLIFIER

One of the more unique applications of step-pulse TDR testing is the adjustment of both the grid and plate lines of a high-power, broadband, VHF transmitter power amplifier. The amplifier uses several tubes in parallel in a normal distributed-amplifier configuration. If the distributed amplifier grid and plate lines are terminated in their characteristic impedance, then a TDR unit can be used while the adjustable line elements are tweaked. The distributed lines do not have to be  $50\text{-}\Omega Z_0$  for the Tektronix Type 1S2 to be useful. As each adjustment is made (all DC power off, but probably with the heaters and bias supplies on), the TDR display will accurately report the true  $Z_0$  throughout the line.

## SIGNAL-GENERATOR OUTPUT IMPEDANCE

The Type 1S2 can be connected to the output terminal of a signal generator to measure its output impedance. If the generator output signal can be turned off while keeping the output circuit active, a clean TDR display can be obtained.

## BROADBAND-AMPLIFIER INPUT IMPEDANCE

Fig. 5-21 shows two TDR pictures of the input circuit of a broadband amplifier. The power was on when Fig. 5-21A was taken to show the good impedance match into a common-base amplifier. The power was off when Fig. 5-21B was taken to show the transistor emitter spatial location.

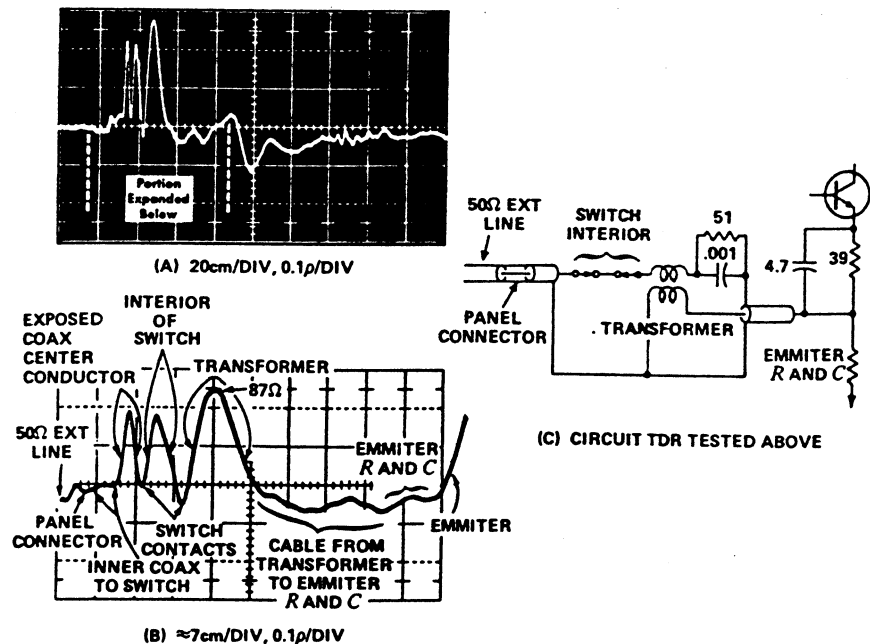


Fig. 5-21. TDR view of broadband-amplifier input circuit.

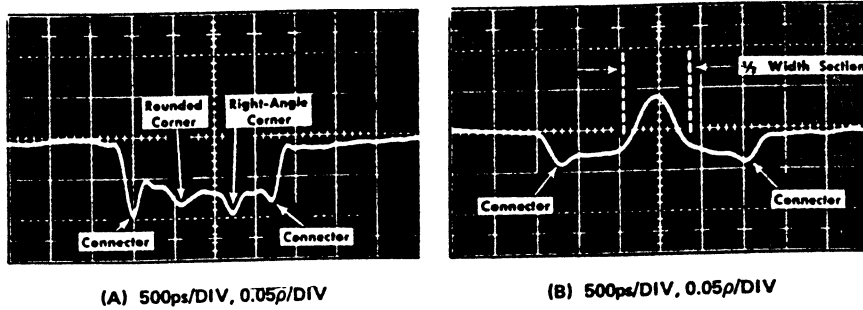


Fig. 5-22. Circuit board assembly  $Z_0$  checked by TDR.

### CIRCUIT-BOARD LEAD IMPEDANCE

Fig. 5-22A shows changes in characteristic impedance of leads along a circuit board assembly. (The board reverse side was fully plated.) The major dip is due to a right angle corner while the minor dip is due to a rounded corner.

Changes in characteristic impedance due to a change in lead width is also plainly seen by TDR. Fig. 5-22B shows an inductive section of line when the physical width of the line was reduced one half for a length of about 1.25 inches.

### FREQUENCY COMPENSATION OF LOSSY CABLES

A lossy coaxial cable connected between one of the Type 1S2 pulsers and the sampler (terminated) permits a view of the cable output signal. Fig. 5-23 shows the same lossy cable described earlier with Fig. 3-8. The top exposure shows how the cable distorts the Type 1S2 1-V pulser while the lower waveform is flatter, because a simple RC compensation network was placed between the pulser and the cable. The TDR unit will permit testing of such compensation networks.

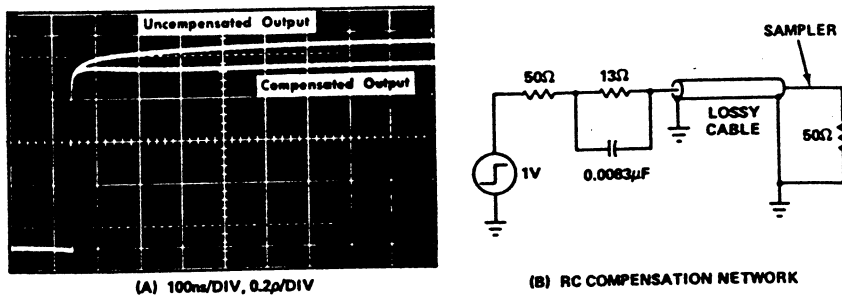


Fig. 5-23. Simple frequency compensation for lossy coaxial cable.



## EVALUATION OF FERRITE BEADS AND CORES

Ferrite beads and cores can be evaluated using the Type 1S2. Simple inductors wound on toroidal ferrite cores are represented by an equivalent circuit which is essentially an inductance in *parallel* with a resistance. The resistance results from core losses and may be typically as low as  $10$  to  $30 \Omega/(\text{turn})^2$ . Both the resistance and inductance characteristics of ferrites can be seen in a TDR display.

Fig. 5-24 shows two displays and the special adapter jig used to test a ferrite bead. The adapter jig is made from half of an insertion unit (Tektronix PN 017-0030-00). The end of the center piece was flattened and a formed piece of #10 copper wire was soldered in place with a ferrite bead included. Thus, there is only a small diameter change of the  $50\text{-}\Omega$  center conductor (pip in both displays) and one turn through the ferrite center. (Use smaller wire for smaller beads.)

Fig. 5-24A shows the basic display.  $L/R$  time-constant analysis is similar to that of Fig. 5-4 and formula (5) of Table 5-5, except the core  $R$  is in parallel with the driving-line  $Z_0$ .

Fig. 5-24B shows the ferrite bead resistance as  $-0.16 \rho$ , or  $36 \Omega$ . (The  $36 \Omega$  is read directly from the curve of Fig. 3-5.) The resistance value of a core is read by finding the curve knee (as marked in Fig. 5-24B) where the inductance effect becomes obvious. The positive pip is ignored.

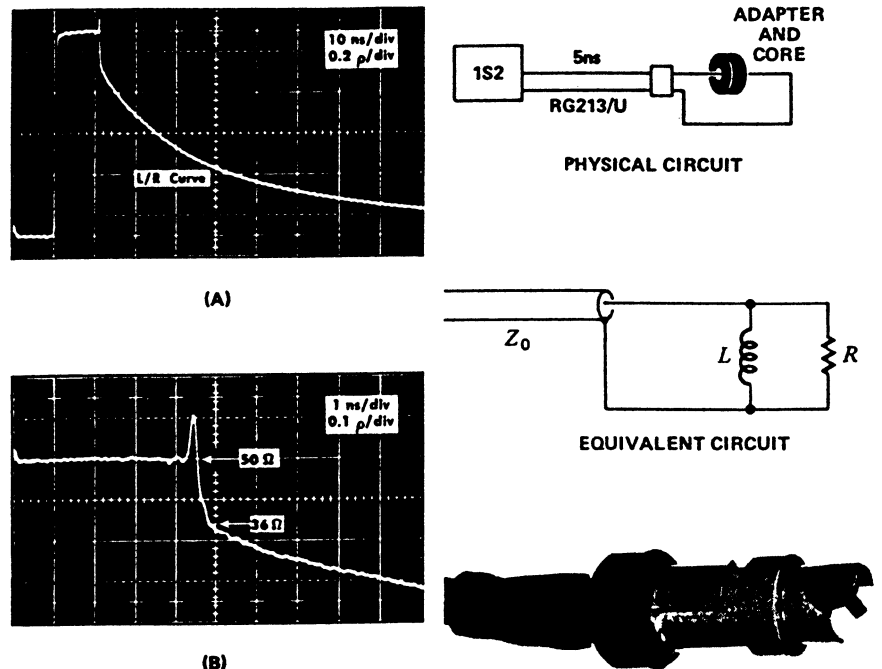


Fig. 5-24. Evaluation of a ferrite core.

## ARTIFICIAL DELAY-LINE BALUN USE IN TDR

The above title is an interpretation of the time-stretch abilities of a magnetic core when used in a coaxial unbalanced-to-balanced pulse transformer. Fast-step-transition pulse transformers are described in detail in an article by C. N. Winningstad<sup>2</sup>. The opening summary of that article is included here:

“The transmission-line approach to the design of transformers yields a unit with no first-order risetime limit since this approach uses distributed rather than lumped constants. The total time delay through the transmission-line-type transformer may exceed the risetime by a large factor, unlike conventional transformers. The extra winding length can be employed to improve the low-frequency response of the unit.

Transformers can be made for impedance matching, pulse inverting, and DC isolation within the range of about 30 to 300 ohms with risetime of less than  $0.5 \times 10^{-9}$  seconds ( $<1/2$  ns), and magnetizing time constants in excess of  $5 \times 10^{-7}$  seconds ( $>500$  ns). Voltage reflection coefficients of 0.05 or less, and voltage-transmission efficiencies of 0.95 or better can be achieved.”

A 50- $\Omega$  to 186- $\Omega$  balun is described in which two 93- $\Omega$  coaxial cables and a toroidal core are used. The basic circuit is included in Fig. 5-25A. In the case constructed, the 50- $\Omega$  to higher  $Z_0$  conversion turned out to be a little greater than 186  $\Omega$  — probably due to the 93- $\Omega$  coaxial cables having a  $Z_0$  greater than their nominal value.

step-signal  
source

impulse-signal  
source

Two uses of the balun are shown. A step-signal source, such as a Tektronix Type 1S2, is used in Fig. 5-25A and Fig. 5-26. Note that the  $L/R$  magnetizing time constant of the core produces a nonflat display for a constant-impedance 186- $\Omega$  transmission line (Fig. 5-26A). An impulse-signal source, such as a Tektronix Type R293 and a sampling oscilloscope in an automated measurement system, is used in Fig. 5-25B and Fig. 5-27. Note that the impulse system does not show the  $L/R$  magnetizing time constant of the core when measuring a constant-impedance 186- $\Omega$  transmission-line termination impedance (Fig. 5-27A).

<sup>2</sup>C. Norman Winningstad, “Nanosecond Pulse Transformers”, *IRE Transactions on Nuclear Science* (March, 1959), NS-6, no. 1, pp. 26-31. Tektronix PN 061-0992-00 for reprints.

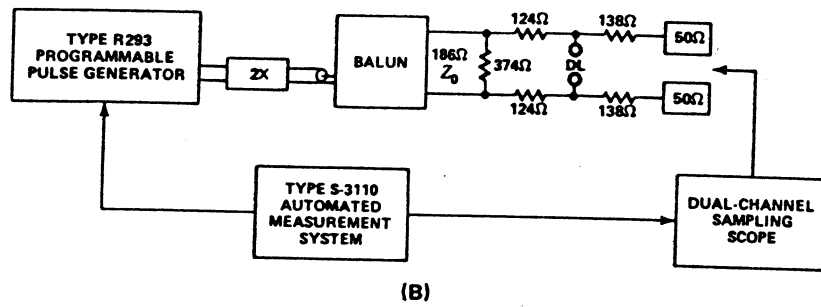
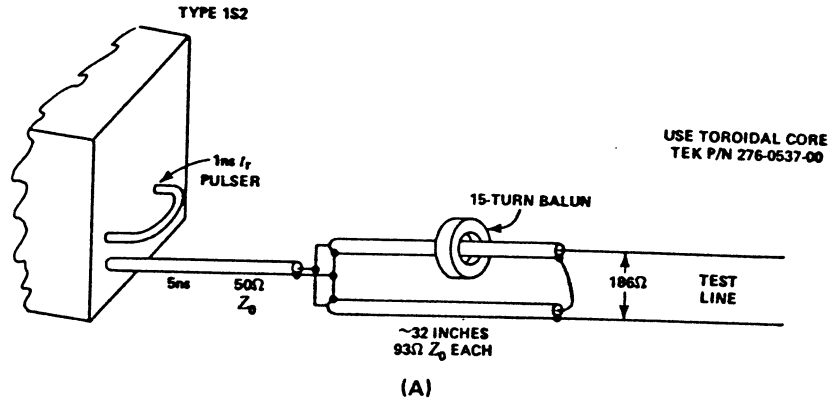


Fig. 5-25. Two TDR systems for checking plug-in-type delay lines. Examples are capable of testing 186-Ω balanced lines.

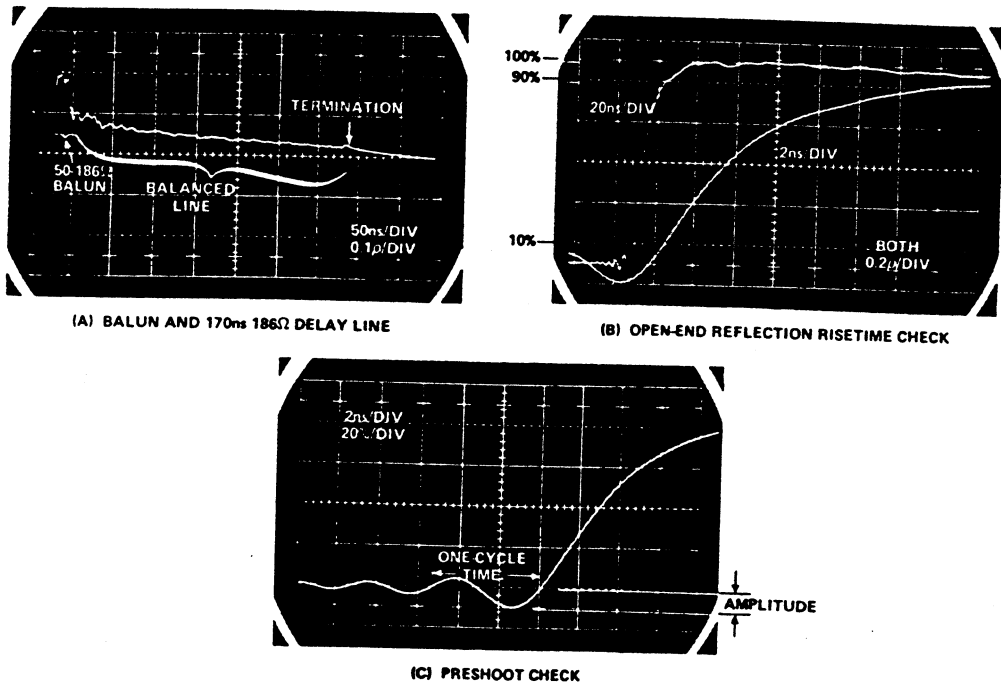
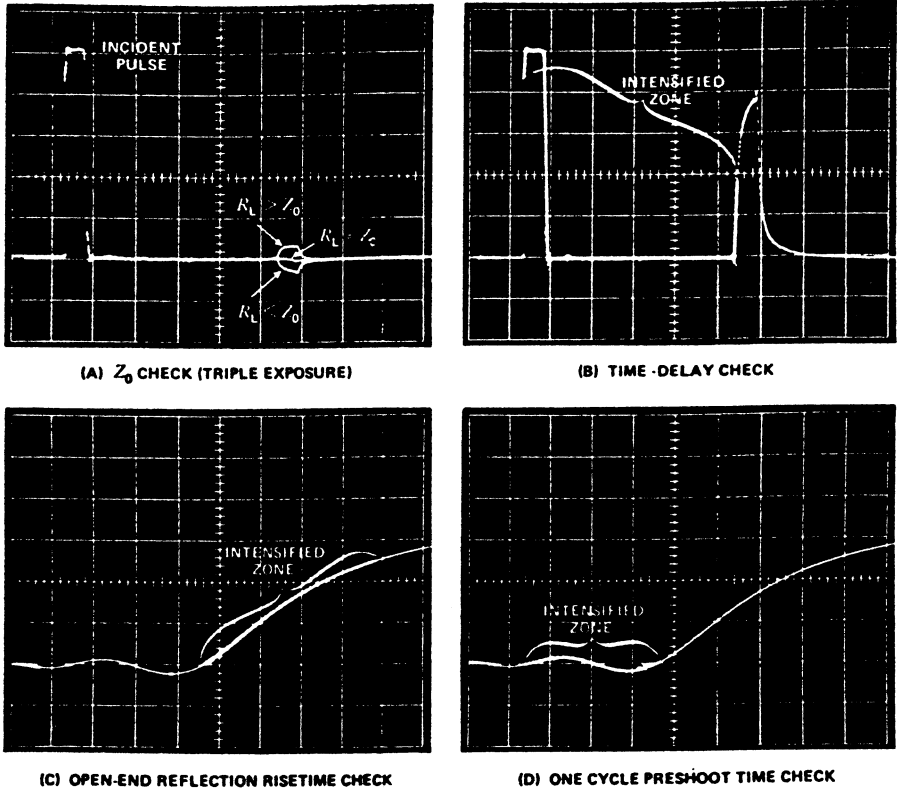


Fig. 5-26. Step-signal TDR (Type 1S2) testing of 186-Ω balanced line. (See Fig. 5-25A.)



**Fig. 5-27. Impulse-signal TDR (Type R293 Pulse Generator and an automatic system) testing of 186- $\Omega$  balanced line. (See Fig. 5-25B.)**

One use of either "balun TDR system" is testing "plug-in"-type balanced delay lines. The line tested in Figs. 5-26 and 5-27 is used in several 500-series Tektronix oscilloscope vertical amplifiers. It is, however, not uncommon to use multiple-tapped delay lines in computers with a tap at each 20 ns along a 200-ns line. The delay to each tap is important and can be quickly measured by an automatic system such as a Tektronix Type S-3110. Such a computer plug-in-type delay line may be tested with a driving pulse that has about a 10-ns risetime, then the system can quickly check a reflected open-circuit risetime (Fig. 5-27C) to be less than some specified number (like 20 ns). (It is common in computer plug-in delay lines to make the risetime measurement between the 20% and 80% amplitude points instead of the 10%-to-90% points as is done in oscilloscope work. Losses through a delay line can also be specified for automatic testing.)

In summary, this TDR application is useful in a production area where untrained personnel do the testing, because an automatic system detects limits specified for the line being tested.



## 6

## A COMPARISON OF SINEWAVE TESTING AND VOLTAGE STEP-FUNCTION TESTING OF COAXIAL TRANSMISSION LINES

Frequency-domain reflectometers, the slotted line and bridges, drive and observe the input terminals of a transmission line as a function of frequency. They do not locate discontinuities on a distance basis. As a result, measurement techniques and unique advantages with such devices differ from those of TDR.

cannot locate  
perfect termination

locating  
small reactances

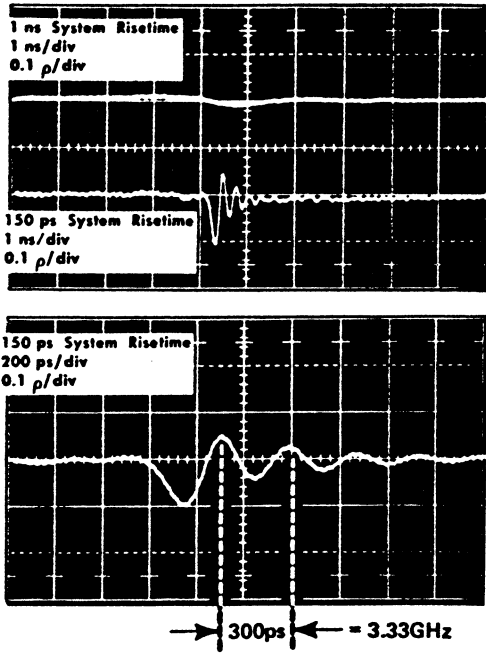
TDR, FDR  
comparisons

A pure resistance measured by either time-domain or frequency-domain devices will appear as an infinitely long lossless transmission line. Thus, a perfectly terminated short length of lossless line will yield the same information to both kinds of testing; neither test system can locate the termination. However, if the termination includes a small inductive or capacitive reactance, both systems will indicate its presence, but the TDR system will show where in the line the reactance is located.

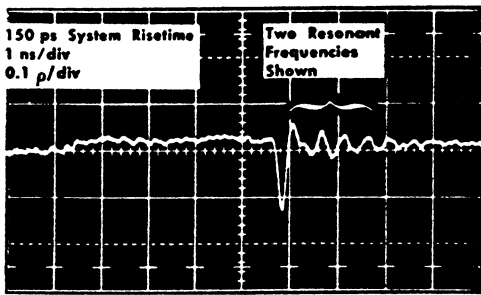
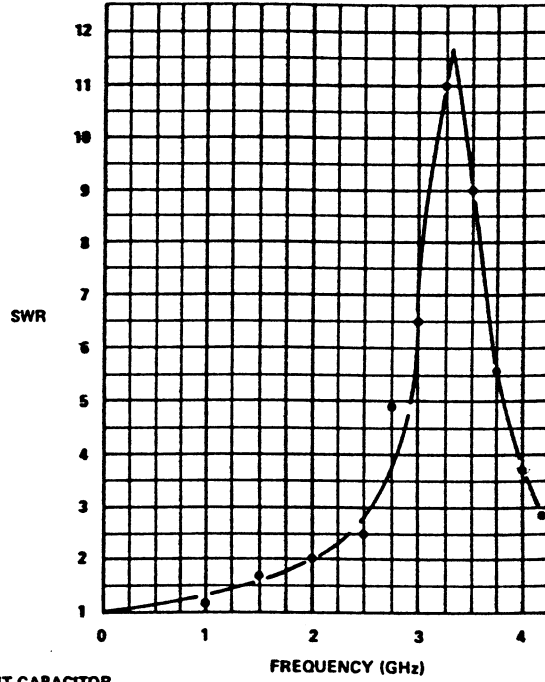
The following comparisons of TDR and frequency-domain (FDR) devices are supported by four specific examples and illustrations.

- 1) FDR measures standing-wave ratio (SWR) directly, but a TDR display can speed FDR testing by locating resonant frequencies of resonant networks prior to FDR testing.
- 2) TDR locates discrete discontinuities and permits analysis of their values. But FDR will indicate two different resonant discontinuities which may be located very close together — TDR may not.
- 3) FDR measures an antenna standing-wave ratio directly while TDR will not. Should a change in SWR indicate problems, TDR will locate faults more quickly and identify the type of fault more rapidly than will FDR. The time-domain display will validate a transmission line to an antenna, while frequency-domain reflectometry cannot, unless the antenna is disconnected and the transmission line terminated.
- 4) TDR can locate small changes in transmission-line characteristic impedance (such as a too-tight clamp holding a flexible line), while FDR will show whether or not the SWR is acceptable.
- 5) Both test systems will quantitatively evaluate single discrete reactances — a higher degree of accuracy is possible with FDR.
- 6) Both TDR and FDR have advantages, each being very valuable in its own way. Thus, the two systems complement each other and both aid where observations and measurements are required.

complementary  
systems



(A) SINGLE SHUNT CAPACITOR



(B) TWO SHUNT CAPACITORS

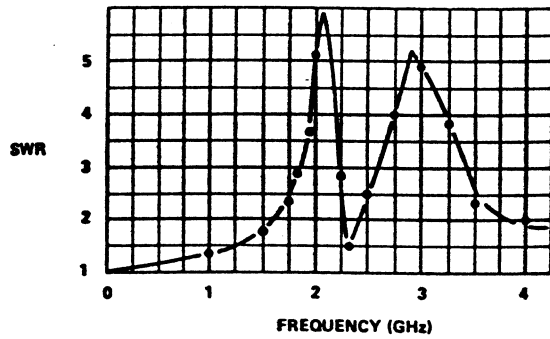


Fig. 6-1. Two examples of discrete shunt capacitors.

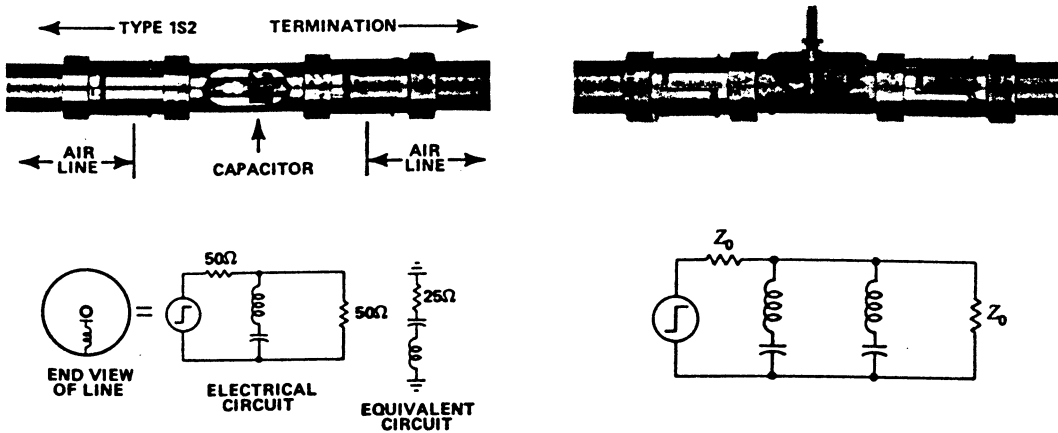


Fig. 6-2. Capacitors measured in Fig. 6-1.



## TDR VERSUS FDR MEASUREMENTS

single  
capacitor

A 1-pF discrete capacitor inserted in parallel with a transmission line will produce almost no TDR indication if the step pulse has a risetime of 1 ns. The same capacitor will produce a significant reflection if the step pulse has a risetime of 150 ps. An FDR test will produce a large SWR at the series resonant frequency determined by the capacitance and its lead inductance. Such a discontinuity would require considerable time for proper FDR testing because of numerous frequency test points, but with a fast-rise TDR system, the capacitance, resonant frequency and spatial location can be quickly determined.

two  
capacitors

Fig. 6-1 shows waveforms and SWR curves of first a single capacitor and then of two capacitors inserted in parallel with a transmission line. Note that the FDR measurement on the right side of Fig. 6-1B plainly shows the two resonant circuits of the two closely spaced small capacitors, while the TDR display at the left shows two resonant frequencies but not in a manner permitting separation of the two capacitors.

The single capacitor used for Fig 6-1A was made of 1/4-inch-wide strip copper, 5/8-inch long, with one end soldered to the side of a component insertion unit (Tektronix PN 017-0030-00) and the other end near the center conductor. The insertion unit was modified to have a continuous center conductor using three inner transition pieces (Tektronix PN 358-0175-00). One of the inner transition pieces was shortened to fit between the two mounted end pieces and then soldered into place. The second capacitor (resonant at 2.1 GHz) was a 0.5- to 1.5-pF piston trimmer with a total lead length of about 5/16 inch. It was adjusted to about 1.2 pF. The piston capacitor was soldered in place in parallel with a strip copper capacitor about 1/8 inch away. It is obvious from both testing methods that neither capacitor was critically damped by the characteristic impedance of the transmission line. The physical and equivalent circuit of the single shunt capacitor is shown in Fig. 6-2. The single capacitor test was made with a shield in place completely covering both openings.

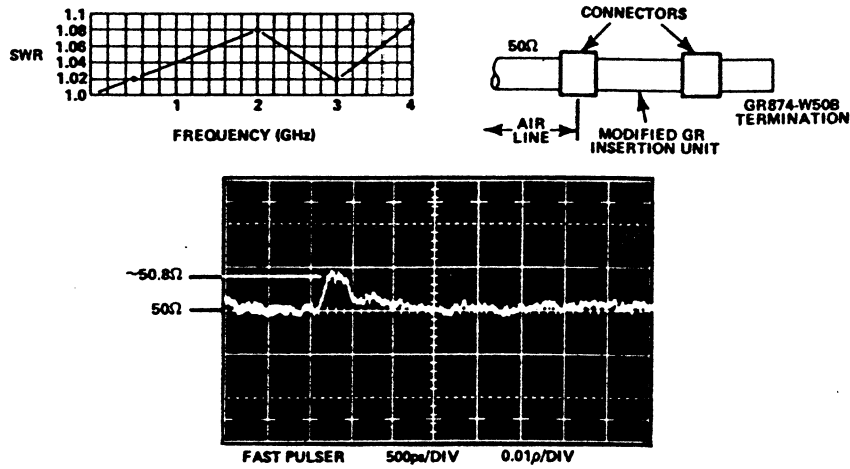


Fig. 6-3. Modified (through-connected) Tektronix insertion unit for testing small components in parallel with 50-Ω line.

locating off-impedance points

Fig. 6-3 shows the ability of TDR to locate an off-impedance point in a transmission line and to quickly resolve its value. The same through-connected insertion unit used in Fig. 6-1A was tested without any component inserted in it. The shield was in place for both TDR and FDR testing.

The TDR display in Fig. 6-3 shows the increased characteristic impedance due to the increased diameter of the outer conductor at the two cutout access slots. Such a TDR display will permit rather rapid correction to be made to the center conductor diameter, if a truly constant impedance through the length of the insertion unit is desired.

The SWR curve shows some changes from a constant-impedance transmission line, but does not help to locate an aberration if it is inside a continuous piece of cable. Either FDR or TDR would help the unit to have a constant impedance, if such a unit were being designed.

TDR timesaving for FDR

Fig. 6-4 shows two TDR and two SWR plots of a simple dipole antenna. The TDR waveforms at the left were photographed first, quickly locating the two radiating resonant frequencies and saving time for the FDR testing. The SWR curves permit a direct evaluation of the antenna radiation

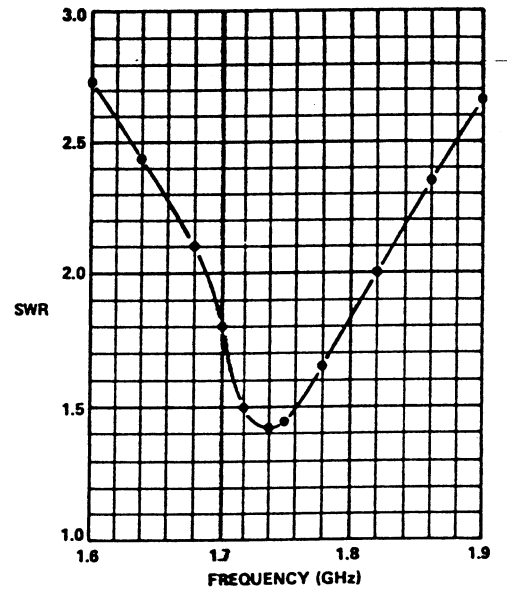
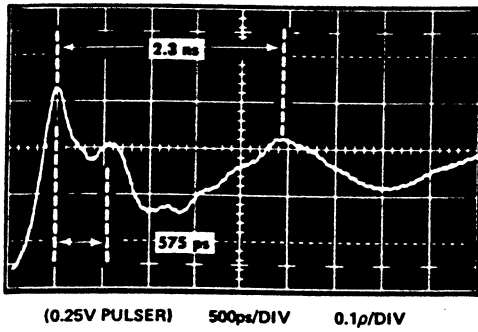
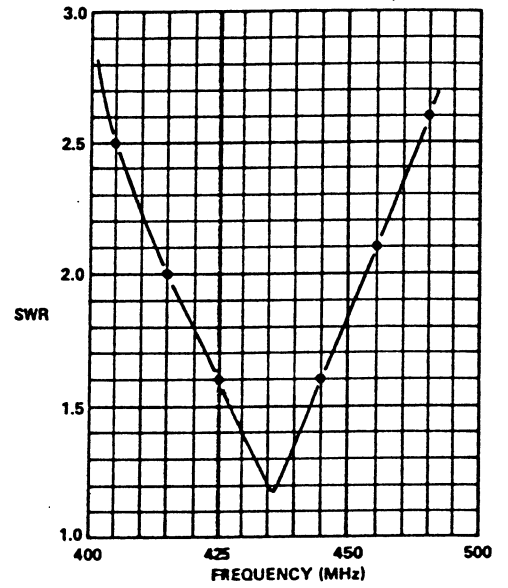
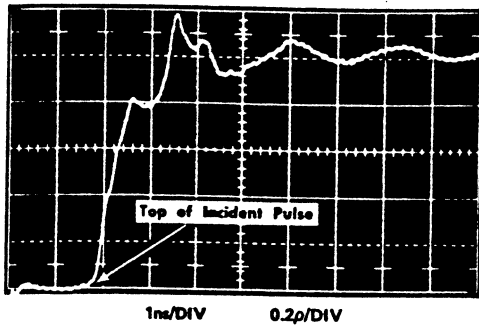
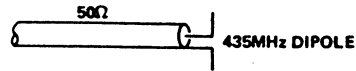
resistance ( $\frac{R_L}{Z_0} = \frac{V_{max}}{V_{min}}$ , if  $R_L$  is purely resistive), while the TDR display

FDR use in antenna design

tells only the transmission-line quality and the radiating resonant frequencies of the nonshorting-type antenna. An antenna-design engineer could use the SWR data and FDR equipment for testing a compensating network to be located at the antenna for minimizing standing waves in the transmission line. The TDR system cannot be used for such design assistance.

TDR SHOWS OPEN CIRCUIT

SWR SHOWS ACCEPTABLE  
ANTENNA RADIATION  
RESISTANCE



ANTENNA RESONANT FREQUENCIES  
SEEN BY TDR:

$$\text{(FUNDAMENTAL) } f = \frac{1}{2.3 \times 10^{-9}} = 435\text{MHz}$$

$$\text{(FOURTH HARMONIC) } f = \frac{1}{575 \times 10^{-12}} = 1740\text{MHz}$$

Fig. 6-4. Two plots of 435-MHz dipole antenna.

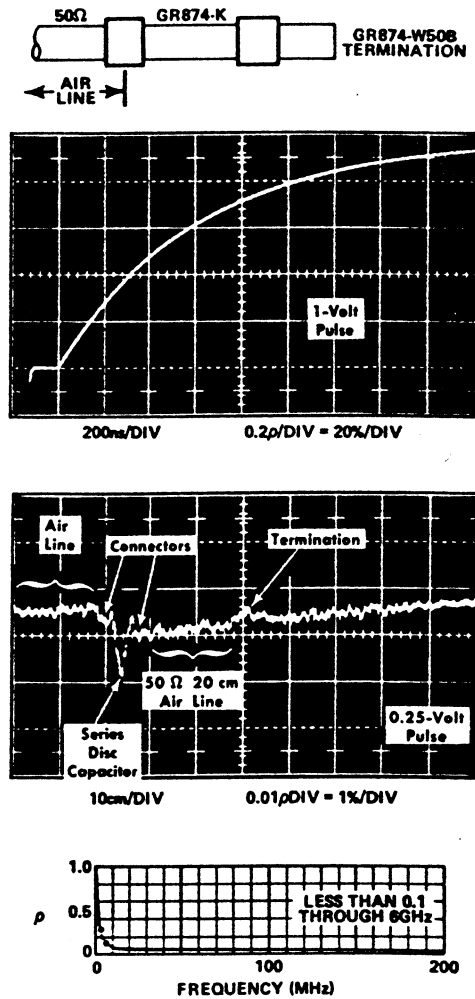


Fig. 6-5. Series blocking capacitor: General Radio Type 874-K.

combining  
TDR and  
FDR tests

Fig. 6-5 shows both TDR and FDR tests of a General Radio Type 874-K series blocking capacitor. The upper TDR display permits direct calculation of the series capacitance, in this case approximately 6.2 nF (0.0062 μF).

The SWR curve shows that the series capacitor does not upset the transmission line significantly except for low frequencies. The middle TDR waveform shows the change in characteristic impedance due to the physical shape of the series capacitor. Note that the disc capacitor reduces the transmission-line characteristic impedance to approximately 49 Ω for only a very short period of time. The same display also permits the precise location of adjacent discontinuities that affect the high-frequency performance. The combined TDR and FDR data tells more about the series capacitor unit than either testing method does alone.

## APPENDIX A

**Derivation Of Second Resistive-Reflection  
Impedance Formula ( $Z_2$ ) In TDR Measurements**  
by Gordon D. Long

Application of formula (5) derived below is found at the end of Chapter 3, page 36.

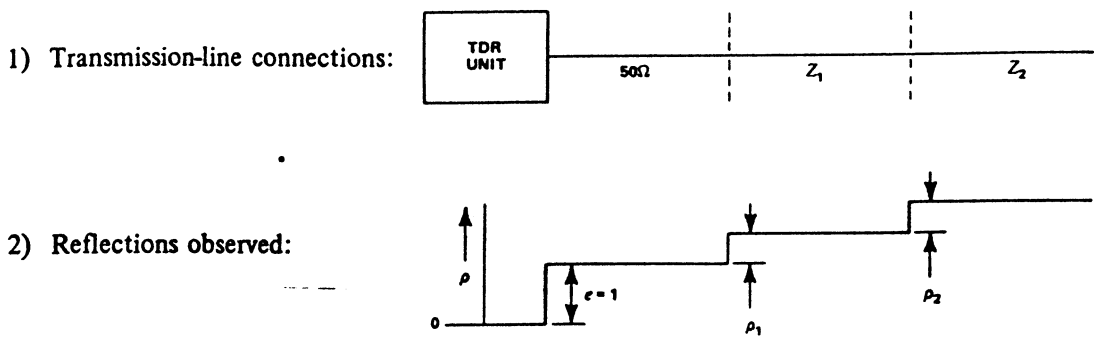


Fig. A-1.

where:  $\rho_1$  is reflection of  $Z_1$  relative to  $50 \Omega$ ,

$\rho_2$  is observed reflection of  $Z_2$  relative to  $Z_1$  (the second reflection).

3) When the incident step is normalized to unity:

The step amplitude transmitted to line  $Z_1$  is

$$V_{1f} = \frac{2Z_1}{Z_1 + 50}$$

The reflection coefficient between  $Z_2$  and  $Z_1$  is

$$\rho_1 = \frac{Z_2 - Z_1}{Z_2 + Z_1}$$

The transmission of return voltage from  $Z_1$  to  $50 \Omega$  is

$$V_{1r} = \frac{2 \times 50}{Z_1 + 50}$$

Thus, the observed second reflection is

$$\rho_2 = V_{1f} \times \rho \times V_{1r}$$

Substituting terms,

$$\rho_2 = \frac{2Z_1}{Z_1 + 50} \times \frac{Z_2 - Z_1}{Z_2 + Z_1} \times \frac{2 \times 50}{Z_1 + 50}$$

$$\rho_2 = \frac{200Z_1}{(Z_1 + 50)^2} \times \frac{Z_2 - Z_1}{Z_2 + Z_1}$$

4) Solving for  $Z_2$  in terms of  $Z_1, \rho_2$ :

$$\rho_2(Z_1 + 50)^2(Z_2 + Z_1) = 200Z_1(Z_2 - Z_1)$$

$$\rho_2(Z_1 + 50)^2 Z_2 + \rho_2(Z_1 + 50)^2 Z_1 = 200Z_1 Z_2 - 200Z_1^2$$

$$\rho_2(Z_1 + 50)^2 Z_1 + 200Z_1^2 = 200Z_1 Z_2 - \rho_2(Z_1 + 50)^2 Z_2$$

$$Z_1 [200Z_1 + \rho_2(Z_1 + 50)^2] = Z_2 [200Z_1 - \rho_2(Z_1 + 50)^2]$$

$$Z_2 = (Z_1) \frac{200Z_1 + \rho_2(Z_1 + 50)^2}{200Z_1 - \rho_2(Z_1 + 50)^2} \quad (5)$$

APPENDIX B

Derivation Of Formula To Determine  
 Small Reactances Viewed By TDR  
 ("Small meaning no pure RC or L/R reflections  
 occur in particular test system.)  
 by H. Allen Zimmerman

PROBLEM:

Given a transmission line with a lumped series inductance somewhere midline, as shown in Fig. B-1, find an expression for  $L$  in terms of observable system parameters.

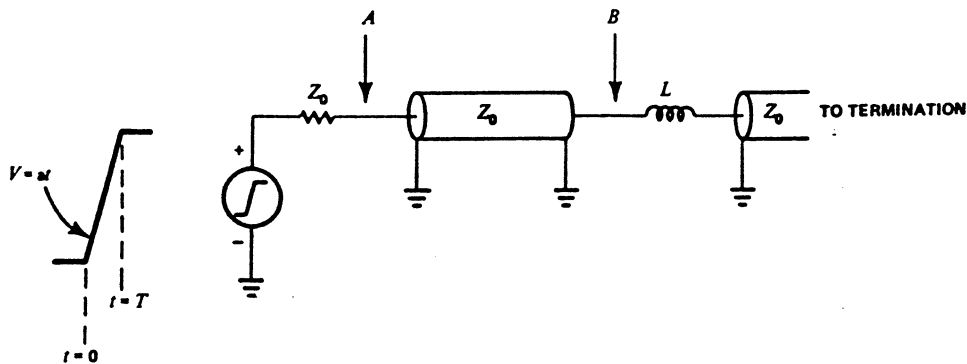


Fig. B-1.

SOLUTION:

Consider the equivalent circuit of Fig. B-2 where the transmission line has been eliminated. With this model, we may easily find an expression of  $i(t)$  through the inductor during application of the ramp. Since the same  $i(t)$  flows through the inductor in Fig. B-1 when the wavefront reaches  $B$ , we may later relate this  $i(t)$  back to the voltage waveform seen as a reflection at point  $A$ .

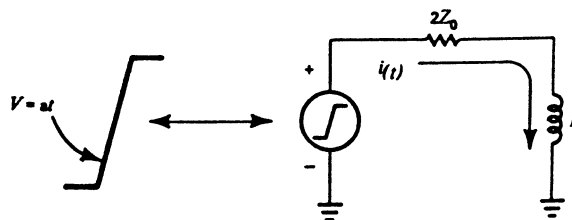


Fig. B-2.

Using the Laplace transforms of the driving waveform and the network impedance, we may write an expression for the transform of the current through the network:

$$I(s) = \frac{E(s)}{Z(s)} = \left(\frac{a}{S^2}\right) \left(\frac{1}{L_s + 2Z_0}\right) \quad (1)$$

or:

$$I(s) = \frac{a}{L} \left[ \frac{-L^2}{S^4 Z_0^2} + \frac{L}{S^2 2Z_0} + \frac{\frac{L^2}{4Z_0^2}}{S + \frac{2Z_0}{L}} \right] \quad (2)$$

which, when transformed back into the time domain, becomes:

$$i(t) = \frac{a}{L} \left[ \frac{L}{2Z_0} t - \frac{L^2}{4Z_0^2} \left( 1 - e^{-\frac{2Z_0}{L} t} \right) \right] \quad (3)$$

or:

$$i(t) = \frac{a}{2Z_0} t - \frac{aL}{4Z_0^2} \left( 1 - e^{-\frac{2Z_0}{L} t} \right) \quad (4)$$

Equation (4) thus describes the current in Fig. B-2 *during the ramp* only. At  $t = T$ , when the ramp ends, it can be shown that  $i(t)$  will settle exponentially from its value to  $t = T$  to the final, steady-state value determined by the steady-state supply voltage,  $aT$ , and the system resistance,  $2Z_0$ .

The equation which describes  $i(t)$  after  $t = T$  is given below:

$$i(t) \Big|_{t \geq T} = \frac{aT}{2Z_0} + \left( i(t) - \frac{aT}{2Z_0} \right) \frac{-2Z_0(t - T)}{L} \quad (5)$$

where  $i(T)$  is given by Equation (4) at  $t = T$ .

Equation (5) is included in this discussion to show that after the ramp ends at  $t = T$ , the current is given by an exponential with a time constant of  $\frac{L}{2Z_0}$  (derivation is left to the reader). Thus, for values of  $L$  which result in a time constant which is *greater than* 4 or 5 times the system risetime,  $L$  can be most easily determined by simply observing the exponential decay (starting at *any point after*  $t = T$ ) and calculating  $L$  from the formula:

$$L = 2Z_0 \times \text{time constant} \quad (6)$$



For values of  $L$  which are *less than* 4 or 5 times the system risetime, observation of the exponential may be distorted to the extent that Equation (6) may give poor results. In this case, another approach may be used as outlined below.

Consider the ramp waveform which travels from  $A$  to  $B$  in Fig. B-1.

When the wavefront arrives at  $B$ , the voltage at that point is given by:

$$\bar{V}(t) = at - Z_0 i(t) \quad (7)$$

where  $i(t)$  is given by Equation (4) and where  $t = 0$  is shifted to be the start of the ramp when seen at  $B$ .

The equivalent circuit of Fig. B-3 shows how the transmission line may be replaced by a lumped source of impedance  $Z_0$  for the purpose of deriving Equation (7).

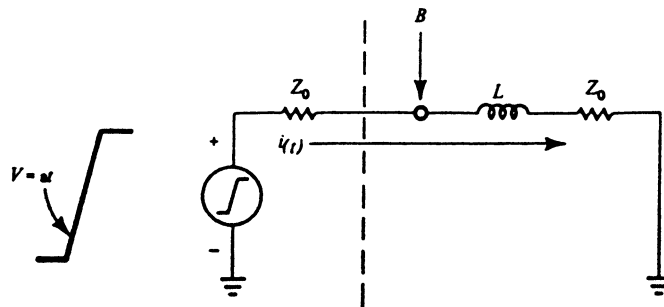


Fig. B-3. Transmission line viewed as "lumped source".

The reflected waveform, as seen at  $A$  in Fig. B-1, will be:

$$\begin{aligned} \sqrt{\text{reflected}} &= \sqrt{(t)} - \sqrt{\text{incident}} \\ &= (at - Z_0 i(t)) - \frac{at}{Z} \end{aligned} \quad (8)$$

and the reflection coefficient will be:

$$\rho(t) = \frac{\sqrt{\text{reflected}}}{\sqrt{\text{incident}}} \quad (9)$$

$$= \frac{\frac{at}{Z} - Z_0 i(t)}{\frac{at}{Z}} \quad (10)$$

$$= 1 - \frac{2Z_0 i(t)}{at} \quad (11)$$

Now, replacing  $i(t)$  in Equation (11) by the expression given in Equation (4), we get:

$$\rho(t) = \frac{L}{2Z_0t} \left( 1 - e^{-\frac{2Z_0t}{L}} \right) \tag{12}$$

The maximum value of  $\rho$  will occur at  $t = T$  and is given by:

$$\rho_{\max} = \frac{L}{2Z_0T} \left( 1 - e^{-\frac{2Z_0T}{L}} \right) \tag{13}$$

This equation is very difficult to solve for  $L$ , but a substitution of variable and graph provide a practical solution.

Let 
$$\alpha = \frac{L}{2Z_0T}, \tag{14}$$

Then 
$$\rho_{\max} = \alpha \left( 1 - e^{-\frac{1}{\alpha}} \right) \tag{15}$$
  
 (8 in Chapter 5)

where  $\alpha$  may be found for a given  $\rho_{\max}$  from the following table and graph:

$\rho_{\max}$	$\alpha$
0	0
0.100	0.1
0.199	0.2
0.459	0.5
0.632	1.0
0.787	2
0.9065	5
0.952	10
0.977	20
0.995	100

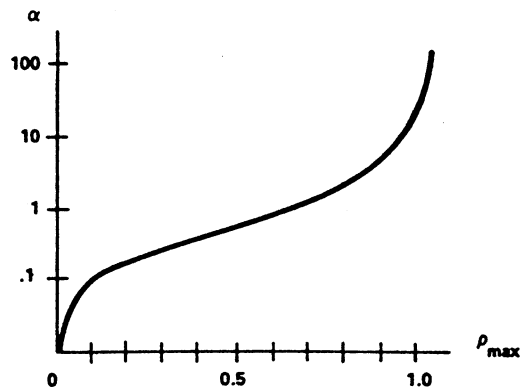


Fig. B-4.

(See Fig. 5-4 in Chapter 5.)

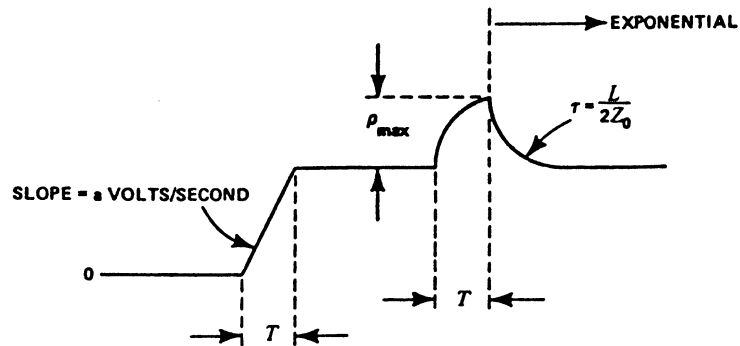


Fig. B-5.

To apply this, one observes the TDR display which resembles the idealized waveform of Fig. B-5 and notes the  $\rho_{\max}$ . From the graph in Fig. B-4, he then finds  $\alpha$ . Now the application of Equation (14) to find  $L$  presents a practical problem since  $T$  is, by definition, the 0-to-100% risetime of the ramp. Since our actual waveform will be fairly linear between its 10% and 90% points, let us say that:

$$0.8T \cong t_r \quad (16)$$

where  $t_r$  is the 10%-to-90% TDR-system risetime observed by opening or shorting the line at the discontinuity in question.

Then we can relate  $\alpha$  to  $L$  by:

$$L = 2.5\alpha Z_0 t_r \quad (17)$$

(7 in Chapter 5)

Note that a  $\rho_{\max}$  of 0.885 indicates that the ratio of the  $\frac{L}{2Z_0}$  time constant to system risetime is about 5:1. One would say that  $L$  should be calculated by this means when  $\rho_{\max} < 0.9$ .

**COROLLARY:**

A shunt-capacitance discontinuity presents a similar problem when  $\frac{CZ_0}{2}$  becomes short with respect to system risetime. A dual solution to the problem for which:

$$\alpha = \frac{Z_0 C}{2T} \cong \frac{Z_0 C}{2.5t_r} \quad (18)$$

or

$$C = \frac{2.5\alpha t_r}{Z_0} \quad (19)$$

(9 in Chapter 5)

where  $\alpha$  is still related to  $\rho_{\max}$  by the graph of Fig. B-4 obtained from a TDR display that resembles Fig. B-6.

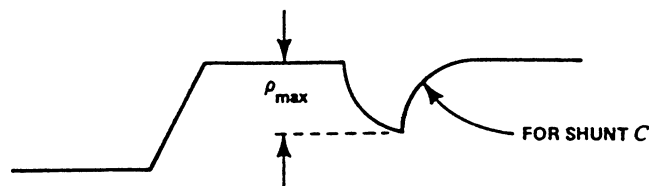


Fig. B-6.

**ASSUMPTIONS:**

The foregoing derivations have been based implicitly on the following assumptions:

- 1) That the actual TDR system may be adequately described by a model having a simple ramp as the pulse source and having a lossless transmission line and ideal sampler.
- 2) That the rounded corners of the actual step transition may be ignored.
- 3) That "dribble-up" line effects are not significant.
- 4) That the sampler is nonloading, nondistorting and of infinitesimal risetime.
- 5) That the element being analyzed is either pure  $L$  or pure  $C$  (e.g., there is no stray- $C$  across the series- $L$  or no stray- $L$  in series with the shunt- $C$ ).

## INDEX

- Amplitude resolution, 39, 41, 43
- Antenna design, FDR use, 92
- Balanced line, 3
  - impulse TDR, 79
- Balun, artificial delay-line, 84-87
- Braided coax, 7 losses, 5
- Broadband amplifier input impedance, 81
- Capacitance per unit length, 3, 7
- Capacitors, 57-60, 63, 66
  - large, 57-60
  - small, 63, 66
- CATV impulse TDR, 80
- Characteristic impedance,  $Z_0$ , 3-4, 6, 7
  - changes, 4
- Circuit-board lead-impedance, 82
- Coaxial cables, 11-20
  - distortion, 14-15
  - frequency response versus
    - pulse response, 11-20
  - load, as a, 8
  - long, 15-18
  - mode of propagation, 19
  - realizable, 5
  - short, 19
  - source, as a, 8-9
- Compensation networks, 82
- Component TDR, 53-68
  - versus FDR, 91
- Cores, ferrite beads and, 83
- Dielectric constant, 7-8
  - discontinuity, locating, 21-37, 68
- Dribble-up, 15, 18-19, 66
- EHV DC line impulse TDR, 75-78
- Fast pulse use, 12, 13
- Feedthrough configuration, 41
- Ferrite beads and cores, 83
- Fourier analysis, 12
- Frequency-domain reflectometry
  - FDR-TDR comparison, 89-94
- Frequency response versus
  - pulse response, coaxial cable, 11-20
  - translation, 11, 12
- Gaussian response, 11, 12
  - curve, 10
- High-frequency losses, 14, 15
- HV line impulse TDR, 68-75
- Impulse TDR, 68-87
  - balanced line, 79
  - balun, artificial delay-line, 84-87
  - broadband-amplifier input impedance, 81
  - circuit-board lead impedance, 82
  - compensation networks, 82
  - EHV DC line, 75-78
  - ferrite beads and cores, 83
  - HV line, 68-75
  - signal-generator output impedance, 81
  - 60-Hz interference, 79-80
  - VHF power amplifiers, 81
- Inductance per unit length, 3
- Inductors, 60-63, 65
  - large, 60-62
  - small, 63, 65
- In-line configuration, 42, 44-46
- Lossy inductor, 62
- Lumped-constant line, 3
- Matched-impedance TDR, 31
- Mismatch, reactive, 54-68
  - large, 54-62
  - small, 62-68
- Mismatched-impedance TDR, 30
- Mismatched tee configuration, 45, 49-51
- Mode of propagation, 19
- Non-reflection time-domain, 59
- Off-impedance, locating, 92
- Ohms/division, 24
- Percent error, 35
- Power-divider tee configuration, 45, 48-49
- Propagation, mode of, 19

- Pulse response characteristics, 14-17
- Pulse response versus frequency
  - response, coaxial cable, 11-20
  - translation, 11, 12
- Reactances, large, 54-62
- Reactances, small, 62-68
  - formula for determining, derivation, 97
  - limitations, 68
  - locating, 68, 89
  - measuring, 66
- Reactive mismatch, 54-68
  - large, 54-62
  - small, 62-68
- Reflection aberrations, 58
- Reflection amplitudes, 22-23
- Reflections, resistive, 26
- Resistive load, 24
- Resistive reflections, 26
- Resolution, TDR, 39-51
  - factors limiting, 40-41
- Rho ( $\rho$ ), 23-24
  - correction, 30-31, 35
- Rho/division calibration, 44-51
- Ringing, 57, 60-61
- Risetime, 11, 15-16
  - test-pulse, selection of, 19-20
- Second-discontinuity reflection
  - coefficient, 31-37
  - derivation of impedance formula, 95-96
  - known impedances, 33-35
  - unknown impedances, 35-37
- Series DC resistance, 5
- Signal-generator output impedance, 81
- Signal propagation velocity, 5-8
  - 60-Hz interference, 79-80
- Skin effect, 5-6
- Time constant, 54-57
- Time-domain reflectometry, 21-37
  - applications, 53
  - component testing, 53, 54-68
  - FDR-TDR comparison, 89-94
  - impulse testing, 68-87
  - major systems, 40, 44
  - resolution, 39-51
- Time resolution, 39, 41, 43
- Transient response, 14
- Transmission line, 3
  - capacitance per unit length, 3, 7
  - coaxial, realizable, 5
  - dimension changes, 4
  - dimension limits, 7, 8
  - EHV DC impulse TDR, 75-78
  - electrical characteristics, 3, 8-9
  - energy, 8
  - HV impulse TDR, 68-75
  - inductance per unit length, 3
  - losses, 5-6
  - nomograph, 8
  - signal propagation velocity, 5-8
- Unbalanced line, 3
- VHF power amplifier tuning, 81
- Voltage reflection coefficient, 23-24
  - correction, 30-37

## LIST OF ILLUSTRATIONS

- Fig. 1-1. "Lumped-constant" transmission lines. 3
- Fig. 1-2. Coaxial-transmission-line impedance nomograph. 8
- Fig. 2-1. An ideal (Gaussian) amplifier amplitude-versus-frequency response curve. 10
- Fig. 2-2. Double exposure. Pulse tests: (A) real-time oscilloscope, 50 ns/div; (B) sampling oscilloscope, 200 ps/div. 13
- Fig. 2-3. 50-MHz dispersion display of 1.5- $\mu$ s-duration 250-ps 10%-to-90% risetime pulse. 13
- Fig. 2-4. Coaxial-cable 0%-to-50% pulse risetime versus length. 16
- Fig. 2-5. RG213/U and RG63B/U ratios of  $t_0$  for 2X change in cable length. 17
- Fig. 2-6. RG11/U and RG213/U distortion to a step signal. Waveforms are reflections from cable open end. 18
- Fig. 2-7. "Dribble-up" output signals from 260-ft RG213/U. 19
- Fig. 2-8. Propagation-mode change in large-diameter transmission line when driven by the Type 1S2 fast pulser. 20
- Fig. 3-1. Circuits showing DC analogy of TDR. 21
- Fig. 3-2. Adding the time dimension to the circuit of Fig. 3-1. 22
- Fig. 3-3. Oscilloscope voltmeter displays for circuit of Fig. 3-2, dependent upon value of  $R_L$  versus  $Z_0$ . 23
- Fig. 3-4. TDR oscilloscope displays for various values of  $R_L$  versus  $Z_0$ . 24
- Fig. 3-5. Values of  $R_L$  versus reflection coefficient when reflection is compared to 50- $\Omega$  transmission line. 25
- Fig. 3-6. Single-resistor discontinuities and their reflections. 27
- Fig. 3-7. Distributed-resistance discontinuities and their reflections. 27
- Fig. 3-8. Waveforms of 1/8-inch-diameter lossy 50- $\Omega$  cable. 27
- Fig. 3-9. Quality RG213/U-cable resistance and  $\Delta Z_0$  characteristics. (Cable tested was 260 feet long.) 28
- Fig. 3-10. Quality RG11/U-cable resistance and  $\Delta Z_0$  characteristics. (Cable tested was 100 feet long.) 28
- Fig. 3-11. Four mismatch conditions that lead to identical reflection coefficients similar to Fig. 3-12A. 32
- Fig. 3-12. Two examples of second-discontinuity reflections. Error of second reflection caused by first discontinuity. 32
- Fig. 3-13. Second-reflection measurement using expanded displays of system shown in Fig. 3-12B. 37
- Fig. 4-1. TDR-system configurations. 41
- Fig. 4-2. Typical TDR resolution. 41

- Fig. 4-3. Application example 5 — demonstration setup. 42
- Fig. 4-4. In-line TDR configuration. 42
- Fig. 4-5. Maximum amplitude resolution. 43
- Fig. 4-6. Maximum time resolution. 43
- Fig. 4-7. Reflection from connector pair. 44
- Fig. 4-8. Three examples of high-resolution TDR connections. Both heads are operating on extender cables, outside the parent sampling unit (vertical-channel plug-in unit). 45
- Fig. 4-9. Displays while calibrating the deflection factor in  $\rho/\text{div}$  using the "in-line" hookup. 47
- Fig. 4-10. Displays while calibrating the displays in  $\rho/\text{div}$  using either "Tee"-hookup TDR system. 48
- Fig. 4-11. Analysis of display when using a "Power-divider Tee." 48
- Fig. 4-12. Regular "Tee" connected to Type S-50 Pulse Generator through a 500-ps section of rigid coaxial line. 50
- Fig. 5-1. Exponential curves and circuit of 6.5-nF capacitor in series with terminated transmission line. 56
- Fig. 5-2. Example of moving display reflection aberrations to obtain a "clean" exponential curve. 58
- Fig. 5-3. Special non-TDR high-speed pulse tests of by-pass capacitors. 59
- Fig. 5-4. Seven-turn coil across end of 50- $\Omega$  line. 61
- Fig. 5-5. Graph for conversion of small reactance observed  $\rho$  to  $\alpha$  for use in formulas (7) and (9). 64
- Fig. 5-6. 16.22 nH coil evaluated by TDR. 65
- Fig. 5-7. Shunt capacitor,  $\sim 0.085$  pF, caused by compressing RG8A/U coaxial cable with pliers. 66
- Fig. 5-8. "Dribble-up" characteristics of two lengths of RG8A/U. 67
- Fig. 5-9. Small series inductor measured 96 cm and 550 cm away from Type 1S2 in RG8A/U coaxial cable. 67
- Fig. 5-10. Special high-voltage impulse-TDR system. 69
- Fig. 5-11. Impulse-TDR resistive-reflection displays. 70
- Fig. 5-12. Impulse-TDR inductive-reflection displays. 70
- Fig. 5-13. Impulse-TDR capacitive-reflection displays. 71
- Fig. 5-14. Comparison of Type 1S2 and special impulse-TDR system. 72
- Fig. 5-15. Complete FM station line using impulse-TDR system. 73
- Fig. 5-16. Three-time-window impulse-TDR plot of FM station 466-foot-long transmission line. 74
- Fig. 5-17. WSU-BPA special Hg pulser and matching network used for testing an EHV DC test transmission line. 76



- Fig. 5-18. TDR trace and line profile for BPA EHV-DC test line. By permission of WSU and BPA. 77
- Fig. 5-19. Type 109 Pulse Generator special application for driving high- $Z_0$  transmission-line TDR system. 78
- Fig. 5-20. Parallel transmission-line impedance relationships between conductors, and between individual conductors and a ground plane. 72
- Fig. 5-21. TDR view of broadband-amplifier input circuit. 81
- Fig. 5-22. Circuit board assembly  $Z_0$  checked by TDR. 82
- Fig. 5-23. Simple frequency compensation for lossy coaxial cable. 82
- Fig. 5-24. Evaluation of a ferrite core. 83
- Fig. 5-25. Two TDR systems for checking plug-in type delay lines. Examples are capable of testing 186- $\Omega$  balanced lines. 85
- Fig. 5-26. Step-signal TDR (Type 1S2) testing of 186- $\Omega$  balanced line. (See Fig. 5-25A.) 85
- Fig. 5-27. Impulse-signal TDR (Type R293 Pulse Generator and an automatic system) testing of 186- $\Omega$  balanced line. (See Fig. 5-25B.) 86
- Fig. 6-1. Two examples of discrete shunt capacitors. 90
- Fig. 6-2. Capacitors measured in Fig. 6-1. 90
- Fig. 6-3. Modified (through-connected) Tektronix insertion unit for testing small components in parallel with 50- $\Omega$  line. 92
- Fig. 6-4. Two plots of 435-MHz dipole antenna. 92
- Fig. 6-5. Series blocking capacitor: General Radio Type 874-K. 94

## LIST OF TABLES

- Table 3-1.  $R_L$  approximations for reflection coefficients of 0.005, 0.01 and 0.02 related to a 50- $\Omega$  transmission line. 24
- Table 5-1. TDR applications chart. 52
- Table 5-2. Single capacitor or inductor TDR displays related to terminated transmission lines. 55
- Table 5-3. Single capacitor or inductor TDR displays when connected across end of transmission line. 55
- Table 5-4. "Large"-capacitor circuits and formulas. 55
- Table 5-5. "Large"-inductor circuits and formulas. 62
- Table 5-6. Type 1S2 suggested impulse duration related to range and magnifier controls. (The RESOLUTION switch must be at its HIGH position.) 69

## BOOKS IN THIS SERIES

### CIRCUIT CONCEPTS

<i>title</i>	<i>part number</i>
Digital Concepts	062-1030-00
Horizontal Amplifier Circuits*	062-1144-00
Oscilloscope Cathode-Ray Tubes*	062-0852-01
Oscilloscope Probe Circuits*	062-1146-00
Oscilloscope Trigger Circuits*	062-1056-00
Power Supply Circuits*	062-0888-01
Sampling Oscilloscope Circuits	062-1172-00
Spectrum Analyzer Circuits	062-1055-00
Storage Cathode-Ray Tubes and Circuits	062-0861-01
Sweep Generator Circuits*	062-1098-01
Television Waveform Processing Circuits	062-0955-00
Vertical Amplifier Circuits*	062-1145-00
*7-book set covering Real-Time Oscilloscopes	062-1180-00

### MEASUREMENT CONCEPTS

Automated Testing Systems	062-1106-00
Engine Analysis	062-1074-00
Information Display Concepts	062-1005-00
Probe Measurements	062-1120-00
Semiconductor Devices	062-1009-00
Spectrum Analyzer Measurements	062-1070-00
Television System Measurements	062-1064-00
Time-Domain Reflectometry Measurements	062-1244-00
Transducers Measurements	062-1246-00